Thermodynamic, Elastic, and Magnetic Properties of Solid Helium*

S. B. TRICKEY,† W. P. KIRK, and E. D. ADAMS
Department of Physics and Astronomy, University of Florida, Gainesville, Florida 32601

Recent experimental studies of solid helium are reviewed with special attention given to specific heat, isochoric pressure, neutron scattering, sound velocity, and magnetic susceptibility measurements. The relationships among the properties are stressed. Low temperature properties of ^{3}He, including exchange, nuclear spin ordering, the melting curve, and Pomeranchuk cooling, are discussed. Phase separation in solid ^{3}He–^{4}He mixtures is reviewed.

CONTENTS

I. INTRODUCTION

Experimental and theoretical investigations of the properties of solid helium have been areas of substantial activity and rapid progress for approximately the past decade. Within the past three years there have appeared three reviews of major aspects of the subject. Chronologically, these are: (1) a review of the lattice-dynamical theories which have been stimulated by the solid helium problem (Werthamer, 1969); (2) a survey of the major phenomena encountered in quantum crystals and the theoretical methods used to treat them (Guyer, 1969); (3) an exhaustive anthology of the magnetic resonance properties of solid ^{3}He (Guyer, Richardson, and Zane, 1971). A very active and fruitful experimental area not treated (except peripherally) by these reviews is the determination of microscopic properties of solid helium using thermodynamic, elastic, etc., techniques.

Sometime prior to the papers just mentioned, the experimental situation in liquid and solid ^{3}He was reviewed by Bernardes and Brewer (1962). So far as the solid phase is concerned, that paper is now mainly of historical value. Somewhat later, a brief summary of NMR work in solid ^{3}He was given by Meyer (1968). Reviews of particular aspects of the experimental situation in solid ^{3}He were also given by Adams (1970), Richardson (1970), and Richards (1971). The basic features of the solid helium systems are well summarized in two monographs (Wilks, 1967; Keller, 1969) as well as in Guyer's (1969) review. At various points in this paper we will recapitulate the appropriate rudiments and leave the exposition of their details to these sources. Comparison with the properties of the other, less bizarre rare-gas crystals can be facilitated by reference to a paper devoted entirely to experiment (Pollack, 1964) and a somewhat more recent review–tutorial effort (Horton, 1968). [There exists a third recent review of the properties of the other rare gas crystals (Smith, 1970), but for our purposes it is less useful than the aforementioned surveys.]

The main aim of the present paper is to provide a comprehensive review of recent progress in the determination of the behavior of solid ^{3}He and ^{4}He using thermodynamic (e.g., calorimetric, strain gauge) or elastic (e.g., ultrasonic) measurements. Some discussion of neutron and x-ray scattering work is also included. Throughout our discussion we will emphasize the experimental motivations and findings. In most cases we limit our review of theoretical considerations to a partial listing of the relevant papers and a commentary on them with respect to experimental results. We adopt much the same attitude toward experimental techniques: our comments are usually limited to a discussion of those procedural features which may have (or are known to have) a significant effect on the experimental findings. When a particular physical observable has been investigated by more than one group of researchers, we usually discuss in detail the experiments which we feel are most instructive, and set our choice in perspective by brief analysis of the merits of the other efforts. We omit, or treat only in passing, those areas which have been relatively inactive since the publication of

* Supported in part by the National Science Foundation.
† Member, Quantum Theory Project, University of Florida.

the monographs by Wilks and by Keller. Examples of such topics are second sound and the ^{4}He melting curve.

The organization of the review is discernible from the Contents; in the remainder of this Introduction we give a brief discussion of those contents and the perspectives underlying our treatment.

At the outset, it is useful to realize that all the macroscopic properties of a solid such as specific heat, thermal expansion, compressibility, sound velocity, etc. are manifestations of the excitation spectrum of the solid. In principle these could all be found by investigating this excitation spectrum directly by the appropriate form of spectroscopy. Indeed, investigations of solid helium by neutron and light scattering have been and are being done. The significant point here is that the direct spectroscopic techniques are by no means sufficiently advanced as to make the macroscopic measurements unnecessary. Thus, the review begins with calorimetry, because of both the conceptual simplicity of the technique and the wealth of peculiar effects uncovered by it. The discussion of the high-temperature specific heat anomaly and its analysis leads naturally to the question of vacancies, and a summary of some unpublished x-ray results. After a discussion of the calorimetric and strain guage investigations of the low temperature specific heat anomaly in bcc ^{3}He, we treat the thermal conductivity measurements: from our vantage point they are of interest mainly insofar as they shed light on the unusual behavior of the specific heat.

The discussion of the various possible mechanisms for the low-temperature specific heat anomaly and of the several lattice-dynamical calculations which have attempted to come to grips with the problem provides a natural bridge to the sound velocity measurements. From there we move to neutron scattering investigations of the lattice dynamics. The emphasis, therefore, of Sec. II and III is the interconnectedness of specific heat, $\partial P/\partial T)_V$, ultrasonic, thermal conductivity, neutron and x-ray scattering measurements and the remarkable number of unusual phenomena those measurements have revealed.

In Secs. IV and V, we turn our attention to the lower temperature region where the spin statistics of the particles plays a dominant role. Section IV surveys the topic of solid nuclear magnetism, with particular attention given to the precision determination of the value of the exchange energy J and to the recently discovered, unanticipated behavior of the isochoric pressure of a sample in a magnetic field. The behavior of solid helium along the melting curve is considered in Sec. V, where we encounter an interesting dichotomy. That is, one aspect (Pomeranchuk cooling) of the melting curve behavior is rapidly being exploited as a low temperature research technique, while the effect of nuclear-spin ordering on the melting curve has just begun to be investigated. A closely related topic which we consider in Sec. V is the effect of high magnetic fields on the melting curve and on Pomeranchuk cooling. Finally, in Sec. VI we review the phase separation of solid ^{3}He–^{4}He mixtures. Although this area has not been subject to dramatic progress in the last few years, we have included it since it has not been reviewed elsewhere.

II. SPECIFIC HEATS

A time honored means of investigating the low-energy excitations in a solid is the straightforward calorimetric measurement of the specific heat. Such a measurement (indeed, any measurement of the specific heat) is restricted to probing the long-wavelength region of the dispersion curves of the relevant excitations. Nevertheless, it is essential that such measurements be performed, if for no other reason than to be sure that the solid holds no surprises in store. For the sake of logical clarity, it is useful to sort out the known excitations and attempt to separate their contributions to the specific heat. Thus, for the moment we will not be concerned about the "magnetic" specific heat of ^{3}He near the nuclear spin ordering temperature T_N ($\approx$2 mK) but will be concerned with C_V at relatively high T.

Many workers have made specific heat measurements; we discuss only the most recent. These have been made by Sample and Swenson (SS, 1967), Edwards and Pandorf (EP, 1965, 1966), Pandorf and Edwards (PE, 1968), Ahlers (1970), and Gardner, Hoffer, and Phillips (1972). Comment on the limitations of the earlier work, particularly with regard to experimental artifacts, may be found in these papers.

Since we are dealing with an insulating inert-gas solid, we expect only "lattice" specific heat. Therefore, it is customary to display the specific heat in terms of Debye θ's, although we do not necessarily expect the Debye model to fit very well. Thus C_V versus T is measured and θ determined from the relation

$$C_V=(12\pi^4/5)R(T/\theta)^3, \qquad T<\theta_0/10, \quad (2.1)$$

where θ_0 is the zero-temperature Debye temperature and R is the gas constant.

The Debye θ as defined in Eq. (2.1) is a temperature dependent quantity since C_V is not, in general, proportional to T^3. We first look at θ_0. The behavior of this quantity is subject to some uncertainty, particularly in the case of ^{3}He, a problem which we will discuss in Sec. II.4. Ignoring this for the present, we show the general behavior of θ_0 verusus molar volume V in Fig. 1. For comparison, the calculated values of θ_0 (deWette, Nosanow, and Werthamer, 1967) in bcc ^{3}He lie above and approximately parallel to the experimental values. (One interesting point to be made here, as in the study of the volume dependence of any other quantity, is the wide range in V available at fairly modest pressures. Helium is more compressible than any other solid: for example, the isothermal compressibility K_T is as large as 5×10^{-3} atm^{-1}. Thus a change in volume of 50%

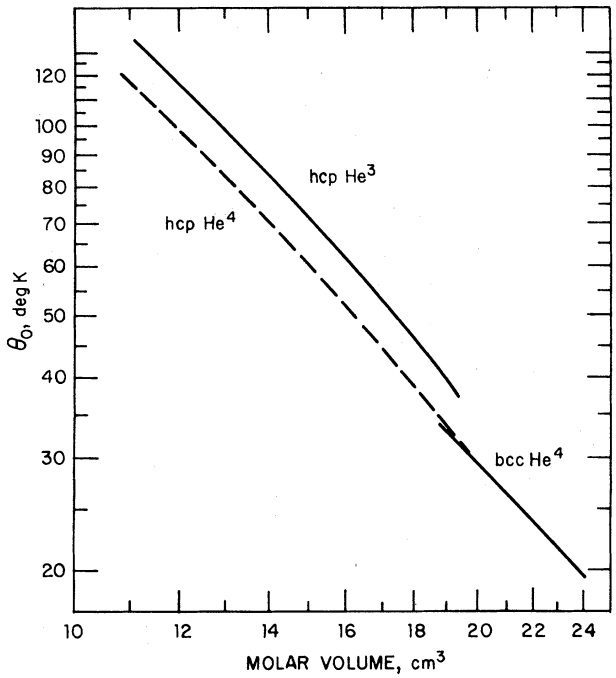

FIG. 1. The molar volume dependence of the zero-temperature Debye temperature θ_0 for bcc ^{3}He, hcp ^{3}He, and hcp ^{4}He. Note that the bcc ^{3}He values are rather uncertain (see Sec. II.4). (After Keller, 1969).

can be achieved with a few hundred atmospheres pressure.)

In the hcp phase, the ratio θ_3/θ_4 of the zero temperature Debye temperatures for the two isotopes is $\theta_3/\theta_4 \approx 1.18$ (SS). For a true Debye solid (classical continuum system), θ_0 scales as $m^{-1/2}$ which implies $\theta_3/\theta_4 = (4/3)^{1/2} = 1.154$. For the hcp phase a self-consistent harmonic calculation (Morley and Kliewer, MK, 1969) gives $\theta_3/\theta_4 \approx 1.23$ over the molar volume range 10.0–16.0 cm^3/mole. The treatment by MK of short-range correlations (by the use of a simple cutoff length) has been questioned (Chell, 1970) in the context of compressibilities, while a calculation on a fcc model (Chell, Goldman, Klein, and Horton, 1970) which included leading anharmonic corrections has also been used to argue for substantial alteration of the MK results. Thus, the comparison of θ_3/θ_4 in the hcp phase with theoretical values is in a state of ambiguity.

II.1. hcp ^{3}He

For a true Debye solid the specific heat is a function only of T/θ_0, so that a single graph of $\theta(T)/\theta_0$ versus T/θ_0 (the "reduced θ versus T curve") suffices to describe such a system. For hcp ^{3}He, SS found it convenient to analyze their data in terms of such a reduced plot (Fig. 2). To do so, it was necessary [because of a low T decrease in $\theta(T)$] to identify θ_0; SS chose $\theta_0 = \theta_{max}$ and ignored the low T behavior for reasons we discuss below. For a Debye solid one would have

$$\partial S/\partial V)_T = \partial P/\partial T)_V = \gamma C_V/V, \qquad (2.2)$$

where $\gamma = -(\partial \ln\theta/\partial \ln V)$ is the Grüneisen parameter, which would be a constant. If C_V and S are functions of T/θ_0 only, then we have $\gamma = \gamma(V)$. But for hcp ^{3}He, the reduced plot shows some slight V dependence. Therefore, we have $\gamma = \gamma(T, V)$. By appeal to thermo-

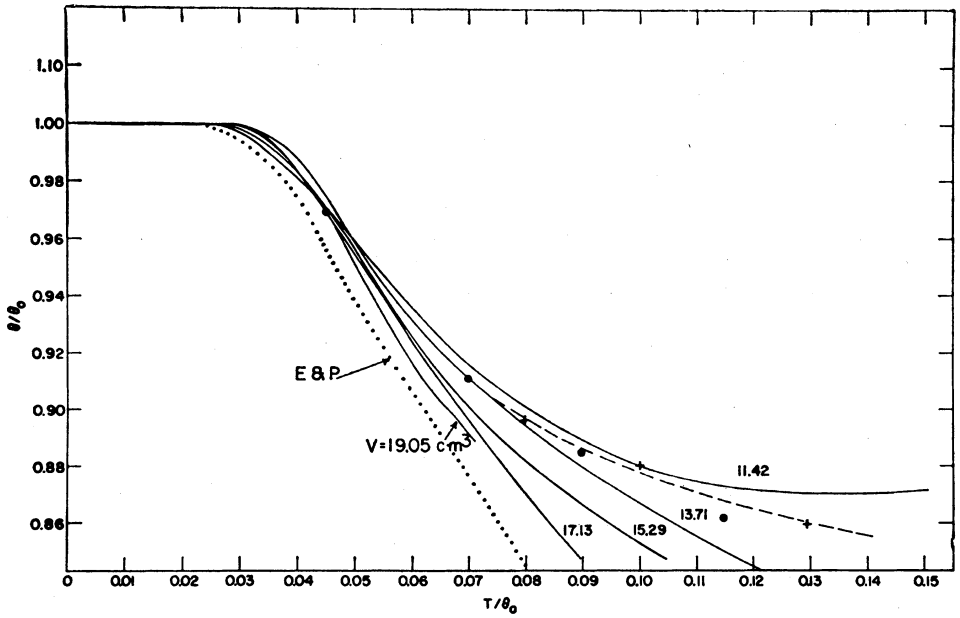

FIG. 2. Reduced θ versus T plot for hcp ^{3}He and ^{4}He. Solid curves, hcp ^{3}He, SS (1967). Dashed curve, hcp ^{4}He ($V = 12.23$ cm^3/mole), SS (1967). Dotted curve, hcp ^{4}He, ($V = 20.9$–16.9 cm^3/mole). +, hcp ^{4}He ($V = 12.22$ cm^3/mole), Dugdale and Franck (1964). "●" hcp ^{3}He ($V = 12.57$ cm^3/mole), Dugdale and Franck (1964). Other molar volumes as shown adjacent to curves. (After SS, 1967).

dynamic relations, the T dependence of γ reduces to

$$\gamma(T/\theta_{\max}, V) = \gamma_0(V) + (V/C_V)(\partial S/\partial V)_{T/\theta_{\max}}.$$

With

$$S = \int_0^T (C_V/T)\, dT,$$

Sample and Swenson evaluated γ with the results shown in Fig. 3. As an increase in γ/γ_0 of only seven percent was found over the range $0.01 \leq T/\theta_0 \leq 0.12$, SS argued that the analysis in terms of the Grüneisen model was appropriate.

As mentioned, SS found a decrease in $\theta_0(T)$ for both bcc and hcp ^{3}He in the region $T/\theta_0 < 0.02$. The behavior was particularly acute in hcp ^{3}He at the lowest molar volume (11.42 cm^3/mole). It was stated by SS that the decrease in θ as T was reduced for hcp ^{3}He was "probably a characteristic of the apparatus." As will become apparent in our discussion of the heat capacity of bcc ^{3}He, it is important that the description of the low-temperature decrease in hcp ^{3}He as an experimental artifact be well founded. The description is in fact supported by two independent pieces of evidence: the very data of SS, and the thermal conductivity work of Thomlinson (1969). We will discuss Thomlinson's results later on; here we give a brief discussion of the experimental effects implicit in the results of SS.

The heat capacity of hcp ^{3}He at 11.42 cm^3/mole is the lowest [i.e., the $\theta(T)$ is the largest] of all the specimens (either hcp or bcc) studied by SS. As noted, SS picked θ_0 by identification with $\theta_{\max}(T)$; in the present case they quoted a value of 128.19 K, at $T = 2.563$ K ($T/\theta_0 = 0.02$). This value corresponds to a sample heat capacity of 0.392×10^{-3} cal/K, while the calorimeter heat capacity at the same temperature is about 2.1 times larger (see Fig. 4 of SS). With this ratio as a clue, one may calculate how much calorimeter heat capacity must be added to a strictly T^3 sample heat capacity in order to give an observed θ equal to that quoted by SS (98 K) at $T/\theta_{\max} = 0.005$ ($T = 0.641$ K). One finds that only 4.85% would be required, without taking into account any uncertainty in the calorimeter heat capacity or the measured θ. Thus, it seems quite reasonable to describe the apparent low-temperature θ anomaly in high density hcp ^{3}He as a direct manifestation of the very small sample heat capacity (compared to the calorimeter used by SS). This description is corroborated by the fact that the hcp ^{3}He runs at higher molar volumes made by SS showed only a rather weak low-temperature drop in $\theta(T)$; as previously noted, the heat capacities of the helium samples in these lower density cases are substantially larger than that associated with 11.42 cm^3/mole.

II.2. hcp ^{4}He

For the hcp phase of ^{4}He there is reasonable agreement between the measurements of EP (1965) and Ahlers (1970), and excellent agreement between

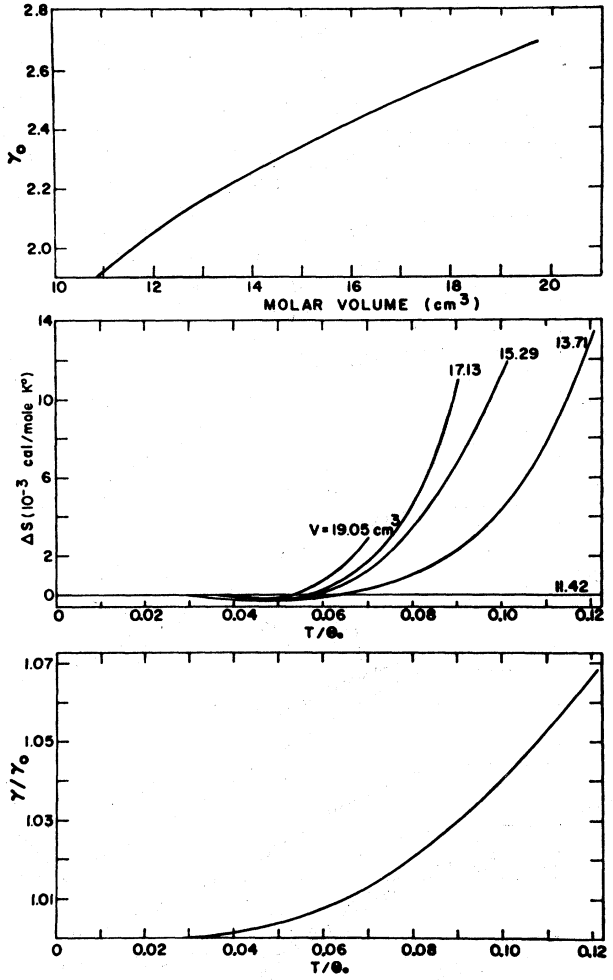

FIG. 3. Dependence of the Grüneisen parameter γ on molar volume and on temperature for hcp ^{3}He as determined by SS (1967).

Ahler's results and those of Gardner, Hoffer, and Phillips (1972). Ahlers stated that the discrepancy between his results and those of EP might be due to an unspecified characteristic of the sample chamber used by the latter workers, but he did not elaborate on the statement. In a private communication (to SBT, 1972), he indicated that his concern was with possible sample density gradients in the sintered-copper "sponge" sample chamber used by EP, but that he is not at all sure as to the precise effect of such difficulties. The investigations by EP and by Ahlers are, if questions of slight discrepancies are cast aside, complementary, for the EP measurements extend down to $T \approx 0.3$ K with reasonable precision, while the lowest temperatures reached in Ahler's high-precision measurements were $T \approx 1.3$ K. [The question of the precision of the EP experiments is a bit confused in the literature, for their error bounds were displayed in a figure in terms of adding or subtracting 1% of the calorimeter heat capacity. Other workers, including Ahlers, seem to have

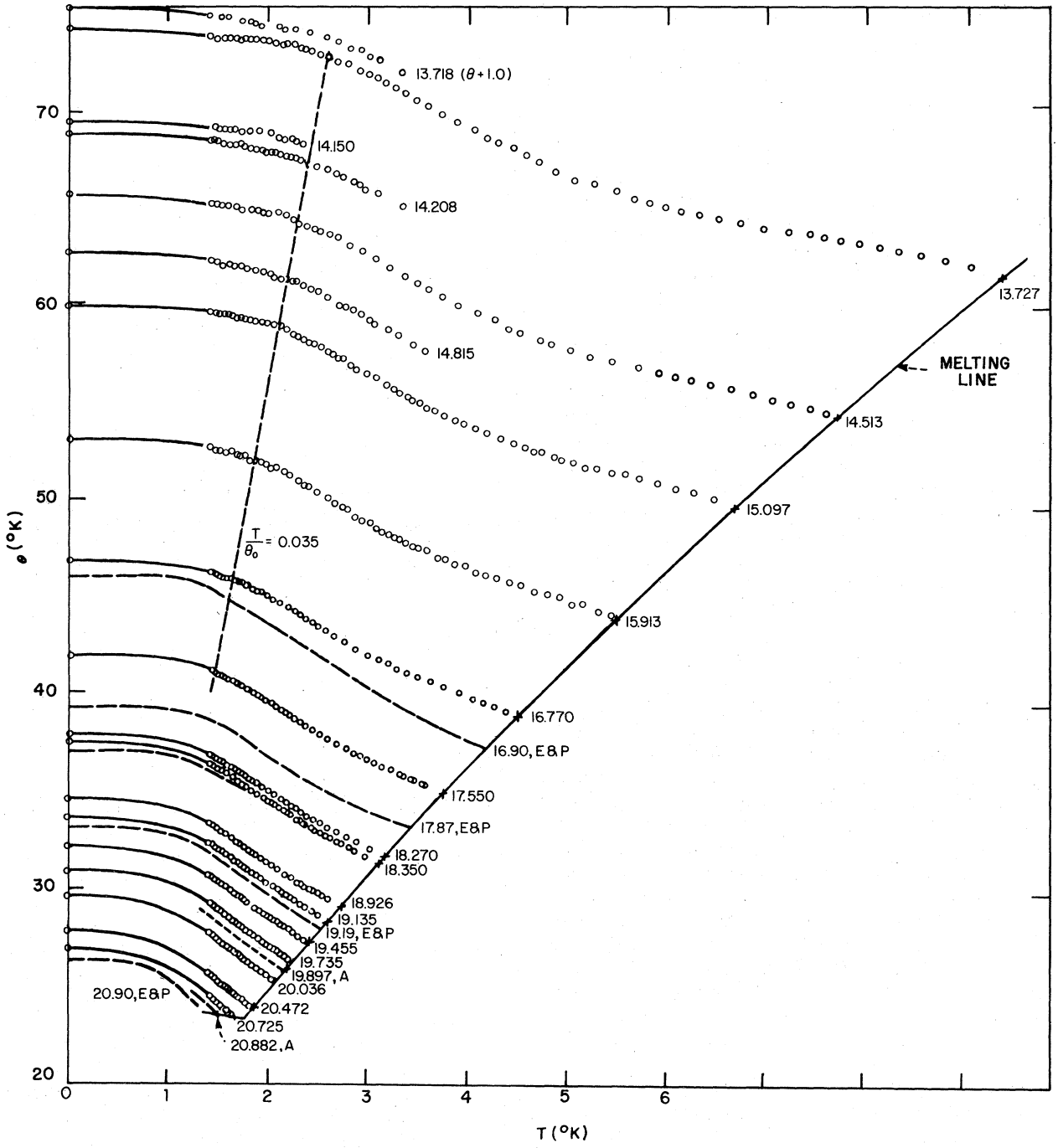

FIG. 4. $\theta(T)$ for hcp ^{4}He. Individual data points from Ahlers (1970). Dashed curves from Ahlers (1964) and Edwards and Pandorf (1965). Note the vertical displacement (by 1 K) of the results for 13.718 cm^3/mole. Molar volumes as shown adjacent to curves.

interpreted this as a statement that the absolute precision was believed by EP to be 1%. A careful reading of the EP comparison of their data with those of Dugdale and Franck (1964) reveals that EP presumed their error bounds to be greater than 1.5% at 5 K, and increasing with decreasing T. (See EP, 1965, p. A822.)]

In Fig. 4 we show temperature-dependent Debye temperatures for hcp ^{4}He from EP and Ahlers for a selection of molar volumes, while in Fig. 5 the corresponding reduced Debye plots are reproduced. Ahlers has analyzed his low molar volume results in the region $T/\theta_0 \leq 0.035$ in terms of the low temperature

heat capacity functional form studied by Barron and Morrison (1957),

$$C_V = a_1 T^3[1+\alpha_1(T/\theta_0)^2+\alpha_2(T/\theta_0)^4] \qquad (2.3)$$

for harmonic solids. For isotropic fcc crystals, Barron and Morrison found $\alpha_1 \approx 50$, $\alpha_2 \approx 10^4$ from model calculations, while Finegold and Phillips (1969) used their high-precision heat capacity measurements on crystalline Ar and Kr to deduce $\alpha_1 \approx 45$. By comparison, Ahlers found (in samples which were free from impurity problems) $21 \leq \alpha_1 \leq 57$ and $2.2\times10^4 \leq \alpha_2 \leq 2.9\times10^4$, values which are in reasonable accord with those for normal close-packed crystals. Of greater significance, Ahlers found that the fit to his data generated below $T/\theta_0 = 0.035$ was adequate to give an acceptable representation of those data up to $T/\theta_0 = 0.045$, in striking parallel with the behavior of other normal solids (Barron and Morrison, 1957).

At higher temperatures, Ahlers found that the reduced θ plot for hcp ^{4}He was in reasonable accord with that determined by Finegold and Phillips (1969) for Ar and Kr. The disagreements are within combined experimental error up to about $T/\theta_0 = 0.10$ for the lower molar volumes, and $T/\theta_0 = 0.08$ for the higher ones. Though we did not mention it previously, SS made a similar comparison with Ar and Kr for hcp ^{3}He, with excellent agreement up through $T/\theta_0 = 0.12$. Thus we believe that it is fair to characterize the behavior of the heat capacity of the hcp phase of both isotopes of helium as that of essentially orthodox inert gas solids without either high or low temperature anomalies.[1]

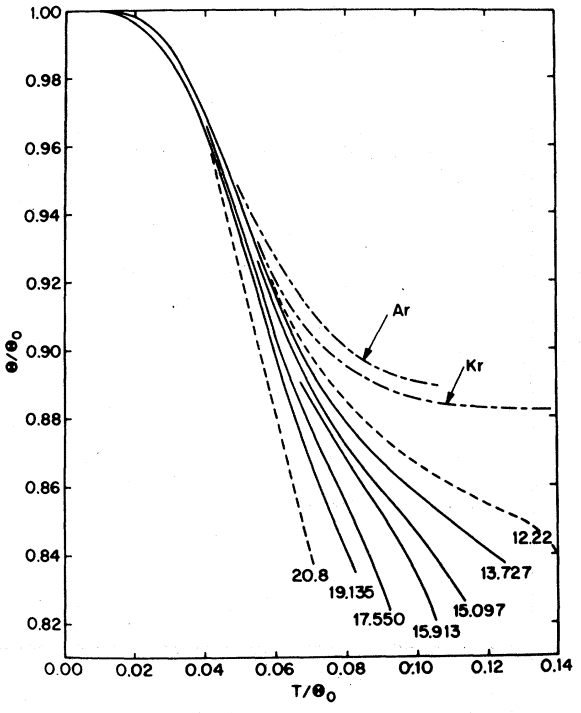

FIG. 5. Reduced θ versus T plot for hcp ^{4}He. Solid curves: Ahlers (1970). Dashed curve: ($V = 20.8$) Hoffer *et al.* (1968). Dashed curve: ($V = 12.22$) SS (1967). Ar and Kr: Finegold and Phillips (1969). (After Ahlers, 1970).

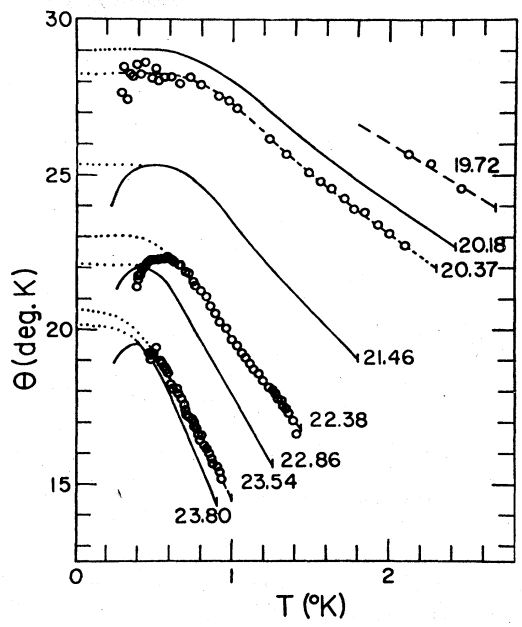

FIG. 6. θ versus T for bcc ^{3}He. Solid curves: SS (1967). Circles and dashed curves: PE (1968). High-T termination of each curve is at the melting temperature. Dotted extrapolations are the $\theta_0 = \theta_{max}$ assumption of SS.

II.3. bcc ^{3}He, High T

The situation in bcc ^{3}He is markedly different from that in hcp ^{3}He, as can be seen in the $\theta(T)$ results of SS and of PE (1968) which are shown in Fig. 6. We defer discussion of the low-temperature decrease in θ, and follow the treatment of SS; they again chose $\theta_0 = \theta_{max}$ and produced the reduced θ curve shown in Fig. 7. If a Grüneisen analysis of these data were attempted, γ would be so strongly T and V dependent as to make the results meaningless. Hence SS studied their data in terms of an excess specific heat, defined by $C_{ex} = C_{obsv} - C_{Debye}$ ($\theta_0 = \theta_{max}$). The problem of determining the mechanism(s) responsible for this excess specific heat then arises. On the basis of earlier diffusion data, Reich (1963) had suggested the possibility that there existed thermally activated vacancies. The specific heat due to such vacancies is (deWette, 1963)

$$C_V/R = A(W/kT)^2 \exp(-W/kT),$$

where W is the energy of formation of the vacancy, k is Boltzmann's constant, and A is a constant of the order of unity.

[1] Low-temperature $\theta(T)$ anomalies were at one time thought to occur in both isotopes and in both phases. The present view is that such behavior is characteristic of bcc ^{3}He only; it is for this reason that we have belabored the question in discussing the hcp phase of both isotopes.

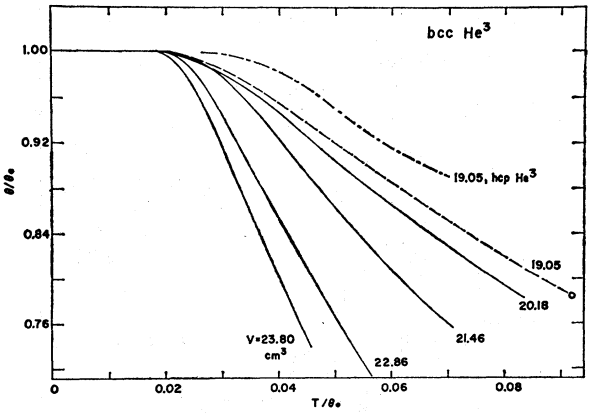

FIG. 7. Reduced θ versus T plot for bcc ^{3}He. The curve at 19.05 cm^3/mole was deduced by SS as plausible from considerations of their other data and their single result (open circle at $T/\theta_0 \approx 0.092$) at that molar volume.

Sample and Swenson were able to fit their bcc ^{3}He data for the excess specific heat rather well with the analytic expression

$$C_{ex}/R = (\phi/T)^2 \exp(-\phi/T), \tag{2.4}$$

where $\phi = \phi(V)$ only, and was chosen to give the best fit. ϕ versus V is as shown in Fig. 8 (note that ϕ corresponds to symbol E in the figure). The resulting values of ϕ are fairly close to the W/k of de Wette (using one adjustable parameter) and to the values of the activation energy found by Reich in diffusion measurements. Thus the hypothesis of vacancy formation seems to give a reasonably satisfactory general account of the excess specific heat at large T. (However, see Sec. II.5.)

Unfortunately, the argument in support of the vacancy formation hypothesis rests on two related assumptions which may well be unreliable. As expressed by deWette and Werthamer (deWW, 1969)), the drawbacks in the SS analysis are: (1) the assumption of a Debye phonon spectrum to determine the "lattice" contribution to the specific heat; and (2) the choice of $\theta_0 = \theta_{max}$. Both assumptions are questionable because of the presence of the low-temperature anomaly (discussed below) in the temperature region of interest and the consequent ambiguity in the characterization of the lattice contribution to the heat capacity.

Because of these difficulties, deWW performed a sequence of analyses, all based on the calculated reduced θ versus temperature relationship obtained by de Wette, Nosanow, and Werthamer (1967). de Wette and Werthamer determined the anomalous specific heat as

$$C_V^{anom}(T/\tilde{\theta}_0) = C_V^{obs}(T/\tilde{\theta}_0) - C_V^{vib}(T/\tilde{\theta}_0), \tag{2.5}$$

with C_V^{vib} chosen to have the theoretically predicted behavior (*not* Debye behavior) and $\tilde{\theta}_0$ some appropriately chosen zero-temperature θ. Since there is no unambiguous way to make this choice, deWW used several methods: (1) $\tilde{\theta}_0 = \theta_0^{SS}$, (the value selected by SS); (2) $\tilde{\theta}_0 = \theta_0^{min}$ so as to keep $C_V^{anom} \geq 0$; and (3) $\theta_0 = \theta_0^{th}$ (the theoretically determined value). They found that the anomalous specific heat could be fitted fairly well by the form

$$C_x = AR(\phi/T)^2 \exp(-\phi/T)[1 - \exp(-\phi/T)]^{-2}, \tag{2.6}$$

with $A = 1$. This is the specific heat of a two-level system with energy level separation $k\phi$ and is, in essence, the expression used by SS [Eq. (2.4)], since the exponential in the denominator is negligible over the range of T in question. The suitability of Eq. (2.6) to the various data analyses is in fact greatest for the SS procedure, because of the more rapid decrease in C_V^{anom}(SS) with decreasing T as compared with the behavior of the C_V^{anom} found by procedure (3) of deWW. This difference in behavior stems from the fact that $\theta_0^{SS} < \theta_0^{th}$, with the result that SS subtracted a larger lattice specific heat from the observed value than did deWW, thus generated a smaller C_V^{anom}. deWette and Werthamer argued that the SS choice of θ_0 artificially depresses the value of θ_0 an indeterminate amount (by

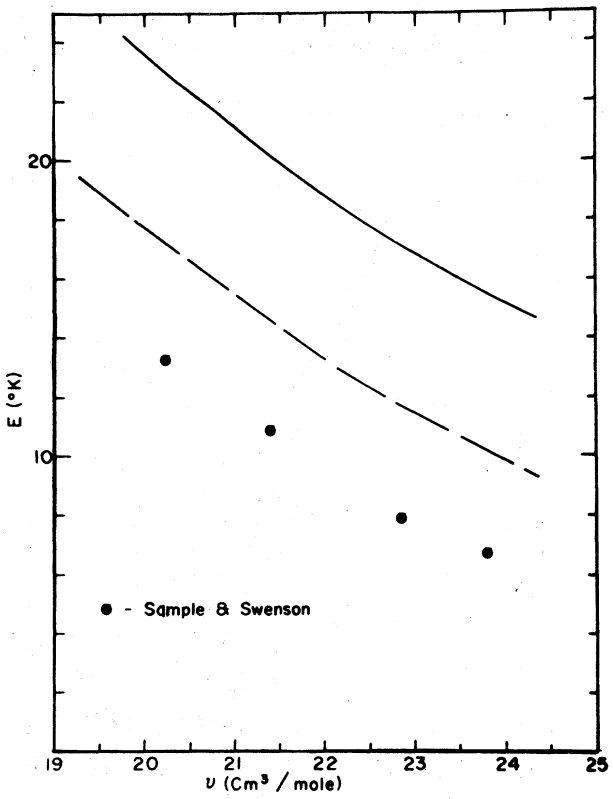

FIG. 8. Molar volume dependence of the activation temperature found by SS in their analysis of the high-T specific heat anomaly in bcc ^{3}He, compared to calculated behavior for localized vacancies (solid curve) and for the lower band edge for nonlocalized vacancies. Both calculations: Hetherington (1968).

inclusion of contributions of uncertain extent from both the low and the high temperature anomalies), and further, that θ_0^{th} is probably too big. Thus they arrived at the conclusion that the quality of the fit of (2.6) is probably overestimated by the SS scheme and underestimated by their own third analysis. This conclusion is weakened somewhat, as deWW pointed out, by the distinct possibility that the combined uncertainties in θ_0^{th} and θ_0^{SS} are not significantly smaller than the difference between the two choices. The elusiveness of the problem is perhaps best appreciated by appeal to Figs. 9 and 10 and to Table I. In Fig. 9 the molar volume dependence of the activation temperature ϕ is plotted for the SS analysis and procedures (2) and (3) of deWW, while Fig. 10 shows the comparison between $C_V^{anom}(T)$ found by procedure (3) and that given by $C_x(T)$ [Eq. (2.6)]. The values of $\tilde{\theta}_0$ for the three procedures are tabulated in Table I for the relevant molar volumes. Here θ_0^{th} is estimated by deWW to have an uncertainty of 10%; they did not provide an estimated uncertainty for θ_0^{SS} but indicated, as noted above, that it is substantially larger than the value of 1% given by SS.

The value $A=1$ in Eq. (2.6) found by deWW would seem to indicate that only vacancies are formed ($A=1$, vacancies only; $A=3.5$, vacancies and interstitials in pairs; $A=4$, vacancies and interstitials singly—see deWette, 1963). However, deWW were careful to point out that their data analyses are sufficiently indeterminate as to make such a deduction quite unreliable. In view of the large root-mean-square displacements of individual helium atoms from their nominal lattice sites (on the order of 30% of the nearest-neighbor distance; see Guyer, 1969), the very notion of a well-defined entity having the usual properties of a vacancy was regarded as questionable by various workers. Hetherington (1968) dealt with this difficulty in very plausible fashion by studying the properties of a nonlocalized vacancy in a bcc ^{3}He lattice. He assumed that the crystal with a nonlocalized vacancy can be described as having a wave function which is a linear combination of crystal wave functions each with a vacancy localized at a different lattice site. This ansatz, coupled with the single-particle ground state theory of the perfect crystal due to Nosanow and co-workers (see Guyer, 1969, for detailed references) yields a band of vacancy excitation energies. The calculated vacancy energies agree only semiquantitatively with those deduced from experiment by SS (see Fig. 8), although the calculated molar volume dependence was found to be quite realistic.

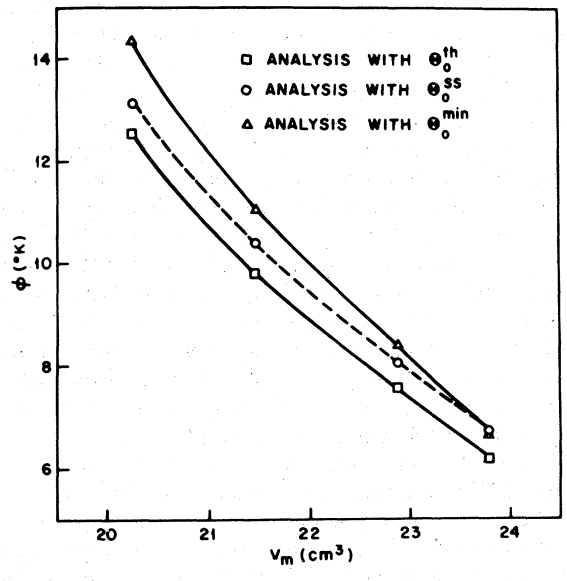

FIG. 9. Activation temperature φ as a function of molar volume as determined from three analyses of the SS data. Dashed curve is the SS result. Upper solid curve is the deWW (1969) result for $\tilde{\theta}_0=\theta_0^{min}$. Lower solid curve is the deWW result for $\tilde{\theta}_0=\theta_0^{th}$. See text for further details. (After deWW, 1969).

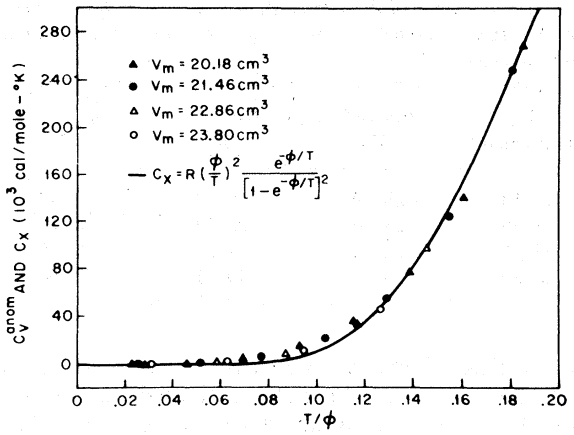

FIG. 10. Comparison of the anomalous specific heat in bcc ^{3}He as determined by deWW (1969) with the exponential form [Eq. (2.6)].

Perhaps the best way to deal with the matter of vacancies in solid helium is by direct observation. Balzer and Simmons (1972) have made a substantial start in this direction by making direct x-ray measurements of the temperature dependent lattice constant $a(T)$ for a bcc ^{3}He crystal held at constant volume. Because of thermal gradient problems, their work has so far been restricted to $T>0.8$ K; in this range they have analyzed their results in terms of the expression

$$-3\Delta a/a_0 = A + \exp[(S-W/T)/k] \qquad (2.7)$$

in which $\Delta a = a(T) - a_0$. Since their experiment probes only thermally activated vacancies, A should be zero; because of the problems so far encountered in going below $T=0.8$ K, they have been compelled to try to determine A along with the activation entropy S and energy W, a situation which prevents them from drawing firm quantitative conclusions. The qualitative

TABLE I. Values of the various $\tilde{\theta}_0$ for bcc ^{3}He found by deWette and Werthamer (1969) by various analyses of the data of Sample and Swenson (1967).

V_M (cm^3/mole)	$\tilde{\theta}_0=\theta_0^{SS}$ (K)	$\tilde{\theta}_0=\theta_0^{min}$ (K)	$\tilde{\theta}_0=\theta_0^{th}$ (K)
20.18	28.99	29.19	33.90
21.46	25.30	25.50	30.98
22.86	22.10	22.20	28.15
23.80	19.64	19.74	26.64

conclusions which can presently be made are these: (a) there do exist thermally activated vacancies in bcc ^{3}He in experimentally detectable concentrations; (b) with the assumption $S=0$, the values of W in Eq. (2.7) which Balzer and Simmons find (over the molar volume range 20–20.9 cm^3/mole) are smaller than, but in reasonable accord with, the SS values of ϕ in Eq. (2.4) (see Fig. 8).

II.4. bcc ^{3}He, Low T

As noted earlier, the discussion we have given of the high-temperature behavior of the heat capacity of bcc ^{3}He ignores the existence of a low-T decrease in θ. Thus, as can be seen from Fig. 6, $\theta(T)$ decreases below $T/\theta_0\approx 0.02$ rather than attaining a constant value, as would be expected for the lattice specific heat of any solid at sufficiently low T. (The choice of θ_0 is not critical to the argument that anomalous behavior is occurring; exact agreement with the elementary criterion for the onset of Debye behavior as $T/\theta_0\leq 0.02$ is not required. Rather, what one sees from Fig. 6 is that almost any plausible choice of θ_0 will place the maximum of $\theta(T)$ at a temperature which would ordinarily be thought of as being in the Debye region.) In the data obtained by PE (1968), the low-temperature anomaly is particularly evident for $V=22.38$ cm^3/mole. This is important since these same workers, using the same apparatus, had earlier found θ for ^{4}He to reach a constant value. Thus it is difficult to attribute the behavior in the case of bcc ^{3}He to an apparatus effect.

For ^{3}He, precautions must be taken to determine that the extra specific heat is not due to some source other than the lattice. For example, other possibilities are that it is caused by ordering of nuclear spins or ordering of small amounts of ^{4}He impurities which are always present to some extent. All such sources were examined systematically by PE who concluded that these could not account for the effect. Although they therefore regarded the effect in ^{3}He as real, not much attention was paid to this. In view of the situation for ^{4}He, the suspicion remained that, with still more precise measurements, the effect in ^{3}He would be shown to be spurious.

In 1969, two rather different experiments were conducted which helped to resolve the question. In the first of these [Henriksen, Panczyk, Trickey, and Adams (HPTA, 1969)], strain gauge techniques (Straty and Adams, 1969) were used to measure accurately small changes in pressure on the sample held at constant volume. From the pressure, one obtains $(\partial P/\partial T)_V$, which is related to C_V by [see Eq. (2.2)]

$$(\partial P/\partial T)_V=\gamma C_V/V. \tag{2.8}$$

Thus a measurement of $(\partial P/\partial T)_V$ will provide about the same information as C_V. There are some advantages to the $(\partial P/\partial T)_V$ method which make it particularly suited to the present problem in which apparatus effects must be excluded: there is neither a calorimeter heat capacity subtraction, nor a filling capillary effect (except near melting), and measurements may be made easily either on warming or cooling.

Measurements of $(\partial P/\partial T)_V$ for both bcc ^{3}He and hcp ^{4}He were reported by HPTA. The ^{3}He samples contained 20 ppm or less ^{4}He, permitting phase-separation effects to be ruled out. (See the discussion by HPTA for details). For the larger molar volumes, there is a sizable contribution to $(\partial P/\partial T)_V$ due to spin ordering. By extending the measurements to quite low temperatures (≥ 20 mK), this contribution was identified, then extrapolated to higher temperatures and subtracted from the total pressure. The resulting $(\partial P/\partial T)_V$ should then be due to only the lattice of pure ^{3}He.

The results of HPTA were presented in the form $\theta\gamma^{-1/3}$ obtained by combining Eqs. (2.1) and (2.8). A plot of $\theta\gamma^{-1/3}$ versus T gave a set of curves quite similar to those of Fig. 6. In Fig. 11, we show the HPTA data in the form $(\partial P/\partial T)_V$ versus T for several molar volumes of ^{3}He and ^{4}He. Because of the rapidly increasing uncertainty in the values of $(\partial P/\partial T)_V$ at lower T, these are not shown below $(\partial P/\partial T)_V=5\times 10^{-3}$ atm K^{-1}. The straight line through the 20.16 cm^3 data is drawn with slope three appropriate to a Debye solid. To within the accuracy of the experiment, in the low-temperature limit the points for the two ^{4}He samples and for the smaller volume ^{3}He sample would fall on a line of this slope. According to Eq. (2.1) this agreement indicates Debye T^3 behavior for the lattice specific heat. For the two larger volume ^{3}He samples, the slope in the low-temperature limit is less than 3, indicating a specific heat in excess of the Debye value. (Only part of the departure of $(\partial P/\partial T)_V$ from the T^3 behavior could be due to the temperature dependence of γ in Eq. (2.8) since γ is constant if $C_V\propto T^3$.) Thus the $(\partial P/\partial T)_V$ measurements support the behavior of θ in bcc ^{3}He determined calorimetrically (Fig. 6).

The second piece of experimental evidence in support of the existence of the anomalous specific heat in bcc ^{3}He which appeared in 1969 was the thermal conductivity work by Thomlinson (1969). In such an experiment, the heat flow is considered to be a diffusive process limited by the mean free path between phonon collisions. The thermal conductivity K is given by the

kinetic equation

$$K = C_V v \lambda / 3, \qquad (2.9)$$

where v is an average sound velocity, and λ is the mean free path. As the temperature is lowered, λ increases, goes through a maximum in the case of Poiseuille flow, and finally reaches a constant value limited by the crystal size. Thus in the low-temperature limit where λ is constant, we have $K \propto C_V$. Figure 12 shows the thermal conductivity of solid ^{3}He as measured by Thomlinson. Curve E, which is for hcp ^{3}He at $V = 19.5$, has the expected slope of 3 for a Debye solid in the boundary scattering region. (This behavior in hcp ^{3}He is the second piece of evidence for the lack of a low-T θ anomaly in hcp ^{3}He which we mentioned earlier.) The other samples, except for A (which had 100 ppm ^{4}He impurity), show evidence of Poiseuille flow as indicated by the enhanced peak in K. Below the Poiseuille flow region, $K \propto T^n$, $n \approx 2.55$, this again is indication of a departure from Debye behavior by C_V at low T in bcc ^{3}He.

A possible difficulty in this interpretation is the fact that specular reflection of the phonons, either at the chamber walls or at crystallite interfaces, could cause a thermal conductivity which was proportional to a power of temperature smaller than three. Thomlinson observed, as noted, that T^3 behavior was found for the hcp phase. Since the hcp crystals in question had higher sound velocities than the bcc samples, the dominant phonon wavelengths in the former situation were longer than in the latter. Since specular reflection is more probable at longer wavelengths, the absence of evidence for it in the hcp phase makes it seem improbable in the bcc phase.

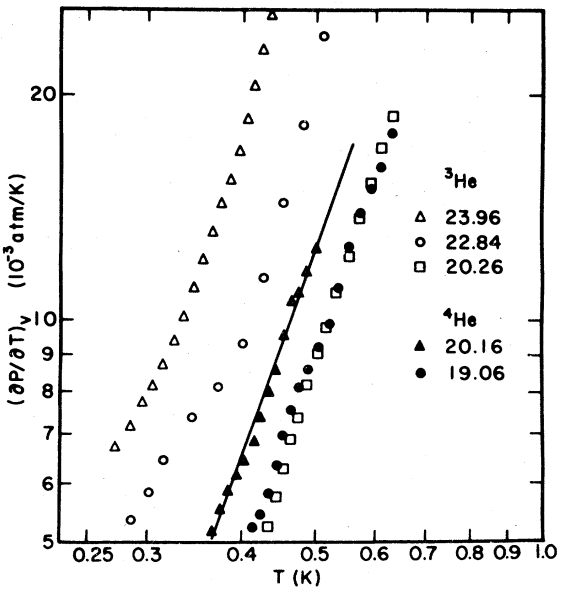

FIG. 11. $(\partial P/\partial T)_V$ as a function of T for bcc ^{3}He and hcp ^{4}He at the indicated molar volumes, as found by HPTA (1969).

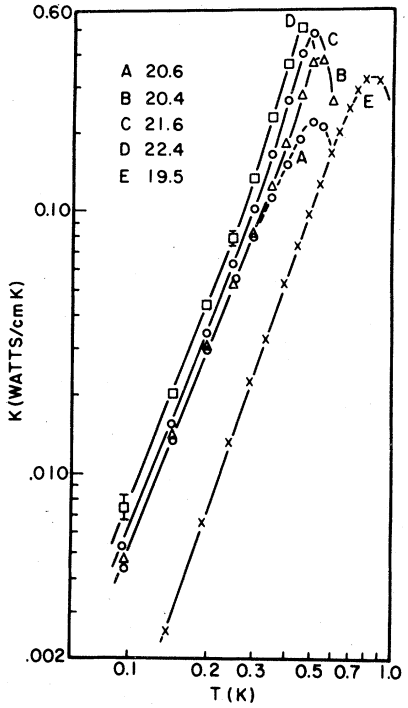

FIG. 12. Thermal conductivity K for bcc ^{3}He. (A, 100 ppm ^{4}He, 20.6 cm^3/mole; B–D, 2 ppm ^{4}He, 20.4, 21.6, 22.4 cm^3/mole, respectively) and hcp ^{3}He (E, 2 ppm ^{4}He, 19.5 cm^3/mole), as determined by Thomlinson (1969).

Because of the existence of four rather extensive studies of the thermal conductivity of hcp ^{4}He (Mezhov-Deglin, 1965; Hogan, Guyer, and Fairbank, 1969; Seward, Lazarus, and Fain, 1969; Fain and Lazarus, 1970), it might be thought that an effort similar to Thomlinson's could be made to confirm the absence of any low-temperature θ anomaly in this phase. Unfortunately, such is not the case, for none of the measurements extended to sufficiently low temperatures to enable a precision determination of the low T dependence of K on T. Mezhov-Deglin stated that the behavior is approximately T^3 for the lowest temperatures investigated, but gave no error bounds; the other workers were primarily interested in Umklapp conductivity, Poisseuille flow, and the Peierls model. The latter predicts K going as a power of T times an exponential; the strong exponential dependence makes a determination of the precise power of T extremely difficult. Thus, it is fortunate that the recent calorimetric data on hcp ^{4}He provide clearcut evidence of normal Debye behavior at low T.

Note added in proof: Recent, high precision heat capacity measurements (S. H. Castles, W. P. Kirk, and E. D. Adams, *Proc. 13th Intern. Conf. Low Temp. Phys.*, Boulder, Colo., 1972, in press) to temperatures as low as $T/\theta_{max} \approx 0.005$ in the molar volume range $21.67 \leq V \leq 24.40$ cm^3/mole, have given dramatic confirmation of the low-T θ anomaly for bcc ^{3}He. These

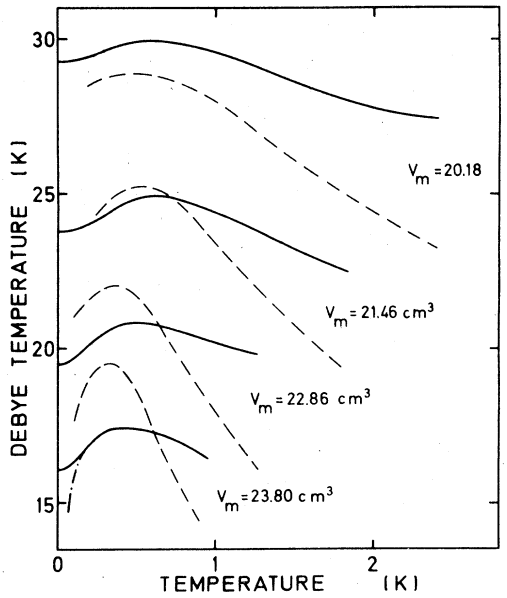

FIG. 13. Comparison of Horner's calculated $\theta(T)$ for bcc ^{3}He with experimental data of PE (1968).

results indicate that the decrease in θ is much larger than had earlier been thought, with the θ's at the lowest T's being of the order of $\theta_{max}/2$.

II.5. θ-Anomaly Mechanisms

A wide variety of mechanisms has been suggested in the search for an explication of the low T anomaly in the heat capacity of bcc ^{3}He. Swenson (1969) suggested the possibility of a Schottky anomaly caused by hydrogen impurities in the sample. The $(\partial P/\partial T)_V$ work of HPTA (1969) took quite specific precautions against such impurities by employing a 5-μ pore size metal membrane filter in a helium-temperature cold trap in the fill line; the low-temperature anomaly persisted. HPTA conjectured that the anomalous θ behavior was a lattice effect arising from a substantially greater elastic anisotropy in the bcc phase than the hcp phase. Their supposition was based on the qualitative behavior (in model fcc solids) of certain integrals which appear as coefficients in the low temperature expansion of $\theta(T)$ in powers of T. The only calculation of $\theta(T)$ available at that time was that of deWette, Nosanow, and Werthamer (1967), which, however, assumed normal Debye behavior at $T<0.5$ K on the basis of the behavior of $\theta(T)$ above that temperature, and so could not be used to test the conjecture of HPTA. A number of workers noted that the absence of a low-temperature θ anomaly seemed to be more firmly established in hcp ^{4}He than in hcp ^{3}He, and attempted to develop a theory based on properties of the ^{3}He nuclear spin system. The only published work specifically along such lines is that of Varma (1970a), who suggested that a phonon mediated indirect spin interaction would yield a specific heat contribution going as T^{-2} (later corrected to be T^{-1}; Varma, 1970b). Guyer (1970) pointed out that both the temperature and impurity-concentration dependence determined by Varma's original model were in significant disagreement with experiment. The corrected model may represent some improvement with respect to experiment, but the extreme brevity of the agrument presented in support of the correction makes comparison with experiment difficult. There are other problems with the procedures employed by Varma, (e.g., his omission of the one-phonon processes in the calculation of the indirect-spin-induced heat capacity), and it seems likely that his model does not in fact provide an adequate description of the mechanism of the θ anomaly.[2] An attempt by Guyer (1971) to develop a description of the anomaly in terms of the tunneling of fermions (as described by a Hubbard model Hamiltonian) was also unsuccessful.

The qualitative suggestion that the phenomenon was a genuine lattice effect associated with extreme elastic anisotropy (and concomitant, pronounced anharmonicity) was converted into a quantitative model by Horner (1970a), who calculated the phonon spectrum for bcc ^{3}He at four molar volumes. He employed the self-consistent harmonic approximation corrected for cubic anharmonicities, then calculated $\theta(T)$ with the aid of the usual harmonic expression. The results of his calculation are shown in Fig. 13, where they are compared with the experimental data from PE (which we first exhibited in Fig. 6). As can be seen, there is at least semiquantitative agreement. Unfortunately, there is also a difficulty. Horner employed one of the several common prescriptions for treating short-range correlations in the context of self-consistent harmonic theory: he replaced the singular interatomic potential with a t matrix. The phonon dispersion curves that resulted exhibited anomalous dispersion (especially in the low-lying transverse [110] branch), which in turn is the cause for the calculated θ anomaly. Glyde (1971) did a similar calculation, over a slightly larger molar volume range, in which he employed a Jastrow effective potential instead of a t matrix. No anomalous dispersion was found. Then, in a subsequent calculation by Glyde and Khanna (1971), the t-matrix scheme was used and anomalous dispersion was found (see also Koehler and Werthamer, 1972). Thus, it would seem that the present lattice dynamical theories are simply not sufficiently refined to resolve the question of the bcc ^{3}He θ anomaly.

Guyer (1972) has extended the idea that the low-temperature θ phenomenon is a lattice dynamical effect by linking it to the *high-temperature* anomaly which we discussed earlier. The connection was achieved with the aid of a simple, two-parameter vacancy-wave model

[2] Note, however, that Varma's idea is not without merit as a clue to a possible phenomenon of intrinsic experimental interest in solid helium. For additional work along these lines, see Meissner (1971) and Silberglitt (1969).

(Guyer, Richardson and Zane, 1971). Guyer fitted the two parameters (an activation energy and a tunneling energy for the vacancy waves) to available NMR data and found that the resulting vacancy specific heat was insufficient to account for the difference between the observed high-T values and the lattice specific heat of a "normal" solid. The "normal" solid employed by Guyer was solid argon. As we noted in our discussion of the heat capacity of hcp ^{4}He, there is a strong similarity between Ar and a form of solid He which does not behave anomalously, so that the use of Ar as a model for the lattice specific heat seems reasonably well founded. The procedure must be distinguished from that of deWW which we discussed earlier: Guyer's scheme determines a *smaller* high-temperature excess specific heat than that found by the method (3) which deWW emphasize. Despite this fact, the vacancy-wave model does not generate anything like sufficient heat capacity to explain the high-temperature θ anomaly, because of its relatively small density of states at energies corresponding to experimental temperatures. Thus, Guyer employed a more conservative estimate of the high-temperature excess heat capacity than those of either SS or deWW and a more refined vacancy model than those authors and was compelled to look for other mechanisms. His suggested alternative is that the excess heat capacity is associated with the phonons, a proposal the plausibility of which is enhanced by the fact that thermal conductivity data for bcc ^{3}He (Bertman, Fairbank, White, and Crooks, 1966), in the temperature range of interest do not seem to be compatible with a T^3 specific heat. However, Thomlinson, (1972) has questioned the basis of Guyer's interpretation of the thermal conductivity data.

After a discussion of the evidence regarding the low-T θ anomaly (much of which we have already considered at length), Guyer completed his linking of the low- and high-T anomalies by a straightforward argument regarding the temperature dependence of the excess specific heats for a system characterized by a phonon free energy plus anomalous high-temperature and low-temperature free energies. Thus, consider the Helmholtz free energy

$$A=-kT[A_P(\theta/T)+A_H(W_H/T)+A_L(W_L/T)], \tag{2.10}$$

where subscripts P, H, L refer to "phonon", "high", and "low", respectively, and W_H and W_L are characteristic temperatures for the respective anomalous contributions to the free energy. Immediately, one has for the specific heat and $(\partial P/\partial T)_V$

$$C=C_P+C_H+C_L, \tag{2.11a}$$

$$\left(\frac{\partial P}{\partial T}\right)_V=\gamma_P C_P+\gamma_H C_H+\gamma_L C_L. \tag{2.11b}$$

By appeal to the experimental data (SS, HPTA), one may then deduce that $\gamma_L\approx-(2\text{–}3)\gamma_P$ and $\gamma_H\approx-(2\text{–}3)\gamma_P$. In other words, the low- and high-temperature anomalies vanish at approximately the same rate with increasing pressure. Having thus argued that both anomalies have their origin in the lattice dynamics and that they have about the same pressure dependence, Guyer suggested that they are in fact one anomaly and should be studied as such. To date, this line of attack has not been developed further.

TABLE II. θ_0 for bcc ^{4}He as extrapolated by Edwards and Pandorf (1966). The listed error in each case is ±0.4 K.

V (cm^3/mole)	20.927	20.932	20.988	21.028
θ_0 (K)	21.2	21.1	20.95	20.8

II.6. bcc ^{4}He

To conclude this section on specific heats, we consider bcc ^{4}He briefly. About a decade ago, it was suggested (Goldstein, 1961) that the bcc phase of ^{4}He (which appears on the ^{4}He P–T diagram as a delicate sliver near the λ line) might have a negative thermal expansion coefficient. Ahlers (1964) studied the heat capacity of the phase and found $(\partial C_V/\partial V)_T<0$, in support of the prediction. Subsequently, Edwards and Pandorf (EP, 1966) reported $(\partial C_V/\partial V)_T$ to be apparently positive, but their results were not conclusive because of the uncertainty introduced by a "premelting" effect. Jarvis, Ramm, and Meyer (1968) have apparently settled the issue: they measured $(\partial P/\partial T)_V$ with strain guage techniques and found it to be positive. Since the compressibility is necessarily positive, the thermal expansion coefficient must therefore be positive also. The heat capacity work of Hoffer (1968) is in accord with this result, for he found $(\partial C_V/\partial V)_T>0$ for ^{4}He; so the predicted unusual thermal expansion behavior is not confirmed experimentally.

The value of θ for bcc ^{4}He was found by EP to be 16.95 K over the entire density range. The agreement with Debye behavior over the temperature range available to EP and Ahlers was within 3% of C_V, using the value given above for θ. It should be noted that at fixed pressure the bcc phase of ^{4}He is at most some 70 mK wide (Wilks, 1967), so that any investigation of the temperature dependence of a quantity in that phase is severely restricted. Hoffer found that $C_V\propto T^4$ approximately, but noted that this merely indicates that there are excited modes with significant dispersion at the temperatures for which the bcc phase exists. He also reported reasonable agreement with the value of θ quoted, but found that θ_0 values extrapolated from his data would be higher (by an unstated amount) than those obtained by EP (see Table II).

Alder, Gardner, Hoffer, Phillips, and Young (1968) considered the previously mentioned "premelting" phenomenon in C_V of bcc ^{4}He in terms of slipping

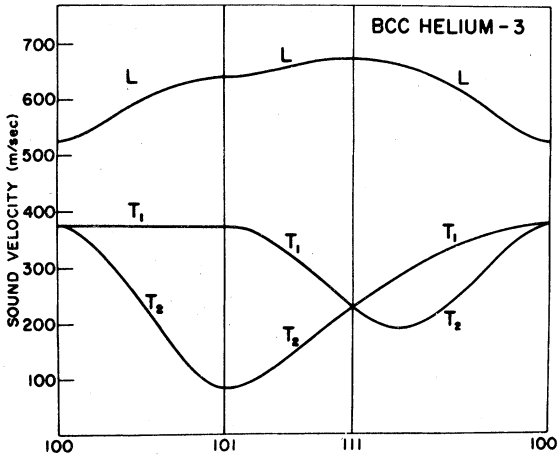

FIG. 14. Sound velocities along principle symmetry lines for single crystal bcc ^{3}He at $V=21.64$ cm^3/mole, as found by Greywall (1971a). See text regarding T_2 mode.

motion excitations found in two-dimensional molecular dynamics studies. The "premelting" manifested itself in their experiments as a smooth, very rapid increase in C_V which began about 0.02 K below the C_V discontinuity which signals the bcc-liquid transition. Ahlers (1972) subsequently re-examined the situation with high precision and concluded that "premelting" did not, in fact occur. Thus, in so far as the phase is subject to examination, the bcc phase of ^{4}He appears to have normal heat capacity characteristics.

III. SOUND VELOCITIES AND ELASTIC PROPERTIES

Experimental investigation of the velocity of sound as a function of direction in single crystals of known orientation is quite important to the understanding of a crystalline system because of the significant variety of experimental and theoretical comparisons which such a determination facilitates. Thus, there are the obvious comparisons of calculated and measured sound velocities, their density and temperature dependences, etc. Additionally, the elastic constants deduced from sound velocity measurements enable the evaluation of the experimental elastic Debye temperature, with obvious implications for the probing of θ anomalies as well as for verifying the identity in quantum crystals of the calorimetric and elastic θ_0 (Overton, 1971; Klein and Martin, 1972). The experimental sound velocities obtained directly may also be compared with those deduced from the dispersion curves generated in neutron scattering experiments.

Until quite recently, the only experimental sound velocity data available for solid helium were those of Abel, Anderson, and Wheatley (1961), Lipschultz and Lee (1965, 1967), and Vignos and Fairbank (1966). This work generated considerable interest, and no small bewilderment, for the results seemed to indicate that the bcc solid was much more nearly elastically isotropic than the hcp phase and further, that the mean sound velocity in the bcc phase was greater than that in the hcp phase, while the Debye temperatures seemed to obey the opposite inequality [see Eqs. (3.1), (3.2)]. To these enigmas we will return shortly. Before that, it is necessary to discuss recent investigations which have used single-crystal samples of known orientation and ascertainable quaility.

III.1. bcc ^{3}He Sound Velocities

The only sound velocity measurements on oriented bcc ^{3}He are those of Greywall and Munarin (1970b) and Greywall (1971a). All the measurements were made at $T=1.2$ K (Greywall, 1971b) and a single molar volume, 21.64 cm^3/mole, with orientation by x-rays. A least-squares fit to their velocity data produced the reduced adiabatic elastic constants:

$$c_{11}/\rho=2.71(\pm0.001)\times10^9 \text{ cm}^2/\text{sec}^2,$$

$$c_{12}/\rho=2.59(\pm0.06)\times10^9 \text{ cm}^2/\text{sec}^2,$$

$$c_{44}/\rho=1.42(\pm0.01)\times10^9 \text{ cm}^2/\text{sec}^2.$$

From these moduli the sound velocities in principal symmetry directions and lines joining them were determined as shown in Fig. 14. It is to be noted that the low-velocity transverse mode (T_2) was calculated from the data obtained in the T_1 and L modes, since Greywall was unable to propagate very soft shear waves particularly near [101].

Greywall calculated the elastic θ_0 from his elastic constants at $T=1.2$ K by means of known relations (Fedorov, 1968) between the elastic constants and propagation velocities in an arbitrary direction and numerical integration of the factor

$$I=(4\pi)^{-1}\int(v_L^{-3}+v_{T_1}^{-3}+v_{T_2}^{-3})\,d\Omega \qquad (3.1)$$

which appears in the expression for the elastic Debye temperature at $T=0$ K,

$$\theta_0=(\hbar/k)(18\pi^2N/V)^{1/3}I^{-1/3}. \qquad (3.2)$$

The result was $\theta_0^{el}=19.5K$ $(+2K, -3K)$ at $V=21.64$ cm^3/mole, with the large uncertainty a consequence of the indeterminancy in the quantity $(c_{11}-c_{12})/2$ which determines the velocity of the T_2 mode along [101]. This value of θ_0^{el} fits very nicely into the interpretation[3]

[3] A very unfortunate misunderstanding has clouded this interpretation. Neither the preliminary report (GM, 1970b) nor the detailed paper by Greywall (1971a) gave an explicit value for the sample temperature. When the initial report of the work was published, Trickey and Adams (TA, 1970) became concerned about the possible effects any temperature dependence in the c_{ij} might have on θ_0^{el}. Based on the information extant at the time (the system working pressure and sample molar volume), they deduced a probable sample temperature in the vicinity of 1.7 K and pointed out that, because of the double-valuedness of $\theta(T)$ and the known temperature dependence of the volume compressibility, there might well be some doubt as to whether θ_0 or θ (1.7) had been found by GM. The actual sample temperature (Greywall, 1971b) was $T=1.2$K (a fact which, regrettably, TA were not able to ascertain from two private communications with GM), so the possible difficulty pointed out by TA did not actually occur.

of the low-temperature bcc ^{3}He θ anomaly as a lattice dynamical effect, for it lies at the end point of a very plausible extrapolation of the calorimetric data (recall Fig. 6).

The elastic constants for bcc ^{3}He indicate that it is highly anisotropic elastically, for the anisotropy factor is

$$A = 2c_{44}/(c_{11}-c_{12}) = 23.6 \qquad (3.3)$$

at $V = 21.64$ cm^3/mole. This large anistorpy has some very interesting experimental consequences which were first pointed out by Wanner (1971). The usual experimental arrangement in sound velocity measurements has a transducer mounted in one wall of the sample cell. Now, the emitted sound beam will not, in general, propagate along a trajectory which is perpendicular to the plane of the transducer producing the sound, but along one which makes some angle Δ_i between the wave normal and the beam direction. The value of Δ_i depends on the wave normal direction and upon the polarization (Musgrave, 1959). Because of this, unless the sound cell has been designed with great care, only a limited range of directions of propagation will be seen (even if any desired orientation of the crystal can be achieved). A typical configuration of the cell is such that unless the angle Δ_i is $\leq 15°$ the beam will miss the receiver entirely and the mode "i" will not be observed.

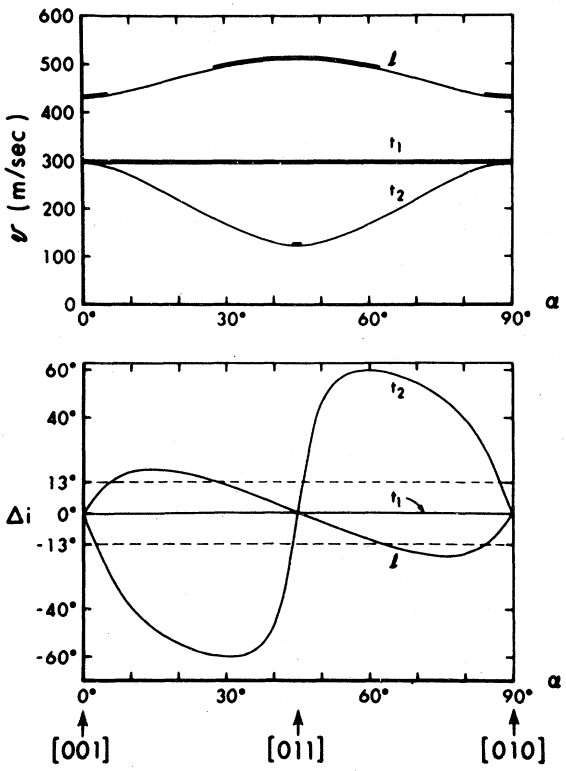

FIG. 15. Longitudinal (l) and transverse (t) sound velocities and beam deviation (from the wave normal) angles Δ_i for different directions α, as computed by Wanner (1971) for bcc ^{3}He with typical elastic constants (see text). Wave normal is in the (100) plane, with α the angle between [001] and the wave normal. For a sample chamber which requires $|\Delta_i| < 13°$ only those velocities indicated by the thicker curve are observable.

TABLE III. Elastic constants for bcc ^{3}He deduced by Wanner (1971) from sound velocity measurements on unoriented crystals in combination with compressibility and θ_0 data. Estimated uncertainty: $\pm 5\%$.

V (cm^3/mole)	c_{11}	c_{12} (10^8 dyn/cm^2)	c_{44}
23.8	2.43	2.05	1.16
23.84	2.44	2.03	1.08
24.06	2.32	1.94	1.05
24.28	2.22	1.86	1.03
24.40	2.17	1.81	1.00

In view of these considerations and the large elastic anisotropy of bcc ^{3}He, Wanner was struck by the apparent isotropy of the transverse velocities found, as we have remarked, in the early work of Lipschultz and Lee (LL, 1967). With $c_{11} = 2.35\times10^8$ dyn/cm^2, $c_{12} = 1.97\times10^8$ dyn/cm^2, and $c_{44} = 1.085\times10^8$ dyn/cm^2 as reasonable values for the adiabatic elastic moduli at $V = 24$ cm^3/mole, Wanner found that sound emitted from the LL transducer with $|\Delta_i| > 13°$ would completely miss the receiver. Figure 15 shows the consequences of this constraint for sound with wave normal in the (100) plane: the T_2 mode is virtually unobservable. An extension of this sort of analysis to a large number of directions (200) in the crystal led Wanner to the conclusion that the transverse data of LL were in fact almost entirely for the T_1 mode. This fact, plus a knowledge of the compressibility K_0 and of θ_0 is sufficient to determine a consistent set of independent elastic moduli, since

$$v_{T_1} = (c_{44}/\rho)^{1/2}, \qquad (3.4a)$$

$$K_0 = -V^{-1}(\partial V/\partial P)_T = 3/(c_{11}+2c_{12}), \qquad (3.4b)$$

and θ_0 is connected to the velocities through Eq. (3.2). A computer fit was generated by varying c_{11} and c_{12} consistently with the measured compressibility (Straty and Adams, 1968; PE, 1968) and θ_0 (taken to be θ_0^{SS}; see Sec. II), for five molar volumes between 23.8 and 24.4 cm^3/mole (see Table III).

With a set of consistent elastic constants, Wanner was able to explicate the two enigmas mentioned at the outset of this section. One puzzle was that $v_{bcc}^{obs} > v_{hcp}^{obs}$ while $\theta_0^{bcc} < \theta_0^{hcp}$ (inequalities are for approximately the same pressure). This pair of inequalities clearly contradicts Eq. (3.1). The explanation is that the apparatus used in the early measurements selectively sampled only the higher velocities in the bcc phase because of the very large Δ_i associated with the lower ones, while in the hcp system the various Δ_i are smaller and a better sample of the velocities is obtained. The other enigma was the apparent high elastic isotropy of the bcc phase with respect to the hcp, especially for the transverse modes. The resolution is quite ironic, for Wanner's

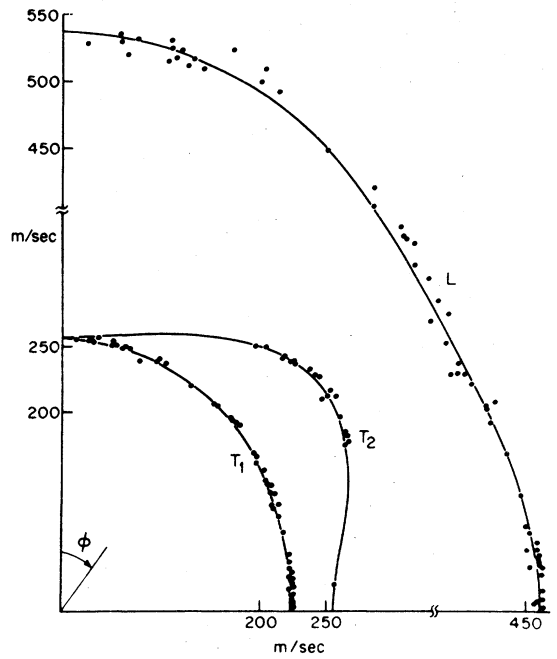

FIG. 16. Polar plot of sound velocities in hcp ^{4}He as a function of the angle ϕ between the propagation direction and the crystalline c axis, $V=20.97$ cm^3/mole. (After Crepeau *et al.*, 1971.)

analysis makes clear that the apparently small elastic anisotropy of bcc ^{3}He was a consequence of its actually large anisotropy, which, as noted, caused a misleadingly small selection of the bcc velocities to be sampled.

The results of the same sort of analysis applied to the bcc velocities obtained by GM (1970b) are of interest, for their elastic moduli generate beam deviations $\Delta_L \geq 20° \pm 1°$ for a few points near the [100] direction. The sample cell geometry employed by GM restricted their observations to waves for which $\Delta_L \lesssim 17°$. Wanner therefore argued that the elastic moduli uncertainties quoted by GM might have to be increased in order to reconcile the calculated and experimental beam deviations. Such an alteration would increase $(c_{11}-c_{12})$ and hence, θ_0^{el}. The magnitude of the alteration was not estimated, though Wanner did comment that high precision measurements in the [110] direction of v_{T2} $(=[(c_{11}-c_{12})/2\rho]^{1/2})$ would be most useful. Given the problems Greywall encountered (recall discussion above) in this connection, Wanner's comments as to the difficulty of such measurements would seem to be well founded.

III.2. hcp ^{4}He Sound Velocities

In the past two years, the results of several studies on oriented single crystals in hcp ^{4}He have been reported. Optical birefringence was used by Wanner and Franck (WF, 1970) and by Crepeau, Heybey, Lee and Strauss (CHLS, 1971) to determine the direction of the "c" crystallographic axis. Since the acoustic propagation velocity in an hcp crystal is a function only of the angle ϕ between the wave normal and the c axis, only the orientation of the c axis need be determined. An extensive discussion of their optical techniques can be found in the paper by CHLS. Greywall and Munarin (1970a) and Greywall (1971a) employed x-ray scattering to determine the orientation and quality of their crystal samples. WF and GM reported longitudinal velocities only, while CHLS and Greywall investigated both transverse and longitudinal polarizations.

The uncertainties in orientation quoted by WF are $\pm 5°$ at $\phi=45°$, $\pm 10°$ at $\phi=10°$ or 80°. By comparison, GM quote $\pm 2°$, independent of ϕ. In addition to the superior determination of orientation, the x-ray technique provides a rather stringent test of crystal quality. Thus, GM rejected almost as many crystals as they used because characteristic features of crystalline defects appeared in the Laue photographs. GM further noted that the visual clarity of the crystalline samples was no indicator of their quality since excellent and poor samples alike were totally transparent.

A typical set of experimental results for hcp ^{4}He is exhibited in Fig. 16. The curves fitted to those data were obtained from best fit elastic constants, about which we will say more later. The peculiar angular distribution of experimental points in the T_2 mode is another feature to which we will return. The molar volume dependence of these velocities is shown in Fig. 17, along with the calculated results due to Gillis, Koehler, and Werthamer

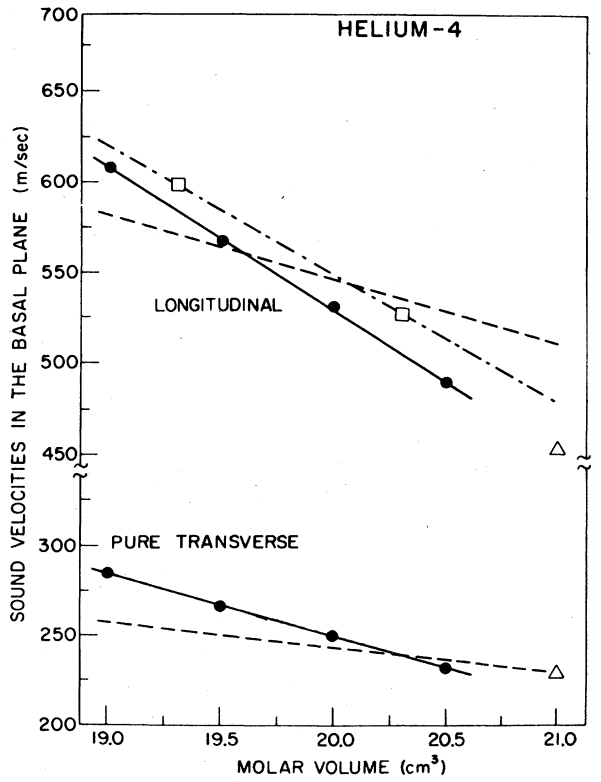

FIG. 17. Molar volume dependence of sound velocities in hcp ^{4}He. Solid dots: Greywall (1971a). Open squares: Wanner and Franck (1970). Open triangles: Crepeau *et al.* (1971). Dashed curves: theory of Gillis *et al.* (1968).

TABLE IV. Reduced elastic constants of hcp ^{4}He. Units: V, cm^3/mole; c_{ij}/ρ, 10^9 cm^2/sec^2. Source of the determination listed in first column. For sources of original sound velocity data, see text. Percent uncertainties in parentheses.

Source	V	c_{11}/ρ	c_{33}/ρ	c_{44}/ρ	c_{12}/ρ	c_{13}/ρ
FW	19.28	3.66(4)	4.72(4)	0.944(4)	2.02(4)	0.954(4)
FW	20.32	2.79(4)	3.60(4)	0.711(4)	1.47(4)	0.665(4)
GM	20.5	2.39($\frac{1}{2}$)	3.1(4)	0.941($\frac{1}{2}$)	1.34($\frac{1}{2}$)	0.64(20)
CHLS	20.97	2.12(1)	2.90(4)	0.652(2)	1.11(2)	0.549(12)

(1968). As WF have remarked, the density dependence predicted by the theory is clearly inadequate. This point was discussed extensively by Gillis *et al.*, who predicted precisely the result shown in Fig. 17, to wit: a fortuitous concordance of theory with experiment at some molar volume between the ends of the range treated computationally.

For an ideal hcp system, there are five independent elastic constants: c_{11}, c_{12}, c_{13}, c_{33}, c_{44}. Of these, only the determination of c_{12} requires knowledge of the velocity in the transverse mode; the other four c_{ij} can be determined, in principle, from the longitudinal velocities (Musgrave, 1959). In the absence of transverse velocity measurements, Franck and Wanner (FW, 1970) have found a way to escape from this dilemma and determine all five of the c_{ij} by showing that in fact only four of them are independent for a hexagonal crystal whose axis ratio, c/a, is independent of pressure. They cite a substantial body of birefringence, x-ray, and neutron diffraction data to substantiate their claim that

$$|\, d \ln (c/a)/dP \,| \lesssim 5\times 10^{-12}\ \text{cm}^2/\text{dyn}. \qquad (3.5)$$

FW then proved for a hexagonal crystal with pressure-independent c/a that

$$c_{12}=c_{33}+c_{13}-c_{11} \qquad (3.6)$$

and that as a consequence the zero-temperature volume compressibility K_0 reduces to

$$K_0=3/(c_{33}+2c_{13}). \qquad (3.7)$$

The existence of Eq. (3.7) enabled FW to avoid having to rely on longitudinal sound velocities exclusively, a reliance which, given the precision of present sound velocity data, would have significantly impaired the precision of the derived elastic constants. Thus, the sequence of determinations used by FW was: (a) extraction of c_{11} and c_{33} from longitudinal velocities in the basal plane and along the c axis respectively; (b) solution of Eq. (3.7) for c_{13}, with values of K_0 from Jarvis, Ramm, and Meyer (1968); (c) determination of c_{44} from the longitudinal sound velocity at $\phi=45°$ and the previously ascertained c_{11}, c_{13}, c_{33}; (d) determination of c_{12} from Eq. (3.6). The velocity data of WF were treated by this procedure to extract the reduced elastic constants at $V=19.28$ and 20.32 cm^3/mole given in Table IV. The results displayed in Table IV due to CHLS ($V=20.97$ cm^3/mole) were found by a computer fit of the analytic expressions given by Musgrave (1959) to both longitudinal and transverse velocities. Greywall (1971a) determined c_{11}, c_{33}, c_{44}, and c_{12} [actually $c_{66}=(c_{11}-c_{12})/2$] from sound velocities at 20.5 cm^3/mole, then, because of some intrinsic limitations in his data, used Eq. (3.6) to find c_{13}. Note that the CHLS work was at 1.32 K and that of GM and of Greywall at 1.2 K (Greywall, 1971b), while the experimental temperature was not reported by WF. In Fig. 18 we show elastic θ_0 values calculated from Eqs. (3.1) and (3.2) as well as calorimetric values for comparison. It should be noted that Greywall's θ_0 values at molar volumes other than 20.5 cm^3/mole are extrapolations from the θ_0 he found at the latter density. His extrapolation procedure was obtained from the empirically observed nearly linear dependence of basal plane and c-axis sound velocities on the molar volume. The relation he used was

$$\theta_0(V)=[(27-V)/6.5]\theta_0(V=20.5). \qquad (3.8)$$

It is evident that the elastic and calorimetric θ_0 values are quite close throughout the molar volume range. Thus, as was first pointed out by FW, the identity of the

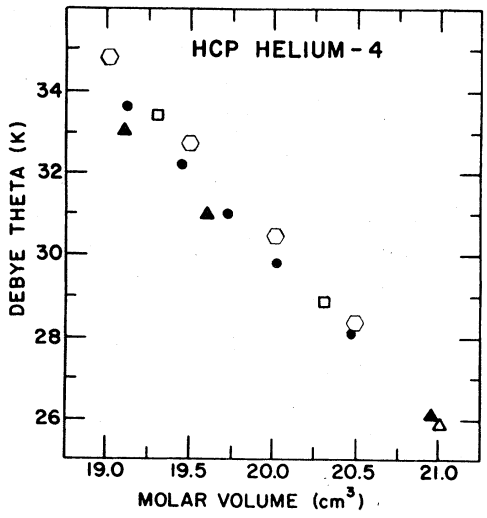

FIG. 18. Elastic and calorimetric θ_0 for hcp ^{4}He as a function of molar volume. Open hexagons: Greywall (1971a). Open squares: Franck and Wanner (1970). Open triangles: Crepeau *et al.* (1971). Solid circles: Ahlers (1970). Solid triangles: Edwards and Pandorf (1965).

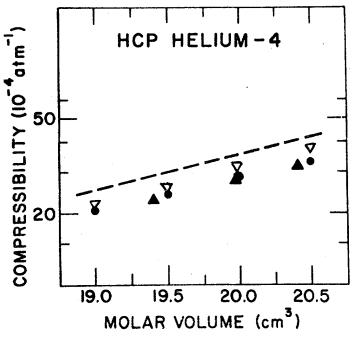

FIG. 19. Comparison of hcp ^{4}He compressibilities as determined from sound velocity (Greywall, inverted triangles), strain gauge (Jarvis *et al.*, solid triangles), and calorimetric (Edwards and Pandorf, solid circles) measurements. Dashed line is theory by Horner (see text).

zero-temperature elastic and calorimetric Debye temperatures seems to hold for hcp ^{4}He, a quantum crystal, just as in more familiar solids.

Greywall (1971a) employed the same extrapolation technique, Eq. (3.8), to study the molar volume dependence of the bulk compressibility in hcp ^{4}He as he had used to investigate θ_0. Thus, he used Eq. (3.7) at $V=20.5$ cm^3/mole, then extrapolated downward in molar volume to the results shown in Fig. 19. The comparisons presented there are to calorimetric (EP, 1965) and strain gauge data (Jarvis, *et al.*, 1968) and to a perturbation calculation due to Horner (1970b). It should be noted that Eq. (3.8) must be used with caution. For example, Greyweall found that the Grüneisen parameters obtained from Eq. (3.8) did not agree well with those determined by Ahlers (1970).

The same sort of beam deviation analysis as Wanner's has recently been applied by Crepeau and Lee (1972) to the hcp ^{4}He data of CHLS. They find that the maximum allowable Δ (17° for their chamber) is exceed by sound in the T_2 mode for polar angles (with respect to the c axis) of propagation in the ranges $17°\leq\phi\leq32°$ and $60°\leq\phi\leq80°$. Reference to Fig. 16 shows that these angular regions are those in which T_2 data were absent in the experiment by CHLS. Thus, the peculiar angular distribution of the T_2 data in hcp ^{4}He which we mentioned earlier is a consequence of anisotropy-induced beam deviations. Though the angular distribution is different in Greywall's hcp ^{4}He data, it would appear that a similar phenomenon occurred. No calculations in confirmation of this conjecture have appeared, however.

III.3. Neutron Scattering in ^{4}He

A fundamentally different means, with respect to those methods so far discussed, of probing the lattice dynamics of a solid is the technique of inelastic neutron scattering. Because of the large neutron capture cross section in ^{3}He, neutron spectrometry is restricted to the study of the various crystallographic phases of ^{4}He, all three of which (hcp, bcc, fcc) have now been investigated to some degree of thoroughness. The work has all been done at Brookhaven (Lipschultz *et al.*, 1967, on hcp; Minkiewicz *et al.*, 1968, on hcp; Osgood *et al.*, 1972, on bcc) and Iowa State (Reese *et al.*, 1971, on hcp; Traylor *et al.*, 1971, on fcc), the appellations which we shall, for convenience, use henceforth. (An investigation of polycrystalline hcp ^{4}He has also been reported: Bitter *et al.*, 1967.) In Table V we give a summary of the neutron scattering experiments which have been reported to date on single crystals of helium. Additional work on the bcc phase is in preparation for publication by the Brookhaven group.

The picture of the hcp phase which has emerged from these investigations is, on the whole, that of a rather surprisingly normal solid. In Figs. 20–22 we present the Brookhaven (1968) dispersion curves for 21.1 cm^3/mole, and the dispersion curves calculated by Gillis, Koehler, and Werthamer (1968) by means of the basic self-consistent harmonic theory with a Jastrow function treatment of the short-range correlations. Though the agreement of theory with experiment is certainly not optimum, it is rather good in view of the absence of adjustable parameters and the *ad hoc* treatment of short-range correlations. The phonons were quite well defined (i.e., the neutron profiles exhibit a readily identifiable peak and a width which is not large compared to the spectrometer resolution), except for observable broadening of the longitudinal optical groups along $[10\bar{1}0]$ rather far from the zone center. Similar behavior was found by the Iowa State workers (1971) at 16.0 cm^3/mole; Fig. 23 gives some of their results for full linewidths at half-maximum for longitudinal phonons along the symmetry direction Δ (crystalline c axis). Clearly, the higher frequency

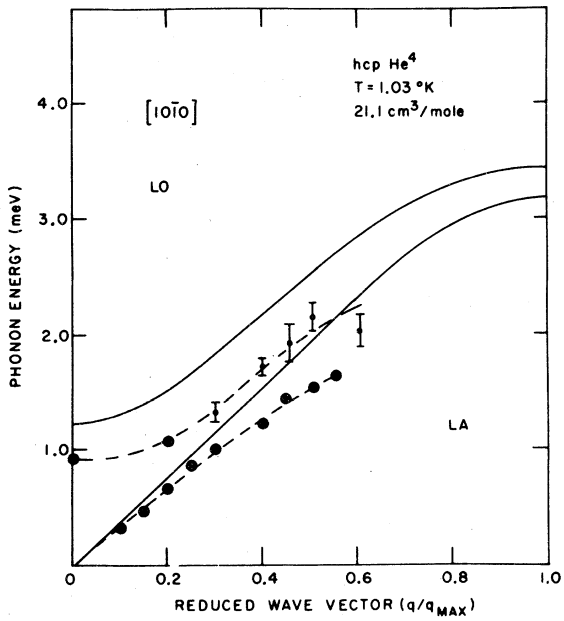

FIG. 20. Dispersion curve for neutron scattering along $[10\bar{1}0]$ in hcp ^{4}He at 21.1 cm^3/mole. Longitudinal polarization. Solid curves are theoretical results of Gillis *et al.* (1968). (After Minkiewicz, *et al.*, 1968).

TABLE V. Summary of inelastic neutron scattering experiments on single crystals of ^{4}He. B: Brookhaven; I: Iowa State.

Group	V (cm^3/mole)	T(K)	Phase	Directions observed
B(1967)	21.1(±0.01)	0.99(±0.05)	hcp	[10$\bar{1}$0]
B(1968)	21.1(±0.01)	1.03(±0.09)	hcp	[10$\bar{1}$0], [0001]
I(1971)	16.02(±0.03)	4.2(±0.1)	hcp	[10$\bar{1}$0], [0001], [11$\bar{2}$0]
B(1972)	21.06(±0.06)	1.620(±0.005)	bcc	[100], [111], [011]
I(1972)	11.72(±0.3)	15.5(±0.25)	fcc	[100], [110]

groups do not correspond to well-defined excitations. An even more pronounced instance of ill-defined excitations was found by the Iowa group while searching for transverse optical modes of perpendicular polarization along [10$\bar{1}$0]. The anomalously broad groups which they encountered are shown as shaded areas in Fig. 24 (note that the TA and TO parallel branches along [10$\bar{1}$0] in that figure were obtained by scaling from the 1968 Brookhaven results). No satisfactory explanation of this phenomenon has been given, though Ruvalds (1971) has suggested a two-phonon resonance as a likely possibility.

For the purpose of calculating the phonon spectrum and Debye temperature, the Iowa group fitted an 18 parameter harmonic force constant model to the results shown in Fig. 24. In the present context, their most interesting result is the extraction of θ_0^{el} as 47.2 K for $V=16.0$ cm^3/mole. The calorimetric value found by Ahlers (1970) can be seen from Fig. 4 to be about 52 K. A similar comparison with θ_0^{el} from sound velocities is also available, as a consequence of the extrapolation formula Greywall (1971a) devised from his data. Thus, we have from sound velocities, via Eq. (3.8), $\theta_0^{el}=47.9$ K at $V=16$ cm^3/mole, though the agreement of this value with the others may be somewhat fortuitous in view of the previously noted limitations associated with Eq. (3.8). (In a private communication to SBT, Sinha has reported that the force constants found by the Iowa group were $c_{11}=19.4$, $c_{12}=12.4$, $c_{33}=26.0$, $c_{44}=5.3$, $c_{66}=3.5$, and $c_{13}=4.76$, all in dynes/cm^2.)

The results of inelastic neutron scattering from fcc ^{4}He are quite similar to those for the hcp phase. The [100] and [110] symmetry directions were probed by the Iowa State workers (Traylor *et al.*, 1971) and, as can be seen from Fig. 25, definition of the phonon peaks deteriorated with increasing frequency. At the highest frequencies, no well-defined phonon peaks were detected. The comparison with theory given in Fig. 25 is for a calculation due to Horner (1971) which used the self-consistent harmonic approximation corrected with the leading component of the lowest order anharmonicity and a t-matrix treatment of the short-range correlations. A comparison with a sequence of increasingly sophisticated self-consistent phonon calculations by Goldman, Horton, and Klein (1970) is also possible in the [100] direction (Fig. 26). The results are easy to summarize: (1) the plain self-consistent harmonic calculation gives frequencies which are everywhere too large (by as much as 25% at the zone boundary); (2) the inclusion of leading anharmonic corrections reduces the frequencies significantly below the experimental values with anomalous dispersion at small wave vectors; (3) the anharmonic treatment including the full lowest order anharmonicity contribution gives frequencies

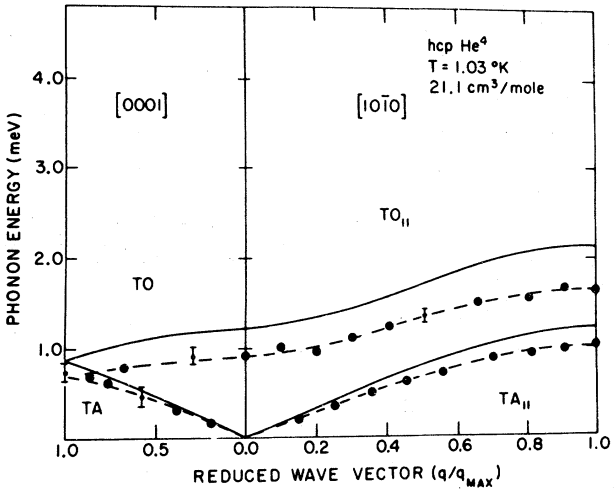

FIG. 21. As in Fig. 20 for transverse modes along [0001] and [10$\bar{1}$0].

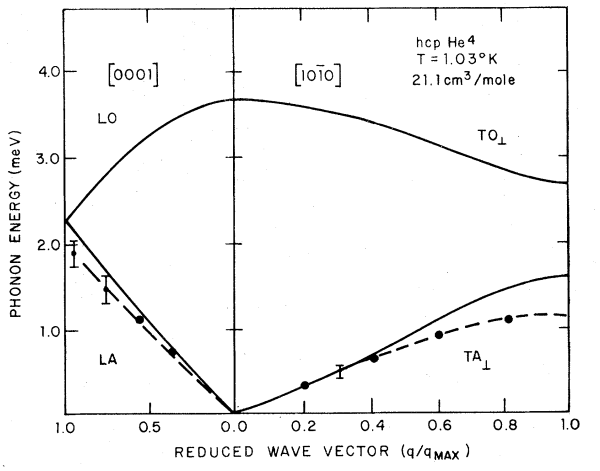

FIG. 22. As in Fig. 20 for transverse modes along [10$\bar{1}$0], and longitudinal modes along [0001].

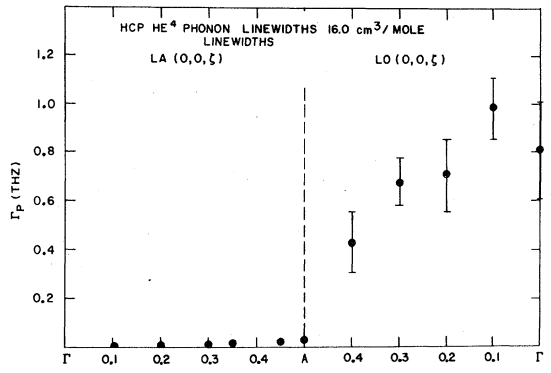

FIG. 23. Phonon linewidths (natural full width at half-maximum) for longitudinal branches along [0001] in hcp ^{4}He at 16 cm^3/mole. (After Reese, *et al.*, 1971).

which are too high by at most 10% at the zone boundary. Since calculation (2) of Goldman *et al.* is the same as Horner's except for the use of a cutoff radius to handle short-range correlations, it is evident once again that interpretation of experimental features using these theories in their present state is a very delicate matter. In a private communication (to SBT, 1972), Sinha has reported the accumulation of [111] transverse data on the fcc phase, again at 11.7 cm^3/mole. He also reported that revised, unpublished calculations by Horner are in better agreement with the fcc data than those shown in Fig. 25.

The most unusual results to come out of neutron scattering experiments on solid ^{4}He have been associated with the bcc phase. The Brookhaven group (Osgood *et al.*, 1972) has measured the dispersion curves along the [100], [111], and [011] principal symmetry directions, with the results shown in Fig. 27. The agreement with the theoretical curve (Glyde, 1970) is probably fortuitous at least in part, since anharmonic corrections introduce noticeable discrepancies. Only a hint of unusual behavior is evident in the dispersion curves; the frequency of the longitudinal branch at the zone boundary in the [100] direction is startlingly high. The situation becomes manifestly strange when the neutron profiles for the L[100] branch are examined. These are displayed in Fig. 28 as a function of the reduced scattering momentum transfer vector $\mathbf{Q}/a^*$ ($a^* = 2\pi/a = 1.525$ Å^{-1}). A comparison of line shapes and uncorrected intensities for first zone and second zone scattering forces the unfamiliar conclusion that equivalent positions have non-equivalent phonon profiles. That the second zone peaks in the vicinity of $Q = 1.6a^*$ should be more intense than those associated with geometrically equivalent positions in the first zone is particularly remarkable, since usual behavior for the Debye–Waller factor would cause the second zone peak to be less intense than the corresponding one in the first zone. A quantitiative comparison of the intensities is possible by use of the one-phonon sum rule (Ambegaokar, Conway, and Baym, 1965) making suitable assumptions about background. The result is a "scaled intensity" which should be independent of Q and be dependent only on spectrometer characteristics. Conventional behavior occurs for $Q < 1.3a^*$ and $Q > 1.7a^*$; in the region about $Q \approx 1.6a^*$ there is as much as four times the expected intensity.

The Brookhaven group described a number of experimental precautions and cross checks to make sure that their results were not a manifestation of an experimental artifact. They produced evidence to show that the phenomenon was unlikely to be due to: (1) contributions from the empty sample cell; (2) scattering from the roton minimum in some unsuspected residual liquid ^{4}He in the sample chamber; (3) scattering from some hcp solid in the sample chamber. They speculated on several possible mechanisms (vacancy formation,

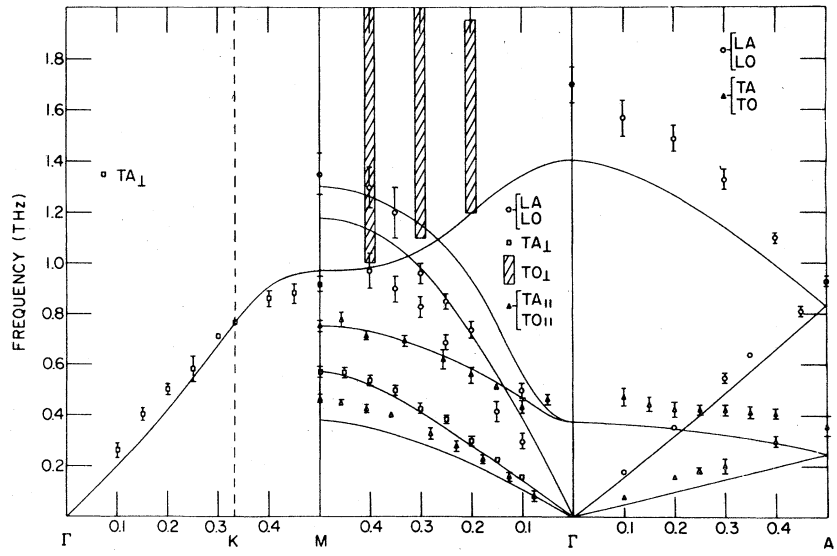

FIG. 24. Dispersion curves for hcp ^{4}He at 16.0 cm^3/mole and calculations of Gillis *et al.* (1968). (After Reese *et al.*, 1971).

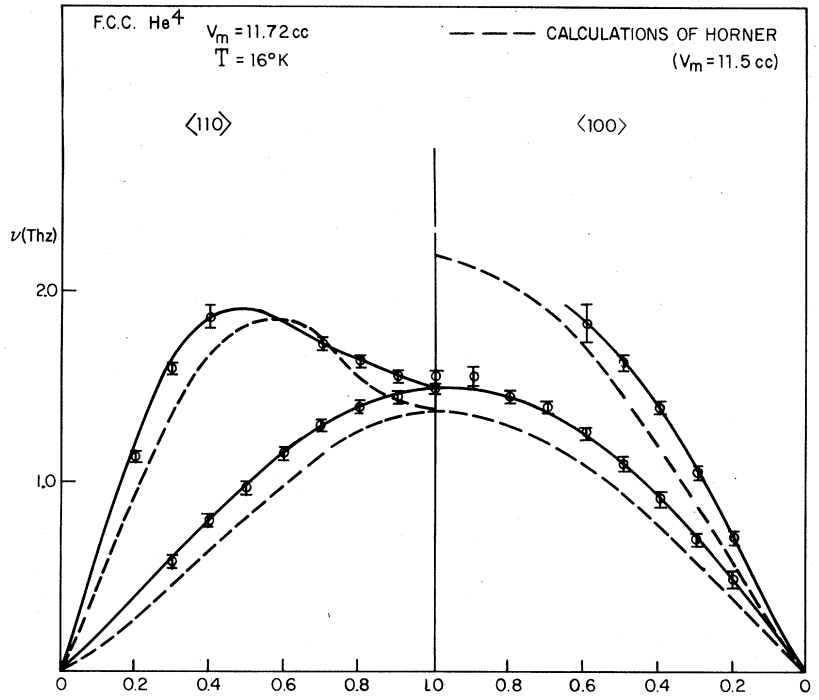

FIG. 25. Dispersion curves for fcc ^{4}He at 11.72 cm^3/mole together with calculated results of Horner (1971). (After Traylor *et al.*, 1971).

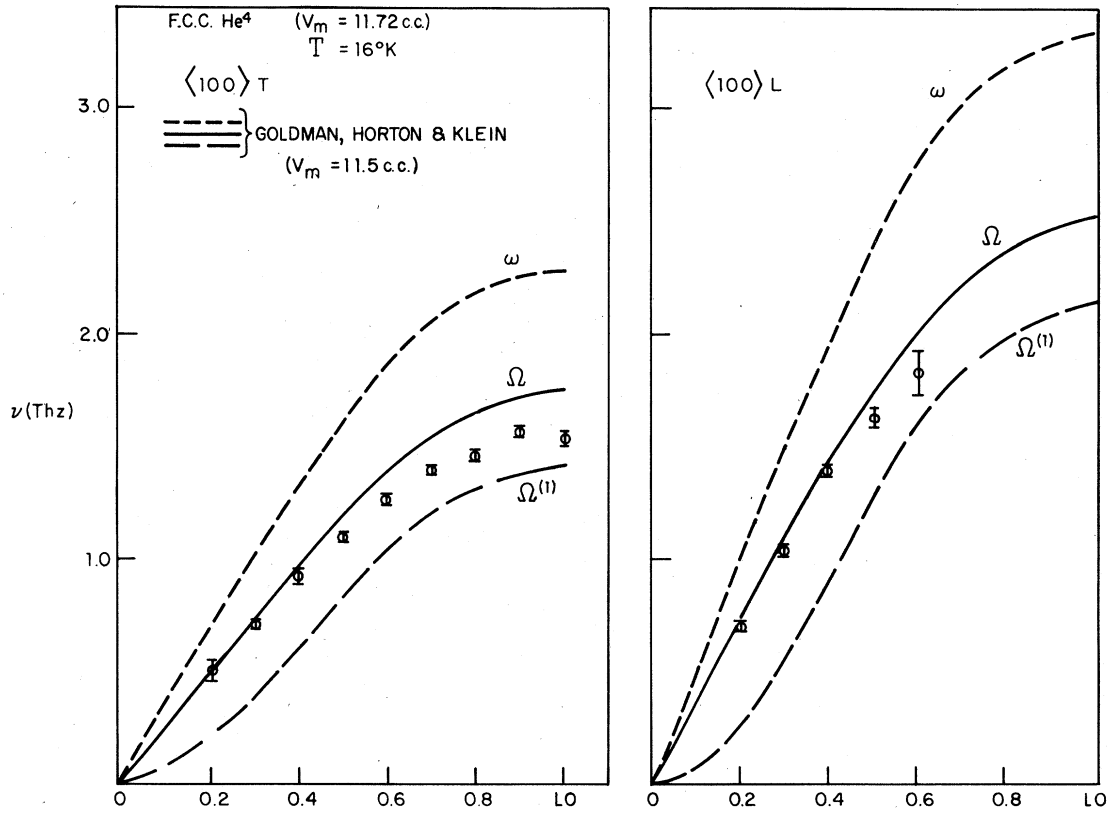

FIG. 26. Comparison of fcc ^{4}He experimental dispersion curve along [100] with three calculations by Goldman *et al.* (1970). See text for details. (After Traylor *et al.*, 1971).

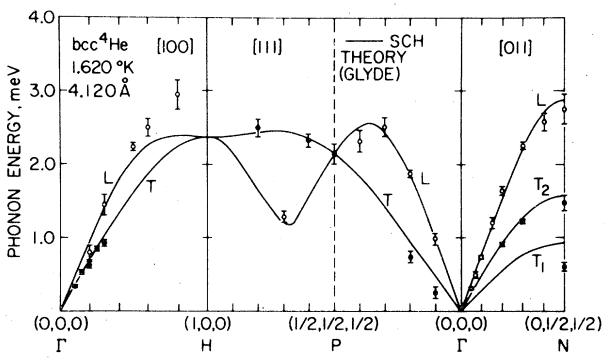

FIG. 27. Experimental dispersion curves for bcc ^{4}He. Solid dots: transverse branches. Open circles: longitudinal branches ($V=21.0$ cm^3/mole). Solid curve: calculation by Glyde (1970). (After Osgood *et al.*, 1972).

vacancy excitation, a rotonlike excitation, severe deviation from orthodox Debye–Waller character) but did not have sufficient information to determine a likely choice among them. Werthamer (1972) considered the effective Debye–Waller factor that arises from the one-phonon sum rule and accordingly replotted the scaled intensity as shown in Fig. 29. The excess intensity is present in the region $Q=2.1$ Å^{-1}, but an unsuspected feature has also appeared, namely, the suggestion of a dip below the usual Debye–Waller factor in the vicinity of $Q=1.2$ Å^{-1}. Werthamer noted that such behavior bears a startling resemblance to the experimental effective Debye–Waller factor for superfluid ^{4}He (Cowley and Woods, 1971) as is shown in Fig. 29. He thus raised the question of the possibility of the solid ground state having a structure much like that of the superfluid liquid (away from the long-wavelength, low-momentum transfer acoustic region). McMahan and Guyer (1972) have, in turn, questioned Werthamer's conjecture on the grounds that an oscillatory Debye–Waller factor (such as that for superfluid ^{4}He) leads, in the solid, to unphysical, negative values of the single particle density in the region of the radial coordinate around 2 Å. At this writing, the entire problem is quite unsettled, without even a clearcut qualitative understanding being available.

Note added in proof: It now seems that the "anomalous intensity" results from an inappropriate identification of the "one-phonon" contribution to the experimental scattering function. The difficulty results from the existence of a long, high-frequency tail to the calculated one-phonon lineshape. This cannot be distinguished from the experimental background in any systematic way. Further, there is no way to remove from the experimental line shape the contributions (arising from the coupling due to cubic anharmonicities) due to the interaction of the one- and two-phonon processes. In consequence, no reliable experimental identification of the one-phonon scattering function as defined in the one-phonon sum rule (Ambeqaokar, *et al.*, 1965) is possible. See V. F. Seans and F. C. Khanna, (Phys. Rev. Letters **29,** 549, 1972) and H. Horner (Phys. Rev. Letters **29,** 556, 1972; *Proc. 13th Intern. Conf. Low Temp. Phys.*, Boulder, Colo., 1972, in press).

IV. EXCHANGE ENERGY AND NUCLEAR MAGNETIC PROPERTIES OF SOLID ^{3}He

Among the fundamental properties possessed by a ^{3}He atom is a *nuclear* spin $I=\frac{1}{2}$ and a magnetic moment $\mu=1.07\times10^{-23}$ erg/G or $-2.12\mu_N$ (μ_N=nuclear magneton). Solid ^{3}He is found to be the simplest known Fermi solid which displays explicit nuclear spin statistics effects in many aspects of its magnetic and thermodynamic behavior. The relative simplicity of this solid also makes it very appealing for theoretical study.

At high temperatures, T, the nuclear spin system is completely disordered, giving a contribution to the entropy of $S=R\ln(2I+1)=R\ln 2$. Eventually S must decrease as T is reduced; thus, at some transition temperature T_c, ordering of the *nuclear* spin system will occur. Pomeranchuk (1950) first showed that a dipole–dipole interaction energy, $\sim\mu^2/(\text{atomic spacing})^3$, in

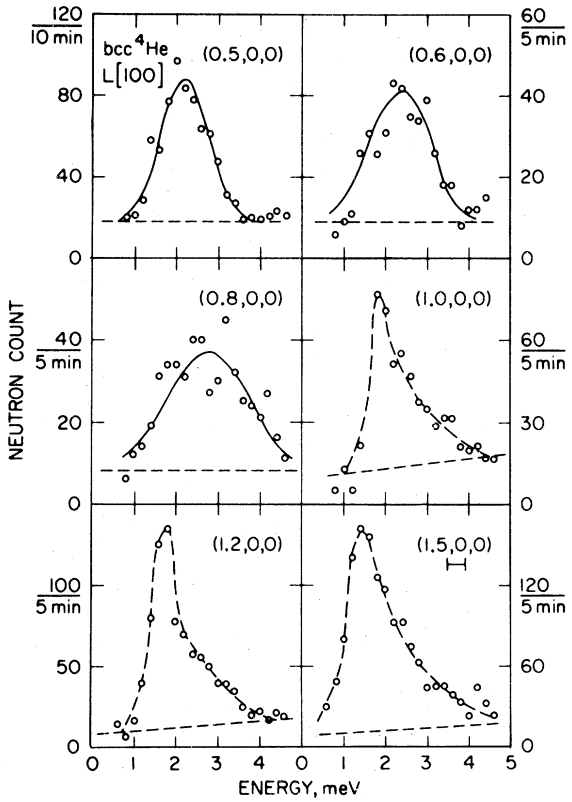

FIG. 28. A selection of phonon lineshapes for bcc ^{4}He along the L[100] branch. Values of Q/a^* ($a^*=2\pi/a=1.525$ Å^{-1}), the reduced scattering vector, as shown in parentheses. Dashed straight lines: estimated background. Solid curves: Gaussian fit to data. Dashed curves: "eyeball" fit to data. Instrumental resolution (full width at half-maximum) is indicated just below the scattering coordinate (1.5, 0, 0). (After Osgood *et al.*, 1972).

^{3}He would lead to a $T_c \simeq 10^{-7}$ K. Such an exceedingly low temperature would present serious problems for laboratory investigations.

What is remarkable in solid ^{3}He is that the effective interaction energy between magnetic moments E_{int} is much larger (three to four orders of magnitude) than the typical dipole–dipole interaction found in the nuclear spin systems of other solids. Thus, in contrast to Pomeranchuk's calculation, Bernardes and Primakoff (1960) pointed out that, in addition to a dipole–dipole interaction energy, there will be a contribution to E_{int} from the quantum-mechanical exchange energy, J, which is a simple consequence of using an antisymmetric wavefunction for Fermi particles. Furthermore, J can be large (in magnitude) compared to the dipole–dipole energy because of the large zero point motion of the ^{3}He atoms ($\approx 30\%$ of the nearest-neighbor distance; see Guyer, 1969) and consequent sizable overlap of the wave functions of neighboring atoms. The degree of overlap is a measure of the probability of exchanging neighboring atoms and hence effectively determines the size of J. Although Bernardes and Primakoff greatly overestimated the exchange energy, their work nevertheless marked the beginnings of a theory of exchange in ^{3}He and also provided stimulus for experimental investigation of the phenomena associated with exchange.

IV.1. Exchange Energy and the Heisenberg Hamiltonian

It will be recalled that the exchange interaction, for which no classical mechanical counterpart exists, always arises in systems of two or more identical Fermi particles. For example, in a two-particle system which consists of spin-$\frac{1}{2}$ particles, the exchange interaction splits the degeneracy of the ground state E_0 by $\pm J$ (the exchange energy, or integral). This gives rise to a triplet energy E_T corresponding to parallel spin alignment and a singlet energy E_S corresponding to antiparallel spin alignment. (The reader is referred to basic quantum mechanics texts for detailed expositions.) The energy difference between the singlet and triplet states is defined as $2J = E_S - E_T$. Thus, the association of a parallel or antiparallel spin alignment with the ground state will depend on the sign of J.

For a many-particle Fermi system, the magnetic properties will depend on the spin alignment induced by the exchange interaction. However, a suitable exact solution for a many-body Hamiltonian has yet to be found; therefore if magnetic properties are to be studied, it is expedient to devise a simple model Hamiltonian dependent only on the spin operators for the particles. Such a model must be arranged to yield an exchange energy which is in agreement with that calculated from some more elaborate theory of the ground state. Dirac (1929) found such a Hamiltonian in the form

$$-\sum_{i<j} J_{ij}[\tfrac{1}{2}+2\mathbf{I}_i\cdot\mathbf{I}_j],$$

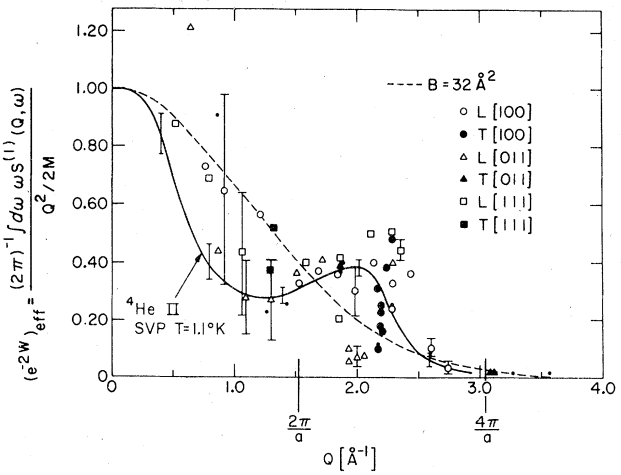

FIG. 29. Effective Debye–Waller factor in bcc ^{4}He (experimental points; Osgood *et al.*, 1972) compared with Gaussian D–W factor (dashed curve, fitted to observed Debye temperature) and the experimental D–W factor for *liquid* ^{4}He (Cowley and Woods, 1971). (After Werthamer, 1972)

where $\mathbf{I}_i$ and $\mathbf{I}_j$ are the nuclear spin operators for the ^{3}He atoms i and j, respectively, and J_{ij} is the exchange energy for the pair (i,j). Only the explicitly spin-dependent part of the Dirac vector model is useful or important to us here for understanding the magnetic properties of ^{3}He. Thus for a crystal of N atoms we consider what is known as the Heisenberg Hamiltonian,[4]

$$\mathcal{H}_H = -2\sum_{i<j} J_{ij}\mathbf{I}_i\cdot\mathbf{I}_j. \tag{4.1}$$

Although the Heisenberg Hamiltonian may be strictly valid for few, if any, actual materials, it is a useful starting point for a theory of magnetic phenomena. On a qualitative basis, $\mathcal{H}_H$ has much appeal because of the possibility of regarding the spin operators $\mathbf{I}_i$ and $\mathbf{I}_j$ as classical spin vectors, whence the energy is lowest for antiparallel spin alignment when $J<0$ and similarly for parallel spin alignment when $J>0$, just as in the two-fermion problem. The subject of the justification for applying $\mathcal{H}_H$ to real crystals is complicated and shrouded with controversy. A detailed discussion of this general topic may be found in Herring (1962), Anderson (1963), Carr (1953), Mullin (1964). Since the work of Bernardes and Primakoff (1960) it has been generally assumed that $\mathcal{H}_H$ is appropriate to describe the magnetic properties of solid ^{3}He. Thouless (1965) has given arguments in support of this assumption: these include the relatively strong localization of the particles and the magnetic isotropy of the crystal. McMahan (1971, 1972a) has refined these arguments. Neverthe-

[4] Various workers from time to time replace the factor 2 in the Heisenberg Hamiltonian, Eq. (4.1), with either $\frac{1}{2}$ or 1. This has led to much confusion, but the use of a factor of 2 is preferred for the following reasons: first the 2 comes about naturally from rather elementary quantum-mechanical considerations leading to a definition of exchange energy for the two-particle problem with wavefunctions normalized to one; and second, the factor of 2 is the more accepted convention; for example, see Footnote 6 of Guyer, Richardson, and Zane (1971), and the Appendix.

less, we note that the question of the validity of Eq. (4.1) is a difficult one.

The Heisenberg Hamiltonian as written in Eq. (4.1) includes exchange between not only nearest neighbors, but next-nearest neighbors, etc. In solid ^{3}He, the probability of second-, third-, etc., neighbor exchange is intuitively small and it has been customary, therefore, to retain only the contributions from nearest neighbors (nn). Hence, for the present discussion, the Hamiltonian used in treating the magnetic properties of solid ^{3}He will be written as

$$\mathcal{H}_{\rm nn} = -2J \sum_{i<j} \mathbf{I}_i \cdot \mathbf{I}_j, \tag{4.2}$$

where the summation is over nearest-neighbor pairs only. In Eq. (4.2), J, the nearest-neighbor pair exchange energy, has replaced J_{ij} and has been factored out of the summation since all magnetic lattice sites and atoms are equivalent throughout the crystal. The magnitude of J determines the temperature at which the magnetic transition to the ordered state occurs. Of course, the sign of J, as discussed above, determines the type of ordering. Considerable theoretical and experimental attention has been devoted to determining J. As will be discussed later, all recent theories of ^{3}He predict $J<0$, or antiferromagnetism. Recently some new experimental results [Kirk and Adams (1971)] and theoretical works [Harris (1971), Zane (1972a) and McMahan (1972b)] appear to challenge the adequacy of the Hamiltonian given in Eq. (4.2); these developments and their implications will be considered later.

In ^{3}He the exchange energy is roughly measured by the overlap of the individual atomic wave functions. Though nonzero, this quantity is small; thus the energy is very small (compared to that for electronic exchange) and the transition temperature can be expected to be quite low. At temperatures far above the transition, the exchange will have very little influence on thermodynamic quantities. These will behave essentially as for a system without magnetic interactions and therefore offer no real possiblity for the determination of J. (It turns out that in one instance the effect of J on a thermal property is observable at $T\sim 0.2$ K.) In contrast, exchange influences dynamic properties such as relaxation times and diffusion at temperatures as high as 1 K. Hence, the first good determinations of J were from NMR measurements of these dynamic properties. [See references in Guyer, Richardson and Zane (1971), Richards (1971), and Meyer (1968).] The analysis of NMR data which leads to a determination of J is rather indirect and involves taking proper account of the local short-range order effects inherent in such a measurement. Hence, the NMR determinations of J have not always been consistent with one another, even with rather high-precision measurements. However, a number of recent determinations, through observation of some thermal equilibrium property, have been made. This type of measurement has the advantage of a more direct interpretation than the NMR experiments and yields the highest precision for J so far attained. We will discuss only the thermodynamic measurements here and refer the reader to the recent review article of Guyer, Richardson, and Zane (1971) for detailed treatment of the NMR experiments. We will make some comparison of the results from the two types of measurement when useful.

If we are interested in the system properties in a magnetic field H, for example the susceptibility, we must add a Zeeman term to the Hamiltonian, Eq. (4.2). The appropriate Hamiltonian is then,

$$\mathcal{H}_{\rm nn} = -2J \sum_{i<j} \mathbf{I}_i \cdot \mathbf{I}_j - H \sum_i \mu_{zi}, \tag{4.3}$$

where we take the H field to be in the z direction, and μ_z is the z component of the ^{3}He magnetic moment. Also it may be that the measurements are in a region of temperature where phonons make a sizable contribution. When needed we will add the appropriate phonon contribution to the observable of interest, rather than augmenting our Hamiltonian.

Given the Hamiltonian $\mathcal{H}$ for the system, thermodynamic properties are obtained from the partition function $Z=$ Trace exp $(-\mathcal{H}/kT)$. The mathematical problem of evaluating Z with $\mathcal{H}$ as in Eq. (4.2) or (4.3) has been the subject of much attention. A lucid review of various effective field theories has been given by Smart (1966). Another approach has been to treat the low $(T<T_c)$ and high $(T>T_c)$ T regions separately and use series expansions in the latter. For $T\gg J/k$, $T\gg\mu H/k$, the high-T series expansions of Z are accepted as giving accurate results. For $I=\frac{1}{2}$, the expansion obtained for ln Z (Baker, Gilbert, Eve, and Rushbrooke, 1967) is

$$N^{-1} \ln Z = F_0(x) + \sum_{s=1} [y^{2s}/(2s)!] F_s(x), \tag{4.4}$$

where $x=J/kT$, $y=\mu H/kT$, and the $F_s(x)$ are themselves series. Several of the coefficients of the $F_s(x)$ series for various lattices have been evaluated by Baker *et al.*

With Eq. (4.4) for Z, useful thermodynamic properties may be obtained by the usual statistical mechanical derivatives for the entropy, isochoric heat capacity and pressure, magnetization, and susceptibility, *viz.*:

$$S = k(\partial T \ln Z/\partial T)_{J,H}, \tag{4.5}$$

$$C_V = T(\partial S/\partial T)_{J,H} = k\beta^2(\partial^2 \ln Z/\partial\beta^2), \qquad \beta = (kT)^{-1}, \tag{4.6}$$

$$P_V(T, H) = kT(\partial \ln Z/\partial V)_{T,H}, \tag{4.7}$$

$$M = (kT/V)(\partial \ln Z/\partial H)_{J,T}, \tag{4.8}$$

$$\chi = \partial M/\partial H = (kT/V)(\partial^2 \ln Z/\partial H^2)_{J,T}. \tag{4.9}$$

At present we are interested in the exchange contribu-

tion in the limit $H\to 0$. In this case, the results are

$$S/R=\sum_{n\geq 0}[(1-n)e_n/2^n n!]x^n, \quad (4.10)$$

$$C_V/R=\sum_{n\geq 0}[n(n-1)e_n/2^n n!]x^n, \quad (4.11)$$

$$P_V(T)=N(\partial J/\partial V)_{T,H}\sum_{n\geq 0}(ne_n/2^n n!)x^{n-1}, \quad (4.12)$$

$$\chi=(N\mu^2/VkT)\sum_{n\geq 0}(\alpha_n/2^n n!)x^n. \quad (4.13)$$

For the bcc lattice, various coefficients are:

$$e_0=\ln 2, \quad e_1=0, \quad e_2=12, \quad e_3=-24, \quad e_4=168, \cdots$$
$$\alpha_0=1, \quad \alpha_1=8, \quad \alpha_2=96, \cdots.$$

Thus we have a number of properties at our disposal which offer the prospect of determining J (or, in some cases, $|J|$). The question of which property is best investigated is one of experimental techniques. In this connection, it should be noted that the first term of a quantity such as χ is J independent and goes as T^{-1}, while the leading contribution from J appears as the coefficient of T^{-2}. By contrast, the leading term in $P_V(T)$ is J dependent. This means that the effects of exchange will be felt at higher temperatures for one quantity than for another, which will in turn affect the uncertainty in the J's so obtained. In studies of magnetic ordering in other systems, C_V (or C_P) and χ have been fairly standard quantities to measure. To date, attempts (Edwards, McWilliams, and Duant, 1962a) to determine J from C_V measurements in ^{3}He have been unsatisfactory, with at best an upper limit on J as the result. Measurements of $P_V(T)$ provided the first, and still most accurate, values of $|J|$ and these will be discussed next.

IV.2. Determination of $|J|$, Thermal Expansion

Equation (4.12) expresses the exchange-energy contribution to the pressure. If we keep only the first two terms, then we can write it in the form

$$P_{V,\mathrm{ex}}=(3R/V)(J/K)^2[\partial \ln|J|/\partial \ln V]\times T^{-1}[1-(J/2kT)], \quad (4.14)$$

where the subscript ex denotes the exchange contribution. At $T\gg J/k$, the second term is negligible, and we have $P_{V,\mathrm{ex}}\propto T^{-1}$, with the constant of proportionality involving only $|J|$ and its volume derivative. Note that the sign of J cannot be determined to this order of T, but that if the measurements were extended to $T\leq 10J/k$, then curvature in $P_{V,\mathrm{ex}}$ versus T^{-1} would reveal the sign of J as a consequence of the second term of Eq. (4.14).

In addition to $P_{V,\mathrm{ex}}$ given by Eq. (4.14), we have a phonon pressure contribution, which for a Debye solid with a Debye temperature θ is

$$P_{\mathrm{ph}}=(-3\pi^4R/5V)(\partial \ln\theta/\partial \ln V)(T^4/\theta^3), \quad (4.15)$$

and a constant P_0 representing the pressure at $T=0$ if $J=0$. The total pressure is then, for $T\gg J/k$,

$$P_V(T)=\frac{3R}{V}\left(\frac{J}{k}\right)^2\frac{\partial \ln|J|}{\partial \ln V}T^{-1} - \frac{3\pi^4R}{5V}\frac{\partial \ln\theta}{\partial \ln V}\frac{T^4}{\theta^3}+P_0. \quad (4.16)$$

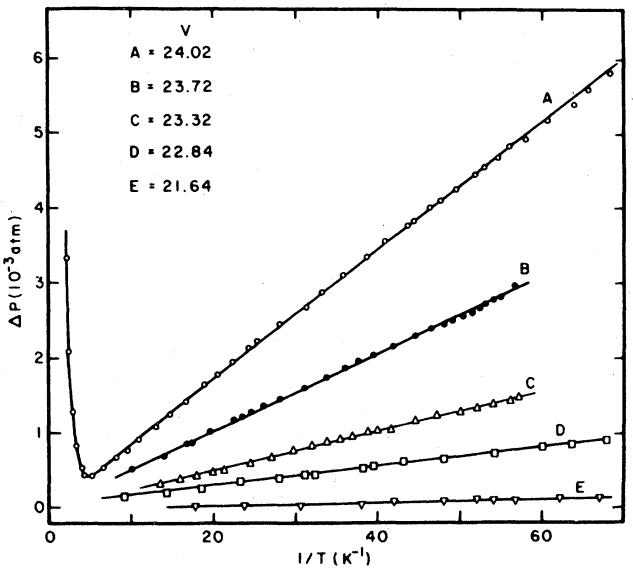

FIG. 30. Pressure difference versus T^{-1} for various molar volumes.[5] For $V=24.02$, cm^3/mole, the high-temperature phonon contribution is shown. For the other volumes, only the exchange contribution is shown. From the slopes in the T^{-1} region, values of the exchange energy are obtained. (After Panczyk and Adams, 1969).

At high T, P_{ph} will be dominant and P_{ex} will be unimportant, while at lower T, the exchange term will dominate. Since the ratio of the two terms goes as T^5, this dominance will switch over from one to the other very quickly, a desirable feature if the two contributions are to be resolved readily experimentally. (Note that the detailed nature of the lattice dynamics, i.e., the use of the Debye model, is not of crucial importance to this argument.)

The measurements of $P_V(T)$ in solid ^{3}He were made by Panczyk, Scribner, Straty, and Adams (PSSA, 1967), and Panczyk and Adams (PA, 1969). In order to make the measurements, which must be done *in situ*, the capacitive strain-gauge technique of Straty and Adams (1969) was used. The values of $|J|$ and $\partial \ln|J|/\partial \ln V$ turn out to be such that at $T\simeq 15$ mK the maximum value of P_{ex} is $\simeq 5\times 10^{-3}$ atm, which requires rather high pressure resolution of the gauge. With a resolution $\Delta P_{\min}\simeq 10^{-6}$ atm, it was possible to examine most of the bcc phase.

The results extending to $T=13$ mK for several molar volumes are shown in Fig. 30 where $P-P_0=\Delta P$ is plotted versus T^{-1} to display the exchange term. For the largest V ($=24.02$ cm^3/mole), the curve labeled A

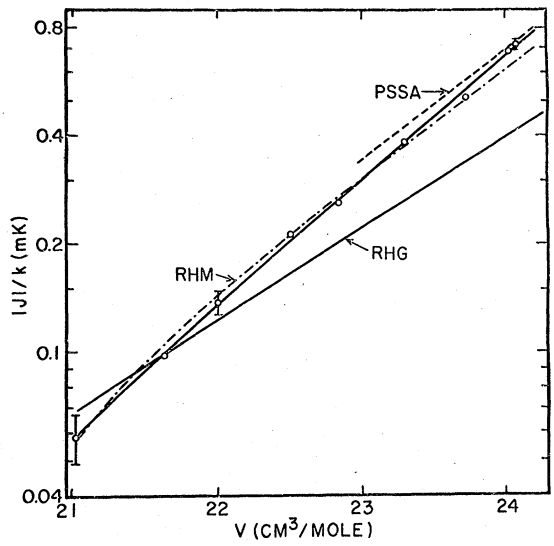

FIG. 31. The exchange energy of solid ^{3}He versus molar volume.[5] Circles: Panczyk and Adams (PA, 1969). PSSA: Panczyk, Scribner, Straty, and Adams (1967). Values given by NMR experiments shown by RHM, Richardson, Hunt, and Meyer (1965); and RHG, Richards, Hatton, and Giffard (1965). Error bars on three circle points of the $P_V(T)$ measurements show the increasing error with diminishing volume. (After Panczyk and Adams, 1969).

in Fig. 30, the phonon contribution is also shown. On the other curves this contribution has been omitted for clarity. From Eq. (4.14) we see that the slope of P_{ex} versus T^{-1} is $(3R/V)(J/k)^2(\partial \ln |J|/\partial \ln V)$. Because of the factor $\partial \ln |J|/\partial \ln V$, measurements at several V are required to permit $|J|$ to be evaluated. This was done by a self-consistent procedure, using a trial value of $\partial \ln |J|/\partial \ln V$ to obtain $J(V)$ from which a new value of $\partial \ln |J|/\partial \ln V$ was obtained, etc. Because $\partial \ln |J|/\partial \ln V$ is virtually constant, the procedure converges in the first iteration. An alternative scheme has been discussed by Panczyk and Adams (1970).

The values of $|J|$ found in the above manner from $P_V(T)$ measurements are shown in Fig. 31 as a plot of $|J|/k$ versus the molar volume.[5] For purposes of comparison, some NMR measurements are shown by the curves labeled RHM (Richardson, Hunt, and Meyer, 1965) and RHG (Richards, Hatton, and Giffard, 1965). From their measurements (open circles in Fig. 31), Panczyk and Adams estimate the uncertainty in $|J|$ to be $<3\%$ for $V=24$, and about 8 and 15% for $V=22$ and 21 cm^3/mole, respectively. The solid line through the circle points in Fig. 31 has a slope $\partial \ln |J|/\partial \ln V = 17.5$ at $V=24$, and 19.2 at $V=22$ cm^3/mole. A convenient set of $|J|/k$ values for various molar volumes (as determined from the $P_V(T)$ measurements) is tabulated in Table VI.

[5] The molar volumes used in Fig. 31 (and in all of Sec. IV) were determined from the V_S versus P_m data of Mills, Grilly, and Sydoriak (1961). If one uses the newer data of Grilly (1971), adjustment of the volume scale must be made *leaving J unchanged*, e.g., $J(V_{MGS}=24.0) \equiv J(V_G=24.14)$. For convenience, a few values for converting V_{MGS} to V_G are given in the Appendix.

From the plot of $|J|/k$ versus V in Fig. 31, one sees that as V decreases so does $|J|$, and furthermore, that the dependence is exceedingly large, $|J| \propto V^{18}$. At first it may seem contradictory that raising the density reduces the exchange. Physically the reason is that as the atoms are brought closer, the wave functions become more localized and there is less overlap. Another way to picture this process is the following: when pressure is applied and the atoms are brought closer together the exchange probability is reduced because the atoms are packed more tightly so that it is more difficult for them to maneuver around each other in a way which avoids their hard cores.

Another interesting result from the $P_V(T)$ measurements of PA is the manner in which the expansion coefficient, α, depends on the exchange energy. The expansion coefficient, like the pressure, will depend on contributions from both the exchange and the phonons. It is related to the pressure by the expression $\alpha = K_T(\partial P/\partial T)_V$, where K_T is the compressibility. As seen from Eq. (4.14), we have $(\partial P_{ex}/\partial T)_V<0$, since $\partial \ln |J|/\partial \ln V>0$ and neither J nor its logarithmic volume derivative is very temperature dependent. On the other hand, from Eq. (4.15) it can be seen that $(\partial P_{ph}/\partial T)_V>0$, since $\partial \ln \theta/\partial \ln V<0$. Therefore at high T, we find $\alpha>0$, and at low T, $\alpha<0$. The line $\alpha=0$ will divide the solid phase diagram shown in Fig. 32 into regions $\alpha>0$ and $\alpha<0$, dominated by phonons and exchange, respectively. For the solid at melting, PA have found that $\alpha=0$ at $T=0.21$ K. This result agrees with the analysis of Goldstein (1967, 1968b) in which the intersection was calculated to be at 0.23 K. Thus the exchange process begins to dominate α [or $P_V(T)$] at $T\simeq 300|J|/k\simeq 0.2$ K. This is higher than will be the case for other thermodynamic properties. For example, for $V\simeq 24$ cm^3/mole, corresponding to large $|J|$, we have $C_{V,ex}=C_{V,ph}$ at $T\simeq 0.14$ K, and for χ only about 5% departure from Curie's law at $T\simeq 0.04$ K is to be expected. The favorable situation which occurs in α or $P_V(T)$ comes about because of the factors $\partial \ln |J|/\partial \ln V$ and $-\partial \ln\theta/\partial \ln V$. The former is ~ 18, while the latter is ~ 2. Thus the strong volume dependence of $|J|$ makes measurement of $P_V(T)$ favorable for displaying nuclear spin-ordering effects.

Another experiment from which values of $|J|$ may be found is the measurement of the melting pressure of ^{3}He, $P_m(T)$. (A more extensive discussion of this will be given in Sec. V.1.) However, except for $T \lesssim T_c$, the effect of exchange on the melting pressure is very slight (see Fig. 47, Sec. V.1). For example, with the present resolution of measurement of P and T, the effect of exchange on the melting curve at $T=20$ mK is barely detectable. From work extending to 2 mK, Johnston *et al.* (1969b, 1970a) have extracted a value of $|J/k| = 0.85$ mK, which, given the limitations of the method, compares favorably with the value 0.72 mK, for the solid at melting, quoted by PA. In principle, the sign of J should be discernible from the behavior of $P_m(T)$, but this requires very precise data. Thus, the results of

TABLE VI. Values of $|J|/k$ from $P_V(T)$ measurements for various molar volumes V.

$\|J\|/k$ (mK)[a]	0.057	0.089	0.135	0.202	0.305	0.450	0.660	0.718
V (cm³/mole)[b]	21.0	21.5	22.0	22.5	23.0	23.5	24.0	24.1

[a] These values of $|J|$ were determined from the smooth curve through the points from the $P_V(T)$ measurements of PA shown in Fig. 31. An estimate of the error can be determined from Fig. 31, also see text.

[b] Consult Footnote 5 for explanation of molar volume values.

Johnson *et al.* could be fitted equally well with $J/k=-0.85$ mK, or $J/k=+1.0$ mK.

IV.3. The Sign of J and the Type of Ordering

From the measurements discussed in Sec. IV.2, we have good values for $|J|$, but the sign of J is undetermined. In order to determine the type of ordering which will occur the sign must be known. In principle, a number of different types of thermodynamic measurements would determine the sign of J as can be seen from the series expansion, Eqs. (4.10)–(4.13). As mentioned previously, $P_V(T)$, if measured down to $T\simeq 7$ mK, would give the sign of J. Perhaps the most direct method of determining the sign of J is through measurement of the nuclear magnetic susceptibility, χ.

From the first few terms in the high-T series expansion, Eq. (4.13), we have

$$\chi=(N\mu^2/VkT)[1+4(J/kT)+12(J/kT)^2+\cdots]. \tag{4.17}$$

Up to and including the second term, Eq. (4.17) may be approximated by the familar Curie–Weiss law

$$\chi=C/(T-\Theta) \tag{4.18}$$

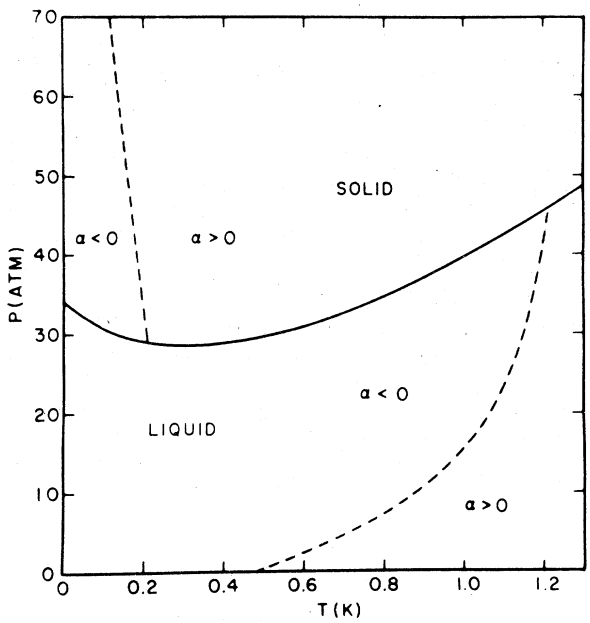

FIG. 32. Phase diagram showing the regions of positive and negative expansion coefficients α in solid and liquid ^{3}He. (After Panczyk and Adams, 1969).

where $C=N\mu^2/Vk$ is the Curie constant[6] and

$$\Theta=4J/k \tag{4.19}$$

is the Weiss constant.[6] An examination of either Eq. (4.17) or Eq. (4.18) shows that departure from the ideal paramagnetic behavior $\chi=C/T$ will yield both the sign and magnitude of J.

It was through susceptibility measurements in fact that the first attempts to determine the ordering temperature in solid ^{3}He were made. The early efforts began with Fairbank and Walters (1957), Fairbank and Adams (1958), and Adams, Meyer, and Fairbank (1960). These early attempts were unsuccessful in determining the sign of J for two reasons: (1) Small amounts of ^{4}He impurities ($\simeq 1\%$) had an unexpectedly large effect on the relaxation times; and (2) The measurements of χ must go to extremely low T and be of good precision to give J. For example, if the temperature dependence is measured to 5%, measurements extending to 50 mK would just reveal the sign of J, and then only set an upper limit on $|J|$. Several other groups of workers (Thomson, Meyer, and Dheer, 1963; Cohen, Pipes, Verosub, and Fairbank, 1968; Richards and Homer, 1969) made subsequent attempts to determine the sign of J; all of these were unsuccessful because of one or both of the above reasons.

In 1969, three groups of workers (Kirk, Osgood, and Garber, 1969; Pipes and Fairbank, 1969; Sites, Osheroff, Richardson, and Lee, 1969, reported, almost simultaneously, measurements of χ made to low enough temperatures to determine that the sign of J is negative. Johnson and Wheatley (1970c) also reported a negative J from a re-analysis of old susceptibility data taken by Anderson, Reese, and Wheatley (1961). In all of the work above the susceptibility was measured by using either a pulse or continuous-wave NMR technique.

Since all of the recent results are in agreement to within the stated accuracy, we will discuss in detail those of Kirk *et al.* which have the greatest precision and are the most extensive: they covered nearly all the bcc phase ($V=21$–24 cm³/mole), a temperature range of 5.3–800 mK and samples with three different ^{4}He impurity concentrations (2 ppm, 125 ppm, and 2000 ppm). As seen from Eq. (4.18), a plot of χ^{-1} versus T

[6] In general, from effective field theories of magnetism we have $C=N\langle\mu^2\rangle/V3k=Ng^2\mu_N^2I(I+1)/V3k$, where $\langle\mu^2\rangle$ is the average of μ^2, g=Landé g factor, and $\mu=g\mu_N I$; $\Theta=2zI(I+1)J/3k$, where z=lattice coordination number=8 (bcc). Note that the factor 4 occurring in the second term of Eq. (4.17) is not unique to the series expansion method but is inherent in the Heisenberg model as given by Eq. (4.3).

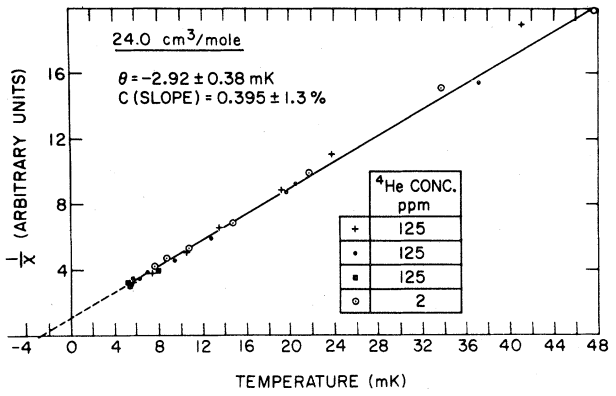

FIG. 33. Inverse susceptibility versus temperature for $V=24.0$ cm³/mole. Straight lines through the data points are least squares fits. (After Kirk *et al.*, 1969, 1970).

should yield a straight line with an intercept, Θ, on the T axis. Such plots for the data of Kirk *et al.* are shown in Figs. 33–36 for various molar volumes,[7] where it is seen that the intercepts Θ are negative, corresponding to antiferromagnetic behavior. With the aid of Eq. (4.19), the values of $|J|$ were computed; these are compared in Fig. 37 with the results of Panczyk and Adams (1969). The error bars shown in Fig. 37 were obtained from an error analysis of deviations of the data from a least-squares fit. As previously mentioned, it is difficult to achieve high precision for J in χ measurements because the temperature has to be resolved extremely well (see discussion at end of Sec. IV.1). For example, although the data of Kirk *et al.* extended to 5.3 mK, the uncertainty in J was 13% at $V=24$ cm³/mole. By contrast, in the $P_V(T)$ measurements (at the same V) which went to 13 mK, an uncertainty of only 3% in $|J|$ was achieved. This situation illustrates

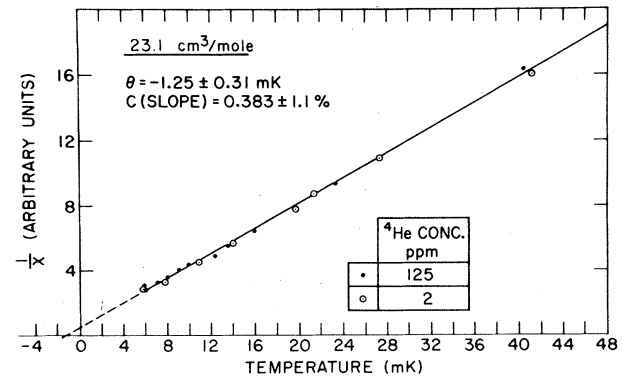

FIG. 34. Inverse susceptibility versus temperature for $v=23.1$ cm³/mole. Straight lines through the data points are least squares fits. (After Kirk *et al.*, 1969, 1970).

[7] A minor result indicating the consistency of the data is that the slopes of the straight lines scaled with the molar volumes as expected from the Curie constant C.

the complementary nature of the two types of data. From χ the sign of J is determined, but the precision is poor; from $P_V(T)$ the precision of $|J|$ is good but the sign is unknown.

By reference to Eq. (4.17), it is clear that contributions from higher-order terms will produce curvature in χ. Hence a χ^{-1} versus T plot could lead to an overestimate of Θ if these higher-order terms are important. One way to analyze for curvature effects and eliminate the possibility of overestimating Θ is to plot χT versus T^{-1}. This type of plot, shown in Fig. 38, was used by Sites *et al.* to analyze their data. Although they had a large amount of data at one molar volume (≈24 cm³/mole), because of limited precision they were able to establish a value for Θ but not for the second-order coefficient of χT. Similarly in the work of Kirk *et al.*, an analysis for curvature was made by means of the χT versus T^{-1} plot, but, again, no determination of the second-order coefficient was possible for the same

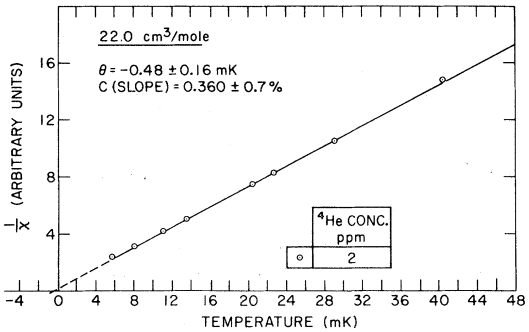

FIG. 35. Inverse susceptibility versus temperature for $v=22.0$ cm³/mole. Straight lines through the data points are least squares fits. (After Kirk *et al.*, 1969, 1970).

reason. However, the data of Sites *et al.* and of Kirk *et al.* yield values for Θ ($V=24$) which are in good agreement.

Although the susceptibility measurements in solid ³He have had a history of unreliable results, the experiments we have just discussed leave little doubt that $J<0$. As discussed in Sec. IV.5, this conclusion has recently been corroborated in an entirely different type of experiment (Kirk and Adams, 1971). We may assume, then, that the magnetic phase transition will be antiferromagnetic, occurring at the Néel temperature T_N. For the bcc lattice, Baker, Gilbert, Eve, and Rushbrooke (1967) have computed the relation for T_N in terms of J, finding

$$T_N=-2.748J/k, \tag{4.20}$$

which, with Eq. (4.19), gives

$$T_N=-0.687\Theta. \tag{4.21}$$

With the more precise values of $|J|$ from Panczyk and Adams (rather than the NMR values), the phase

transition should occur for the solid near melting ($V=24.1$ cm³/mole) at $T_N=2.0$ mK. A summary of values of T_N and J/k computed from the recent susceptibility data is given in Table VII.

As indicated in Sec. IV.1, the experimental results which we have discussed up to this point have been interpreted using the Heisenberg Hamiltonian with nearest-neighbor interactions only, $\mathcal{H}_{nn}$. The conclusions given above concerning the Néel temperature assume the validity of this Hamiltonian. A recent experiment which we shall discuss fully in Sec. IV.5, has provided evidence that the situation is more complicated and that the simple Heisenberg model may not be adequate for the interpretation of the magnetic properties of solid ^{3}He. If such be the case, the conclusions we have given regarding the Néel temperature may require revision.

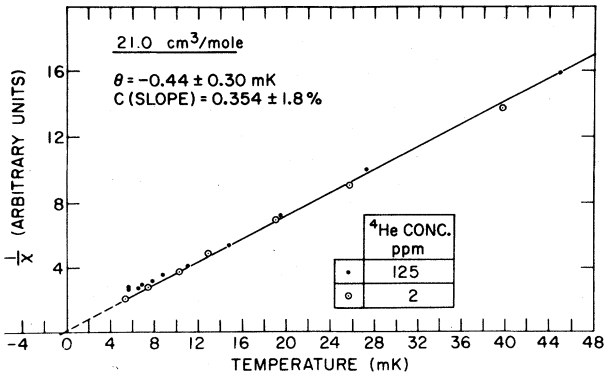

FIG. 36. Inverse susceptibility versus temperature for $v=$ 21.0 cm³/mole. Straight lines through the data points are least squares fits. (After Kirk *et al.*, 1969, 1970).

IV.4. Brief Comparison of Exchange Theories with Experiment

The vigorous and diverse experimental efforts regarding exchange which have taken place in the past ten to twelve years have been paralleled by a wide variety of attempts at a calculationally feasible theory of exchange. As in the experiments, there are two basic tasks confronting any theory, namely, to predict the kind of ordering and the magnitude of $J(V)$. To undertake such an endeavor is, first of all, to undertake the development of a theory of the ground state of the system, no small task in itself. Thus, a comprehensive review of even the basic structure of the many theories would take us far afield. We confine our remarks to general comments on the comparison with experiment and some of the suspected causes of the discrepancies encountered.

The early treatment of exchange by Bernardes and Primakoff (1960) is mostly of historical interest. Later and more extensive work has been carried out by Nosanow (1964), Nosanow and Mullin (1965), Hertherington, Mullin and Nosanow (1967) Nosanow and Varma (1968, 1969), Mullin, Nosanow and Steinback (1969), Varma and Nosanow (1970). A somewhat different approach to an exchange theory has been provided by Guyer and Zane (1969, 1970). Other contributions to the theories on exchange have been given by Hartmann (1964), Thouless (1965), Mullin (1968b), Glyde (1969, 1970), Ebner and Sung

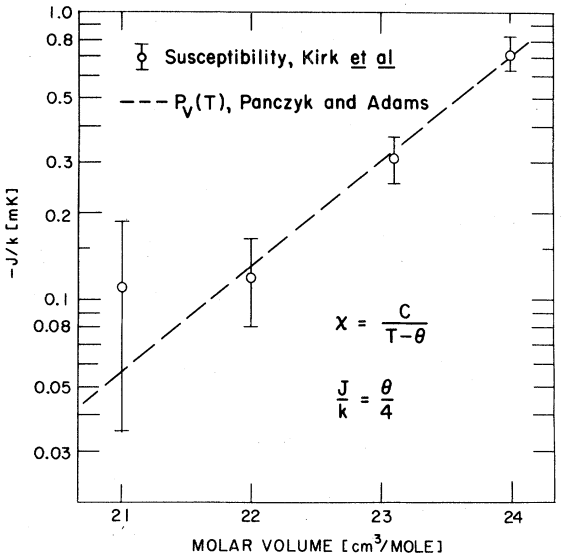

FIG. 37. The exchange energy versus molar volume.[5] Comparison of values obtained from susceptibility and $P_V(T)$ experiments. Dashed curve of $|J|/k$ from Panczyk and Adams (1969). Circles with error bars from Kirk *et al.* (1969, 1970). (After Kirk *et al.*, 1969, 1970).

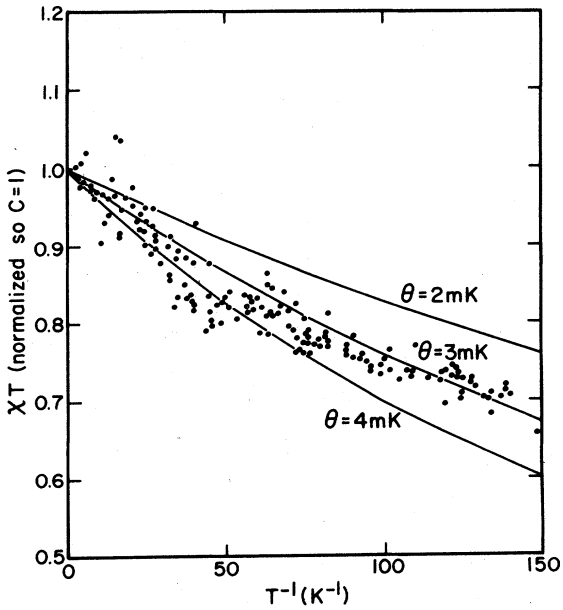

FIG. 38. χT versus T^{-1} with χ in units of the Curie constant. Solid lines are theoretical curves [using Eq. (4.17)] for different values of the Weiss Θ. (After Sites *et al.*, 1969).

TABLE VII. Susceptibility Measurements. Values of the exchange energy and Néel temperature computed from the Weiss constants of various molar volume solids.

Molar volume[a] (cm^3/mole)	Θ (mK)	J/k (mK)	T_N (mK)	Experiment
24.0	−2.92±0.38	−0.73±0.10	2.0±0.26	Kirk[b]
24.1	−3.0±0.3	−0.75±0.08	2.1±0.2	Sites[c]
24.2	−3.5±0.4	−0.88±0.10	2.4±0.3	Johnson[d]
24.2	−4.89±2.0	−1.22±0.50	3.4±1.37	Pipes[e]
23.1	−1.25±0.23	−0.31±0.06	0.86±0.16	Kirk[b]
23.6	−3.98±2.0	−1.00±0.50	2.73±1.37	Pipes[e]
23.3	−1.52±2.0	−0.38±0.50	1.04±1.37	Pipes[e]
22.0	−0.48±0.16	−0.12±0.04	0.33±0.11	Kirk[b]
21.0	−0.44±0.30	−0.11±0.08	0.30±0.21	Kirk[b]

[a] See Footnote 5.
[b] Kirk, Osgood, and Garber (1969).
[c] Sites, Osheroff, Richardson, and Lee (1969).
[d] Johnson and Wheatley (1970c).
[e] Pipes and Fairbank (1969).

(1971), McMahan (1971, 1972a), and Østgaard (1972). Critiques and some review of these various theories have been given by Guyer (1969), Brandow (1971), and McMahan (1971).

According to Brandow (1971), McMahan (1971), and Østgaard (1972), the seemingly wide variety of approaches of the above workers are, in fact, closely interrelated. In a private communication (to WPK, 1972), McMahan has observed that all the above workers have calculated values of J by a form of reduction of the many-body problem to a two-body problem and furthermore if one uses the full many-body integral expression for J one gets results which are smaller, by factors of three to six for nearest-neighbor distances of 3.75 to 3.45 Å, respectively, than those obtained from the two-body approximations. Brandow and Østgaard have both emphasized the three distinguishable contributions which dominate the exchange energy. These are the tunneling (due to overlap and present even in a system of free fermions), interaction (due to the interatomic potential in an uncorrelated, i.e., Hartree–Fock, system), and correlation (due to the symmetry requirements on that portion of the wave function which treats short-range correlation) energies. Both Brandow and Østgaard have argued that the various theories differ most strikingly in the way in which they treat, approximate, or neglect these three contributions. Perhaps the most trenchant comment on exchange theories as a class is due to Guyer (1968) who pointed out that even if a particular theory were to give $J(V)$ in reasonable accord with experiment, very little would have been learned, since a "back of the envelope" calculation involving nothing more than the Debye temperature for the system and some plausible estimate of single-particle overlap will also yield reasonable agreement with experiment. (Guyer in fact displayed precisely such a calculation.)

The modern theories of exchange all predict $J<0$. However, a substantial controversy has arisen as to whether this result is inherent in the theories or is the result of delicate (and potentially unrealiable) cancellation of large numbers. In McMahan's scheme (1972a), the sign is manifestly a consequence of the formalism, but Brandow has claimed that this advantage was obtained at the price of relying on a surface-integral expression over a surface on which the wave function is intrinsically ill defined, with the result that a large uncertainty in the calculated magnitude of J has been introduced.

A comparison of the experimental molar volume dependence of the exchange energy, $|J|/k$, with some of the more recent theories is given in Fig. 39. It should be noted that many such plots have appeared in the literature with erroneously good comparisons resulting from ignored differences in the definition of J; see McMahan (1971) and the Appendix for a very careful discussion of this point. The agreement shown in Fig. 39 between the theory by Østgaard and experiment should not be taken too seriously, for Østgaard himself has pointed out that his calculations involve a significant number of approximations and uncertainties. In particular, he has emphasized the sensitivity of his results to the Gaussian width parameter which characterizes his unperturbed single-particle functions; McMahan has made the same point with regard to a number of the theories.

In summary, we believe that it is fair to say that at present the question of concordance of theories of

exchange with experiment is seriously overshadowed by questions concerning the structure of the theories themselves.

IV.5. Behavior of $P_V(T, H)$ in High Magnetic Fields

In the previous discussion of nuclear-spin ordering and magnetic effects in solid ^{3}He we have found a rather satisfactory picture. The various thermal and magnetic properties measured in the different experiments have given results that either confirmed or agreed with one another to within estimated uncertainty. A common element in all these measurements is that only the lowest-order term in J of the series expansions has been measured and compared. Since effective field theories are able to produce the lowest-order term in the high-T series expansion for various magnetic properties of a solid, it is not too surprising to find the agreements above. The experiments have not provided a true test of the Heisenberg model Hamiltonian in Eq. (4.3).

In order to make a detailed comparison between theory and experiment, the measurements in low magnetic field need to extend well into the critical region near $T_c = 2$ mK. However, as Goldstein (1968a) has pointed out, a detailed comparison should be possible in the paramagnetic region at temperatures well above T_c if one applies a large magnetic field. Referring to Eq. (4.7), and including several terms in $x = J/kT$ and $y = \mu H/kT$ we have for the pressure in a magnetic field,

$$P_V(T, H) = (RT/V)\,(\partial \ln |J|/\partial \ln V) \times [3x^2 - \tfrac{3}{2}x^3 + \cdots + y^2(2x + 12x^2 + 52x^3 + \cdots) + y^4(-1.33x - 23x^2 + \cdots)]. \quad (4.22)$$

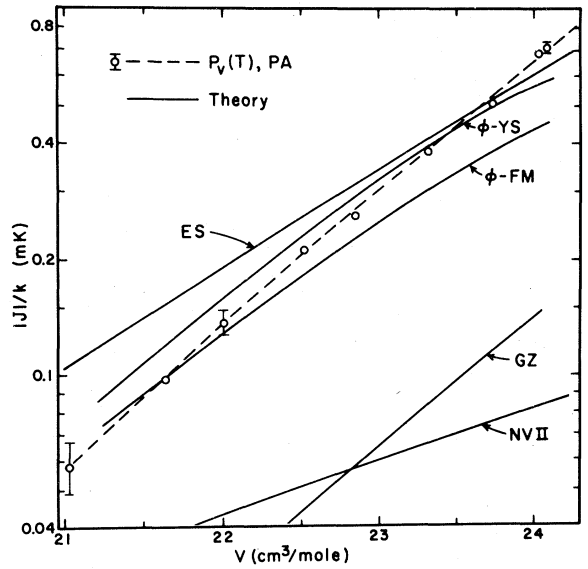

FIG. 39. The exchange energy versus molar volume[5] showing the comparison of $|J|$ values from $P_V(T)$ measurements, dashed curve from Panczyk and Adams (1969), with the values given by various theories, solid curves. ES, Ebner and Sung (1971); Ø–YS, Østgaard (1972) using a Yntema–Schneider potential; Ø–FM, Østgaard (1972) using a Frost-Musulin potential; NVII, Nasanow and Varma (1969); and GZ, Guyer and Zane (1969). All values of $|J|$ are shown using the convention $2J = E_S - E_T$; see Sec. IV.1 and the Appendix. Therefore, as pointed out by McMahan (1971, 1972a), the results reported by NVII have been divided by four; and those reported by GZ divided by two.

In Sec. IV.2 we remarked that pressure measurements in zero field, which extended to $T \simeq 15$ mK, required only the quadratic term in x and therefore depended only on $|J|$. In the presence of a large field, the term in y^2x of Eq. (4.22) can be comparable to the first term in x^2 and hence will reveal the sign of J. Also the extent to which this expansion for $P_V(T, H)$ fits the data should provide a test of the adequacy of the Heisenberg model, Eq. (4.3), or of the expansion resulting from it.

Two groups of workers (Osgood and Garber, 1971; Kirk and Adams, 1971) have made measurements of $P_V(T, H)$. Osgood and Garber reported the very disconcerting result that the magnetic field has no effect, i.e., $P_V(T, H) = P_V(T, O)$. Shortly afterwards Kirk and Adams reported results for which there was a large effect of the field. They suggested that the null result of Osgood and Garber was because of thermometry errors brought about by magnetoresistance of the carbon-resistor thermometer which was used.[8] Osgood (1971) has also expressed the view that relaxation effects were a contributing factor. It appears that the data of Osgood and Garber do not represent the correct equilibrium behavior of $P_V(T, H)$; thus, in the remainder of this section we will discuss only the results of Kirk and Adams.

Kirk and Adams (1971, 1972) measured $P_V(T, H)$ in applied fields of $\simeq 0$, 40, 60, and 70 kG for molar volumes of 23.34 and $\simeq 24.0$ cm^3/mole over a temperature range of 17–130 mK. The results in the form ΔP vs T^{-1} are shown in Figs. 40–42. Here we use $\Delta P = P_V(T, H) - P_0$, where P_0 is a constant pressure which remains in the absence of J and H. The zero of ΔP, i.e., the value of P_0, for each curve was determined by requiring that it extrapolate through zero at $T^{-1} = 0$. (This extrapolation was subject to some uncertainty, particularly at the higher fields.) Open and closed symbols indicate data taken on warming and cooling, respectively.

From these data it is evident that the strong magnetic fields have a pronounced effect on the pressure. A number of conclusions can be drawn. As was mentioned in Sec. IV.3, the observed effect indicates $J < 0$, or antiferromagnetic ordering. Examination of Eq. (4.22), shows that this follows from the downward curvature of $P_V(T, H)$. This argument relies on the Heisenberg

[8] Kirk and Adams used two resistance thermometers, one in the field and one in zero field. They used the one in zero field for determining T, since the other exhibited strong magnetoresistance. If the resistor in the field were used as a thermometer, the resulting incorrect temperature scale was such that it almost exactly canceled the field effect on $P_V(T, H)$, producing the same apparent null result as that of Osgood and Garber.

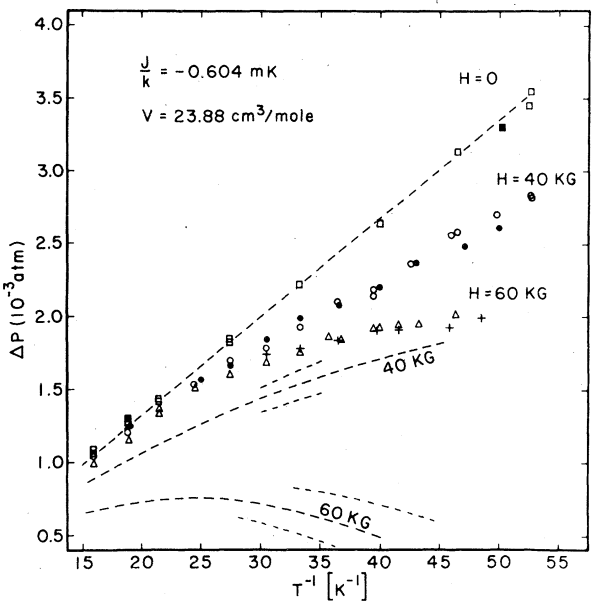

FIG. 40. Pressure differences versus T^{-1} for $V=23.88$ cm^3/mole[5] in fields of 60, 40, and 0.5 ($H\approx 0$) kG. Various symbols for a given H are for different traversals of the temperature region. The dashed curves are calculated behavior based on the Heisenberg model, Eq. (4.3). (After Kirk and Adams, 1971).

model ($\mathcal{H}_{nn}$) used in obtaining Eq. (4.22). As we shall discuss shortly, these results call into question the adequancy of $\mathcal{H}_{nn}$ in ^{3}He. Therefore, an argument not requiring reliance on $\mathcal{H}_{nn}$ would be more satisfactory. This can be provided by thermodynamics.

In a magnetic field the Helmholtz free energy differential is

$$dA=-SdT-PdV-MdH. \tag{4.23}$$

Since dA is an exact differential, the Maxwell relation follows

$$(\partial P/\partial H)_{V,T}=(\partial M/\partial V)_{H,T}. \tag{4.24}$$

We will consider an effective exchange energy, J_e, which is not necessarily the same as the J used in Eq. (4.3), and will be thought of as a parameter to characterize the magnetization $M=M(J_e)$. Ferromagnetic behavior will correspond to $J_e>0$,[9] and antiferromagnetic behavior to $J_e<0$. Expanding the right side of Eq. (4.24) by the chain rule, we have

$$\begin{aligned}(\partial P/\partial H)_{V,T}&=(\partial M/\partial V)_{H,T}\\&=(\partial M/\partial J_e)(\partial J_e/\partial V)\\&=(\partial M/\partial J_e)(J_e/V)(\partial \ln|J_e|/\partial \ln V).\end{aligned} \tag{4.25}$$

[9] Under exceptional circumstances, $J_e>0$ could also correspond to antiferromagnetic ordering when a positive exchange energy of next-nearest neighbors is larger than the negative exchange energy of the near neighbors. However, $J_e<0$ will never correspond to ferromagnetic ordering. [See Smart (1966), for details.]

Physically, we expect M to be a non-decreasing function of J_e, i.e., $\partial M/\partial J_e\geq 0$. Although discussed and analyzed in terms of J in $\mathcal{H}_{nn}$, the $P_V(T,0)$ measurements show that $\partial \ln|J_e|/\partial \ln V>0$. Therefore, the sign of J_e in Eq. (4.25) is the same as that of $(\partial P/\partial H)_{V,T}$, which from the Kirk and Adams experiment is negative. This experiment then provides an elegant confirmation of the expected antiferromagnetic ordering shown by the χ measurements.

The dashed lines shown in Figs. 40 and 41 are computations of $P_V(T,H)$ using Eq. (4.22), and the J values obtained in zero field and with $\partial \ln|J|/\partial \ln V=17.5$; whereas in Fig. 42 the dashed curves were computed using $\partial \ln|J|/\partial \ln V=18.1$. Only the terms explicitly written out in Eq. (4.22) were used on the computations; higher-order terms contribute $<1\%$. The dashed short lines near the ends of the computed curves in Figs. 40 and 41 are for fields differing by ± 3 kG from the central curve. In every case the magnitude of the effect of the field is much less than would be expected from Eq. (4.22). A quantitative disagreement of about a factor of 2 is apparent for the data given in Figs. 40 and 41, and in Fig. 42 the discrepancy is almost a factor of 2.5. The data agree in a qualitative manner with the $P_V(T,H)$ expression given in Eq. (4.22). That is, for a particular molar volume the pressure data taken in the various magnetic fields scales as H^2 to within experimental error. Qualitative agreement with Eq. (4.22) is also indicated by the fact that

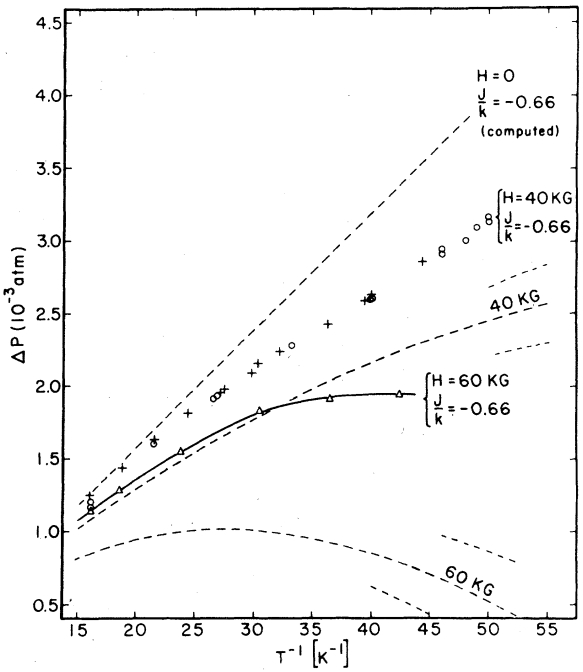

FIG. 41. Pressure differences versus T^{-1} for 24.0 cm^3/mole[5] in fields of 40 and 60 kG. Various symbols for a given H are for different traversals of the temperature region. The curve through the 60 kG data is simply to connect points. Dashed curves are calculated behavior based on the Heisenberg model, Eq. (4.3). (After Kirk and Adams, 1971).

at a high enough field and a small J the pressure is observed to go through a maximum as shown by the data in Fig. 42. The reason for the quantitative discrepancy between the theory using the Heisenberg model, Eq. (4.3), and experiment is not entirely clear at the time of this writing: However, a number of possibilities can be readily suggested. Among these are the inclusion of nearest-neighbor two-body exchange only, the adequacy of the Heisenberg model, and the convergence or correctness of the series expansion, Eq. (4.4). The last possibility seems unlikely to be the source of the trouble. As we will discuss shortly, the explanation may lie in the fact that higher-order exchange has been neglected.

In order to rule out spurious effects, several checks have been made in the experiments of KA. Samples made with different amounts of ^{4}He impurities ($\sim$2 ppm and 400 ppm) did not show different behavior of $P_V(T, H)$. The capacitance of the empty strain gauge in $\sim$0 and 40 kG fields was observed and found to have no temperature dependence. The strain gauge had a resolution of 2×10^{-6} atm with no indication of hysteresis. The values of the magnetic field, produced by a superconducting solenoid, were verified using a search coil. Special precautions were taken to eliminate effects of the large magnetic fields in temperature measurements. Thermal equilibrium times for the sample were checked and found to be short, <1 minute for $V\approx24.0$ cm^3/mole in 60 kG. These short times are confirmed by the recent high-field χ measurements of Johnson, Paulson, Giffard, and Wheatley (1972) for solid ^{3}He on the melting curve, for $T>5$ mK. At higher fields and smaller V, longer relaxation times were found (Kirk and Adams, 1972) and the approach of the system to equilibrium was followed. Thus it can be concluded that the drastic departure of $P_V(T, H)$ from the behavior expected on the basis of $\mathcal{H}_{nn}$ is a real effect.

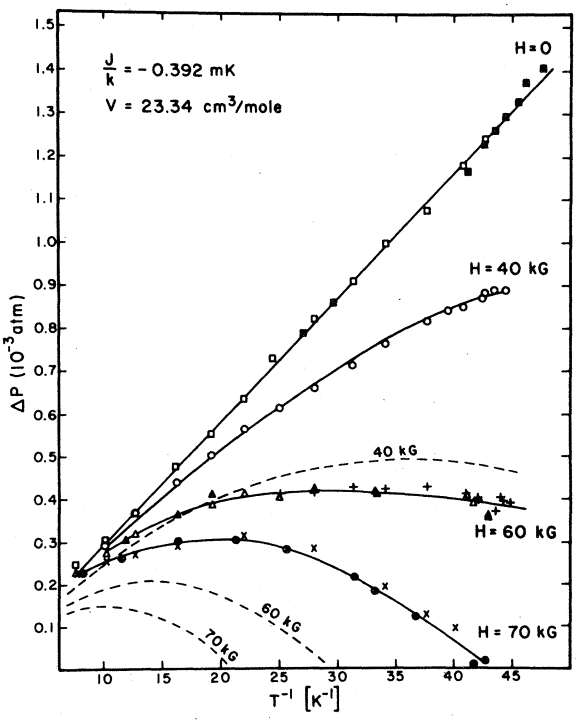

FIG. 42. Pressure differences versus T^{-1} for $V=23.34$ cm^3/mole[5] in fields of 70, 60, 40, and 0.5 ($H\approx0$) kG. Various symbols for a given H are for different traversals of the temperature region. The curves through the data at different fields are simply to connect the points. Dashed curves are calculated behavior based on the Heisenberg model, Eq. (4.3). (After Kirk and Adams, 1972).

A possible explanation for the unexpected behavior of $P_V(T, H)$ has been offered by Zane (1972a, b). As we have already stressed, the Heisenberg Hamiltonian considered in Eq. (4.2) included only nearest neighbor pair exchange J, which we will now designate as J_2. However, Zane has suggested that to this Hamiltonian there should be added a triple exchange term

$$\mathcal{H}^{(3)}=2J_3\sum_{i<j<k}(I_i\cdot I_j+I_j\cdot I_k+I_k\cdot I_i), \qquad (4.26)$$

where J_3 is the exchange energy of three particles permuted cyclically at sites (i, j, k).

The important feature of the term $\mathcal{H}^{(3)}$ is that effectively it leads to ferromagnetic ordering between next-nearest neighbors in solid ^{3}He. Thouless (1965) first pointed out that in ^{3}He two-particle exchange should be antiferromagnetic, while three-particle exchange should be ferromagnetic. Above the transition temperature, the tendency for ferromagnetic ordering of next-nearest neighbors will then lessen the influence of a magnetic field on the behavior of some thermodynamic properties of the solid, such as $P_V(T, H)$.

Using a Hamiltonian which is the sum of Eqs. (4.3) and (4.26), Zane finds for the thermodynamic pressure,

$$P_V(T, H)=(RT/V)(d\ln|J_2|/d\ln V)\times\{3x^2[1-6a(1+b)+48a^2b^2]+\cdots+2xy^2(1-9ab)+\cdots\}, \qquad (4.27)$$

where

$$a=-J_3/J_2, \qquad x=J_2/kT,$$

and

$$b=\frac{d\ln|J_3|/d\ln V}{d\ln|J_2|/d\ln V}.$$

Zane made some rough estimates of the quantities a and b, but basically considered them as adjustable parameters. The value $b=3/2$ was assigned, and a was given trial values of 1/30, 1/25, and 1/20, for computing $P_V(T, H)$ from Eq. (4.27). Comparison with some of the experimental results of Kirk and Adams is shown in Fig. 43. With $a=1/20$, the agreement between the theoretical and experimental behavior is greatly improved. The fact that only small values of a are needed for agreement is surprising and indicates how sensitive the $P_V(T, H)$ measurements are to the effects of three-particle exchange.

Comparing the expression of Zane for $P_V(T, H)$, Eq. (4.27), to that computed from $\mathcal{H}_{nn}$, Eq. (4.22), one

sees that, with the inclusion of three-particle exchange, a renormalization of the values of J_2 $(=J)$ will be required to preserve the observed zero-field behavior of $P_V(T)$. Zane finds that the values of $|J|$ obtained by Panczyk and Adams (1969) from $P_V(T)$ must be increased by about 30% to 50%. In a similar way, Zane's calculations would renormalize the J's obtained in χ measurements, increasing them by about 70%. This renormalization would cause some deterioration of the existing good agreement between J's found in χ and $P_V(T)$ experiments.

One possible effect of three-particle exchange is an increase in T_N over that expected using $\mathcal{H}_{nn}$. A more complicated expression than Eq. (4.20) for T_N, involving J_2 and J_3 or the effective nearest-neighbor and next-nearest-neighbor exchange $J(\text{nn})$ and $J(\text{nnn})$, is required. Such a relationship is not known accurately, but an idea of the expected T_N may be found by scaling the molecular-field results for nn plus nnn exchange so that the nn contribution is the same as that derived from the high-T series expansion based on $\mathcal{H}_{nn}$. Using the resulting expression for T_N and Zane's theory, a calculation from $P_V(T)$ data gives $T_N=2.25$ mK, while suceptibility data indicate $T_N=2.8$ mK. The approximations made introduce considerable additional uncertainty in T_N in each case. As we will discuss in Sec. V.1, a transition has been reported at 2.65 mK.[10] If this transition should prove to be the expected antiferromagnetic one, three-particle exchange may provide an explanation for its location at 2.65 rather than 2.0 mK.

The above suggestion by Zane for explaining the behavior of $P_V(T,H)$ appears to have considerable merit. However, it does provide an extra degree of freedom in the form of the parameter a. McMahan (1972b) has recently tried to evaluate a from careful many-body calculations using Monte Carlo methods. These calculations have been able to verify that solid ^{3}He has a ferromagnetic three-particle exchange, although determination of a definite numerical value for a has not been possible so far.

A recent computation by Harris (1971) provides additional information regarding the adequacy of the Hamiltonian, $\mathcal{H}_{nn}$. He has computed values of the fourth moments in bcc and hcp solid ^{3}He using $\mathcal{H}_{nn}$ as given in Eq. (4.2). For the bcc phase, he found values that were incompatible with the experimental NMR results of Richardson, Hunt, and Meyer (1965), and Richardson, Landesman, Hunt, and Meyer (1966). However, for the hcp phase the values of the fourth moments were compatible with the experimental results. In the hcp phase, Zane (1972b) finds that there is three-body exchange but that the exchange Hamiltonian can be described by a single parameter and is therefore structurally identical to $\mathcal{H}_{nn}$. This structure precludes the possibility of deducing a value of J_3/J_2 by experiment. $P_V(T,H)$ should be describable in terms of a single exchange parameter J_2. This result is another example of the relatively normal character of the hcp phases of solid helium compared to the bcc phases. Experimental verification of this would provide strong support for the triple-exchange hypothesis; however, this would be extremely difficult because of the small value of J_2 at the higher densities.

[10] In a recent preprint Osheroff, Gully, Richardson, and Lee (1972) have reported measurements of the susceptibility of the liquid ^{3}He in their Pomeranchuk cell. They interpret these measurements to indicate that the effects occurring at 2.65 mK are due to behavior of the liquid rather than a transition in the solid as first claimed by Osheroff, Richardson, and Lee (1972).

V. THE MELTING CURVE OF ^{3}He AND COOLING BY MEANS OF THE POMERANCHUK EFFECT

V.1. The Melting Curve (In Zero Magnetic Field)

Interest in the low temperature melting curve of ^{3}He can be traced to the work of Pomeranchuk (1950). His conclusions were based on a comparison of the behavior of the entropies of the liquid and solid at melting. The liquid entropy should be approximately linear in temperature, characteristic of a Fermi liquid. However, the entropy of the solid should have the value $R\ln 2$, characteristic of a disordered spin system, until some quite low temperature where nuclear-spin ordering occurs. The implications of this on the melting curve slope are seen from the Clausius–Clapeyron equation

$$(dP/dT)_m=(S_L-S_S)/(V_L-V_S). \qquad (5.1)$$

Although the change in volume on melting, V_L-V_S,

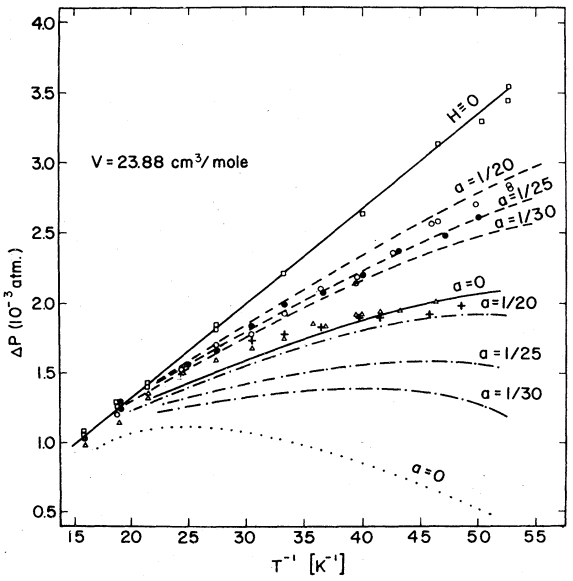

FIG. 43. Pressure difference versus T^{-1}. Comparing data from experiment of Kirk and Adams (1971) shown in Fig. 40 with theoretical calculations by Zane (1972a). For $H\approx 0$ kG: squares, experiment; solid line, theory without triple exchange. For $H=40$ kG: circles, experiment; dashed lines ($a=1/20$, 1/25, 1/30), theory with triple exchange; solid line ($a=0$), theory without triple exchange. For $H=60$ kG: triangles and crosses, experiment; dot-dashed lines ($a=1/20$, 1/25, 1/30), theory with triple exchange; dotted line ($a=0$), theory without triple exchange. (After Zane, 1972a).

may be slightly temperature dependent, we know that it must remain positive since the solid is the higher pressure phase. Thus the sign of $(dP/dT)_m$ will be the same as that of $S_L - S_S$. This situation is illustrated in Fig. 44.

The most striking conclusion of Pomeranchuk was that there should be a minimum in the melting curve at the point where the entropies are equal. Below this temperature, the melting curve slope is negative, except very near $T=0$ where spin ordering occurs in the solid. Early efforts to observe the minimum were unsuccessful because of the use of the blocked-capillary technique. Later it was realized that this method would not reveal a minimum (Roberts and Sydoriak, 1954). The first measurements of the melting pressure which showed the minimum were made by Baum, Brewer, Daunt, and Edwards (1959) using an *in situ* technique for observing the pressure.[11] A number of subsequent workers have studied the melting curve in the vicinity of the minmum, which is now well established at $T_{\min}=0.318$ K, and $P_{\min}=28.94$ atm (see Scribner, Panczyk, and Adams, 1969, and references cited therein).

Before discussing the behavior of the melting curve in the vicinity of the nuclear-spin ordering temperature of the solid, we will consider the temperature dependence of the change in volume on melting. As is apparent

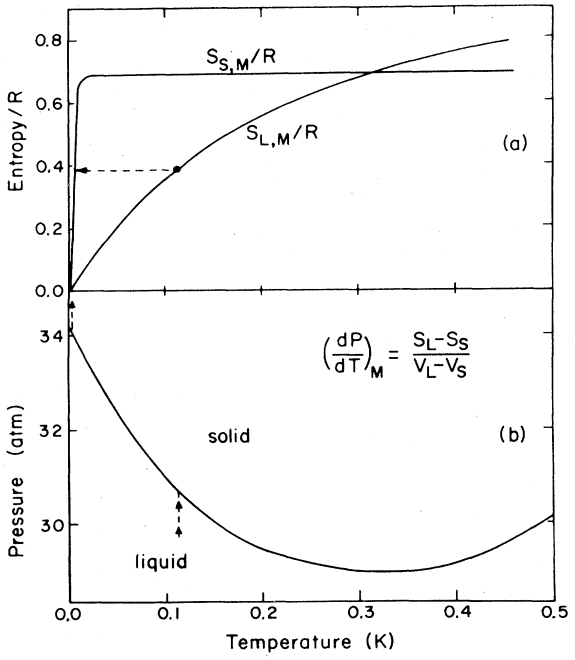

FIG. 44. The entropies of liquid and solid ^{3}He at melting and the melting curve. The dashed arrows illustrate cooling by the Pomeranchuk effect. (After Richardson, 1971).

[11] That a minimum exists had been indicated previously by observation of warming during adiabatic melting of ^{3}He below $T\approx 0.4$ K (Fairbank and Walters, 1957), and by use of a dielectric constant technique to determine the location of the minimum (Lee, Fairbank, and Walker, 1959).

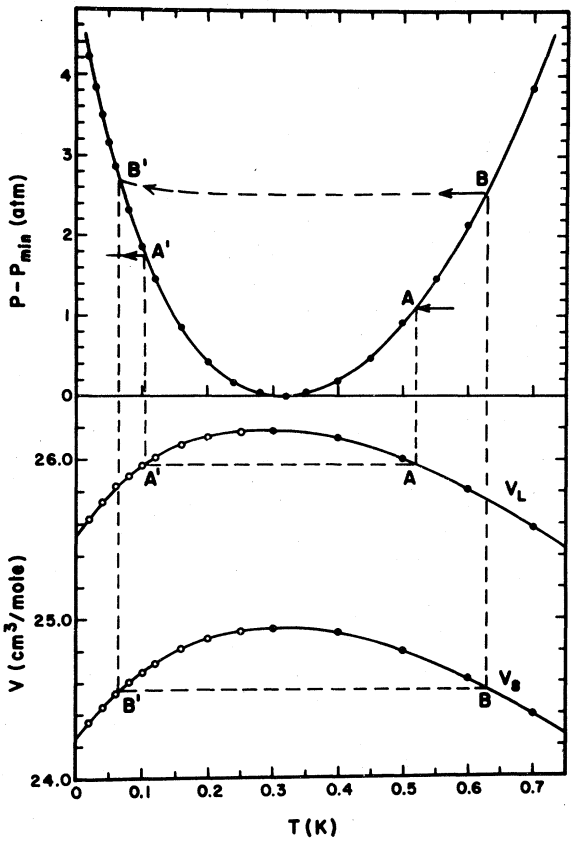

FIG. 45. The ^{3}He phase diagram in the P–T and V–T planes. P versus T, Scribner *et al.* (1969, 1972); V_L, V_S for $T>T_{\min}$, Grilly (1971); V_L, V_S for $T<T_{\min}$, Scribner *et al.* (1969), using the Grilly results. The isochores AA' and BB' illustrate the procedure of Scribner *et al.* (1969) for determining V_L, V_S for $T<T_{\min}$.

from Eq. (5.1), this quantity is needed for a full quantitative understanding of the melting curve. Mesaurements of the liquid and solid molar volumes at melting for $T>T_{\min}$ were made several years ago (Grilly and Mills, 1959; Sherman and Edeskuty, 1960; Mills, Grilly, and Sydoriak, 1961). Grilly (1971) has recently made new measurements between 0.26 and 1.8 K, which have higher precision than the earlier ones. Some values for various quantities at melting are given in the Appendix.

Until recently, no values for the molar volume were available for $T<T_{\min}$. Because of the melting-pressure minimum, the procedure used earlier for $T>T_{\min}$ cannot be used in this region. Scribner *et al.* (1968, 1969), using the procedure illustrated in Fig. 45, have determined the molar volumes at melting relative to values at $T>T_{\min}$. A constant volume sample was maintained by a solid plug in the filling capillary (which always had some portion at $T\lesssim T_{\min}$), then the sample was cooled along an isochore. From the data of Mills *et al.* (1961), the volumes V_L at point A or V_S at point B were determined. Then the temperatures of points A' or B', which are at the intersections of the isochores with the melting curve, give points on the

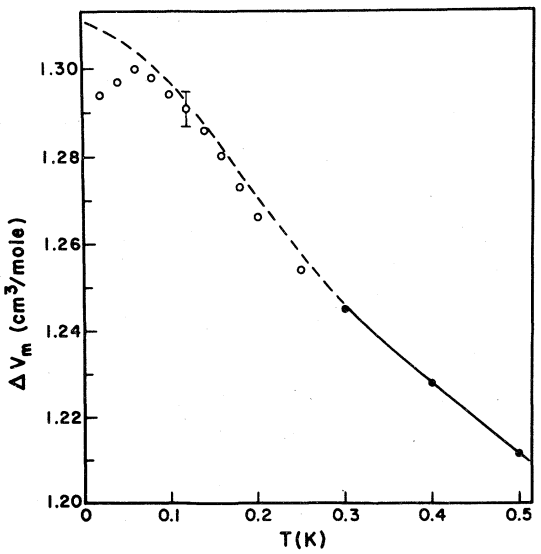

FIG. 46. Volume change of ^{3}He on melting. Solid circles: smoothed results of Grilly (1971). Open circles: smoothed results of Scribner *et al.* (1969), using Grilly results. Dashed curve: calculation of Grilly.

curves $V_L(T)$ or $V_S(T)$, respectively. By following several different isochores, both $V_L(T)$ and $V_S(T)$ were determined down to 17 mK. The difference, $V_L - V_S$, gives $\Delta V_m(T)$, the volume change on melting. The higher-temperature data (Mills *et al.*, 1961) had indicated that $\Delta V_m(T)$ was approaching a constant value of 1.20 cm^3/mole near $T_{\min}$. Instead, Scribner *et al.* (1969) found that $\Delta V_m(T)$ continued to increase to about 1.28 cm^3/mole at the lowest temperature of the measurements. Using the new data of Grilly (1971) for V_L and V_S about $T_{\min}$, the results of Scribner *et al.* have been re-analyzed, and are presented in the Appendix. The behavior of $\Delta V_m(T)$ is shown in Fig. 46. Although the results of Scribner *et al.* (1968, 1969) are the only experimentally determined $V_L(T)$, $V_S(T)$, and $\Delta V_m(T)$, calculations of some of these quantities have been made. Anderson, Reese, and Wheatley (1963) did a self-consistent calculation, using Eq. (5.1) and various experimental results, in which they obtained $V_L(T)$ (assuming $V_S = V_S(P)$ only). More recently, Goldstein (1970b) and Grilly (1971) have made calculations using values of the expansion coefficients and compressibilities to extrapolate V_L and V_S. The agreement with the measured values is generally good when one takes into account the new data of Grilly for $T > T_{\min}$. The detailed behavior of $\Delta V_m(T)$ below about 30 mK is still somewhat uncertain.

We now turn our attention to the melting curve below $T_{\min}$, paying particular attention to the region $T \sim T_N$. The minimum in P_m, discussed previously, occurs because we have classical behavior of the spins in the solid ($S = R \ln 2$) but the liquid entropy is that of a degenerate quantum liquid. As the quantum effect of spin ordering in the solid occurs at $T \sim T_N$, the melting curve should again show interesting behavior. (Our discussion at this point will be based on the assumption that the magnetic phase transition in solid ^{3}He will be as expected from the Heisenberg model with nearest-neighbor interactions only. Recently discovered effects by Kirk and Adams (1971) (see Sec. IV.5) and particularly by Osheroff, Richardson, and Lee (1972) may necessitate revisions in the resulting conclusions.[10])

On the basis of the Clausius–Clapeyron equation, many authors have calculated $P_m(T)$ and other melting properties near T_N (Bernardes and Primakoff, 1960; Anderson, Reese, and Wheatley, 1963; Thompson and Meyer, 1967; Goldstein, 1967, 1969; Scribner *et al.*, 1969). The general features expected as we go below $T_{\min}$, which were discussed first by Bernardes and Primakoff, are that the melting pressure should rise with increasing negative slope, pass through an inflection point T_{infl}, then reach a maximum, followed by a region of positive slope before leveling off with zero slope at $T = 0$ in compliance with the third law of thermodynamics.

In recent years a number of efforts have been made to observe the low-temperature behavior of the melting curve. Scribner *et al.* (1968, 1969), in work extending to 17 mK, were the first to apply the highly sensitive capacitive strain-gauge technique for meauring pressure. Because of inadequate thermal contact between the thermometer and the sample, the magnitude of the measured slope below 40 mK tended to be too large. With the measured ΔV_m, the consistency of Eq. (5.1) was established. Zeisse (1968) made measurements to 13 mK, but with poor temperature accuracy because of a low signal-to-noise ratio in calibrating his NMR thermometer.

Neither of the works mentioned above went to low enough temperatures to see the behavior expected at $T \to T_N$. By differentiating the Clausius–Clapeyron equation (with the approximation $\Delta V_m = $ const.), we see that T_{infl} should occur where $C_L = C_S$. The liquid specific heat at melting can be estimated from the data of Abel, Anderson, Black, and Wheatley (1966). Direct measurements of C_S have not been made. But, using the series expansion (Eq. 4.6) and a value of $J/k = -0.72$ mK appropriate to the solid at melting near $T = 0$ (Panczyk and Adams, 1969), C_S may be calculated. The resulting temperature for the inflection point is $T_{\text{infl}} \approx 7$ mK. Confirmation of the inflection point at about this temperature has been provided by measurements of Johnson *et al.* (1969b, 1970a), which were the first to be made in the few-mK region. Their slopes are shown in Fig. 47.

As the temperature of the solid is lowered below the Néel point, the entropy will drop rapidly toward zero while that of the liquid should be linear in T (assuming Fermi liquid behavior).[10] The maximum in P_m will occur where $S_L = S_S$. Again the specific heat data of Abel *et al.* (1966) provide an estimate of S_L. Assuming that the solid entropy is correctly given by spin-wave

theory (Van Kranendonk and Van Vleck, 1958), we have

$$S_S/R=6.87\times10^{-3}(kT/J)^3$$

since the lattice entropy is several orders of magnitude smaller. Then setting $S_L=S_S$ gives $T_{\max}\approx0.5$ mK for the position of the maximum of P. The decrease in pressure between $T_{\max}$ and absolute zero is expected to be only $\sim10^{-5}$ atm and will be difficult to observe.

Recently Osheroff *et al.* (1972), using Pomeranchuk compressional cooling (discussed in Sec. V.3), have studied the melting pressure of solid ^{3}He. The pressure was measured using a capacitive strain guage; the nuclear susceptibility of platinum or copper, measured by NMR techniques, served as a thermometer. Below about 3.5 mK, the thermometer and the melting solid were not in equilibrium. Therefore, instead of showing $P_m=P_m(T)$, P and T were shown versus time t for a slow compression and decompression. At a pressure corresponding to a temperature of about 2.65 mK, dP/dt changed discontinuously by a factor of 1.8. Also dT_{Pt}/dt was discontinuous as shown in Fig. 48. Osheroff *et al.* argued that the discontinuity in dP/dt must be due to a discontinuity in dP/dT. If this conclusion is correct, the implications are most profound, since the solid would have undergone a first-order transition instead of the expected second-order magnetic phase transition.[10]

Johnson, Symko, and Wheatley (1972) have reported a rapid decrease of the diffusion coefficient and transverse relaxation time at low temperature which they interpret as supporting the findings of Osheroff *et al.* However, there were problems with interpreting the work because neither the fraction of solid in the pick-up coil nor the absolute temperature was known.

Because of the non-equilibrium nature of the measurements in their experiment, the inferences of Osheroff *et al.* are subject to criticism. A combination of the large increase in specific heat of the solid near the magnetic

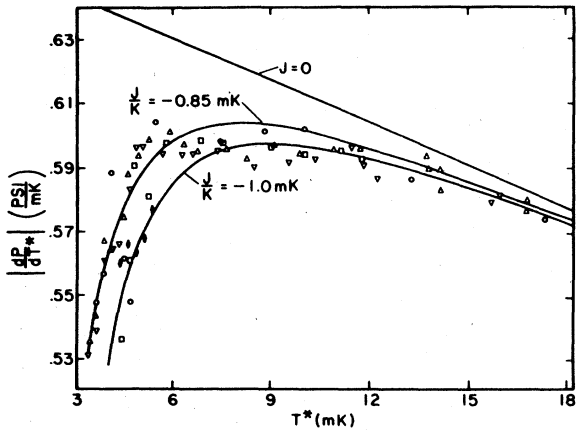

FIG. 47. The ^{3}He melting curve slope versus T^*, the CMN magnetic temperature. The various symbols are for different runs. (After Johnson *et al.*, 1970a).

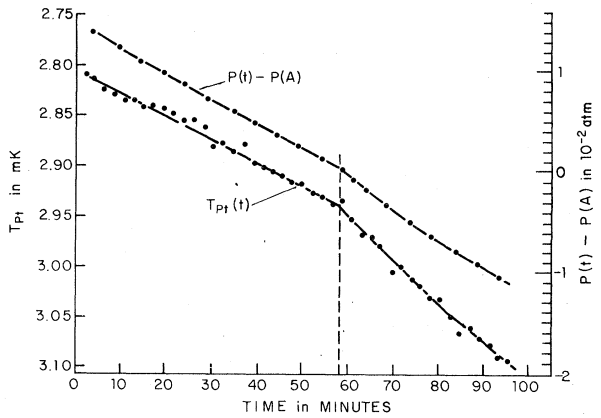

FIG. 48. ^{3}He melting pressure and platinum thermometer temperature versus time during a Pomeranchuk compression. (After Osheroff *et al.*, 1972).

transition and possible changes in thermal conductivity could cause dP/dt to be discontinuous while dP/dT is not. Such a criticism of the work has been made by Horner and Nosanow (1972) who suggest that Osheroff *et al.* have observed the expected magnetic second-order transition. With a ferromagnetic three-body exchange in addition to the antiferromagnetic two-body exchange (see Sec. IV.5), the Néel temperature would be higher than previously expected. Obviously much more experimental work is required to settle this question. If the conclusions of Osheroff *et al.* are corroborated in further work, determining the nature of the phase transition will be one of the most interesting and active areas of research in the next few years.[10]

V.2. Magnetic-Field Dependence of the Melting Curve

Since the melting curve slope is proportional to S_L-S_S and S_S is modified by the application of a strong magnetic field [see Eq. (5.2) below], while S_L is affected very little, $(dP/dT)_m$ and $P_m(T)$ should be field dependent. This was first discussed by Goldstein (1968a) who made extensive calculations using the high-temperature series expansion of the partition function for the Heisenberg Hamiltonian, Eq. (4.4). In connection with the effect of a magetic field in compressional cooling (to be discussed in Sec. V.4), Walstedt, Walker, and Varma (1971) have calculated the behavior of $P_m(T, H)$ for $H=74$ kG using molecular-field theory. Their results are shown in Fig. 49. It is seen that there is a sizable effect on P_m even at $T=20$ mK. At this temperature we have $P_m(H=0)-P_m(H=74\text{ kG})\approx0.04$ atm, which is easily detectable with present strain gauges. However, other experimental considerations make observation of this pressure change extremely difficult. For instance, in comparing $P_m(T, H=0)$ with $P_m(T, H=75\text{ kG})$, if T differs by as much as 1 mK, a corresponding change in $P_m=0.04$ atm

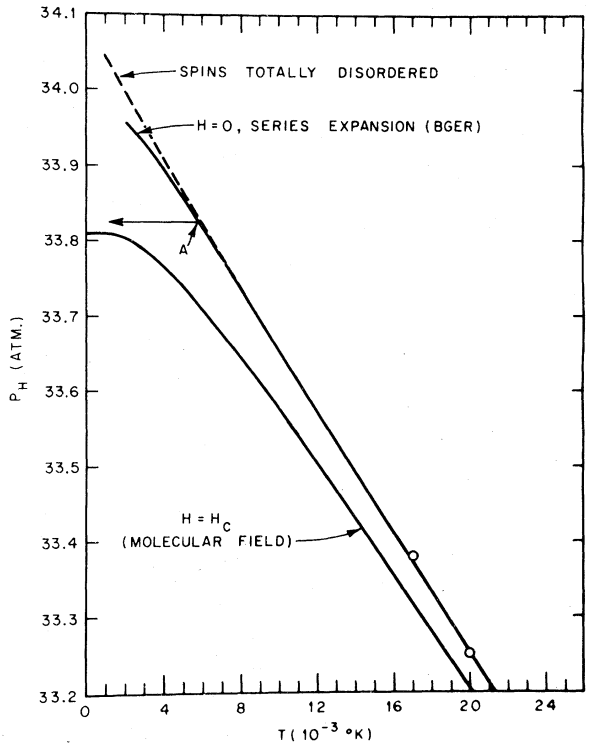

FIG. 49. Calculated behavior of the ^{3}He melting pressure near $T=0$. (After Walstedt *et al.*, 1971).

occurs. Thus, very precise reproducibility in temperatures under conditions of $H=0$ and $H=74$ kG is required.

A number of experimenters have observed the melting pressure in a magnetic field. Kirk and Adams (1971) first reported such observation, finding a depression of 0.03 atm in 60 kG at 20 mK. Osheroff *et al.* (1972) made measurements in fields up to 13.4 kG, down to 5 mK, and found results in agreement with calculations based on the high-temperature Heisenberg expansion, Eq. (4.4), The most extensive measurements have been made by Johnson, Rapp, and Wheatley (JRW, 1971, 1972a). These were made in fields as large as 63.6 kG and at temperatures as low as 5 mK, which were measured by the γ-ray anisotropy from ^{54}Mn. Originally JRW assumed that the measured melting curve in 2.12 kG agreed with the theoretical curve and made an adjustment of the temperature, which became of increasing importance below 12 mK, to secure this agreement. With this temperature adjustment applied to all the data the effect of the higher magnetic fields was considerably greater than expected theoretically.

JRW (1972) have since renalyzed their data using a different assumption. They argued that, because of incomplete saturation of the host iron for the ^{54}Mn in low fields, the thermometry should be more reliable at high fields. Thus they assumed that the measured melting curve in 63.6 kG agreed with the theoretical curve. With this assumption imposed at higher temperatures, the low-temperature points fell at too high a pressure compared to the theory. Again the discrepancy was assumed to be due to a difference in temperature between the thermometer and the ^{3}He as a result of self-heating in the thermometer. A temperature adjustment which brought the 63.6 kG experiment and theory into agreement was applied to all the data. This time the low-field results did not agree with theory.

In all of the above discussion, the theoretical calculations referred to make use of the Heisenberg Hamiltonian with nearest neighbor interactions only, $\mathcal{H}_{nn}$. Since these calculations were made, the inadequacy of this Hamiltonian in representing the high-field behavior of $P_V(T,H)$ of the solid has been seen (Kirk and Adams, 1971), and we are led to the question of how this should affect the high-field melting curve. The nature of the effect can be seen by examining the expression for the solid entropy, which is approximately proportional to $(dP/dT)_m$ since S_L is small at temperatures of interest. From $\mathcal{H}_{nn}$ and Eq. (4.5) we have

$$(dP/dT)_m\tilde{\alpha}S_S/R = \ln 2-\tfrac{3}{2}x^2+x^3+\cdots -\tfrac{1}{2}y^2[1+8x+36x^2+\cdots]+\cdots, \quad (5.2)$$

where $x=J/kT$, $y=\mu H/kT$. Unless we have $y\to 1$, the effect of the field on the melting curve is small. Even in the case $y\to 1$, the leading term in the series which is the coefficient to $y^2/2$ is unity. The details of exchange enter only in the next term $8x$. Thus the melting curve in a high field is rather insensitive to the details of exchange and departures from calculated behavior using $\mathcal{H}_{nn}$ should be quite small. These details are brought out only in $P_V(T, H)$ of the solid where exchange occurs in the leading term of the series coefficient of y^2, the constant term having been removed on taking $\partial \ln Z/\partial V$ [see Eq. (4.22)]. In the experimental work on the melting curve in a high field discussed above, only the measurements of JRW were at sufficiently large values of x and y to be sensitive to the details of exchange. But in their case any possibility of observing such effects was removed by the uncertainty in their temperature scale which they adjusted to force agreement between experiment and theory using $\mathcal{H}_{nn}$.

V.3. Cooling by Means of the Pomeranchuk Effect

Our aim here will be to give the basic ideas involved and to indicate the types of experiments being done with this method of cooling. The original literature, cited below, should be consulted for the details needed to implement the method.

Following his calculation which showed that the melting curve of ^{3}He should mave a minimum, Pomeranchuk (1950) suggested that adiabatic compression along the melting curve below the minimum would produce cooling. This is illustrated in Fig. 44, where it is seen that the final temperature reached should be in the vicinity of T_N, the spin-ordering temperature of the solid. The large change in entropy of the solid, $R\ln 2$, near T_N makes this method competitive with others such as adiabatic demagnetization in terms of cooling ability.

The soundness of Pomeranchuk's idea was recognized, although it was not until 15 years later that the first attempt was made to put it into practice. One reason for this reluctance can be seen on comparing the mechanical work involved in the compression $\Delta W = P_m(V_L - V_S)$ to the heat which is extracted at constant temperature $\Delta Q = T(S_S - S_L)$. Over the range of interest ΔQ is $\approx 1\%$ of ΔW. This is of no concern if the work can be done completely reversibly. But, because of friction in the compression process, it is never completely reversible. Thus, if the frictional heating is $\gtrsim 0.01\Delta W$, there will be no cooling at all.

Anufriyev (1965) was the first to demonstrate that the frictional heating could be kept small. Starting at 50 mK, he reached a temperature of less than 20 mK (the actual temperature was probably much lower than this, but was not known because of thermometry problems). Because of the minimum in the melting curve, the compression of the ^{3}He must take place through deformation of the chamber walls. (For complete solidification a change in volume $\Delta V_m/V \approx 5\%$ is required.) To accomplish this Anufriyev used a flexible ^{3}He chamber surrounded by a second chamber which could be pressurized with liquid ^{4}He. With a ^{4}He pressure of <25 atm in the outer chamber, a pressure ~ 34 atm, sufficient to solidify the ^{3}He, is achieved in the inner chamber, the difference being supplied by the tension in the walls. All subsequent workers have used this scheme or some variation of it.

Since Anufriyev's work, Pomeranchuk cooling has been used extensively by Johnson, Wheatley, and co-workers and by Lee, Richardson, and co-workers. Johnson, Rosenbaum, Symko, and Wheatley (1969a) reached a temperature of about 2 mK. Since then they have used Pomeranchuk cooling to study the melting curve, as has already been discussed (Johnson *et al.*, 1969b, 1970a, 1970b, 1971, 1972a), and spin polarization of solid ^{3}He (Johnson *et al.*, 1972b). The Cornell group has used this method of cooling to study the susceptibility of solid ^{3}He (Sites, Osheroff, Richardson, and Lee, 1969), spin diffusion in liquid ^{3}He (Corruccini, Osheroff, Lee, and Richardson, 1971), and nuclear-spin ordering of the solid[10] along the melting curve (Osheroff *et al.*, 1972).

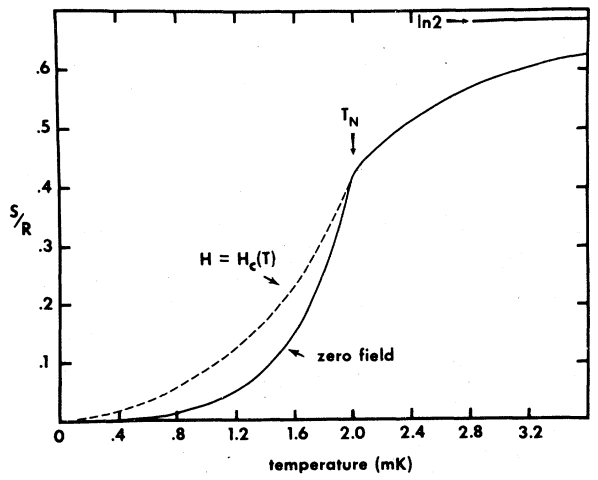

FIG. 50. Estimated variation of entropy with temperature for solid ^{3}He assuming isotropic nearest-neighbor exchange. (After Wolf *et al.*, 1971).

As is clear from the above, Pomeranchuk cooling is ideally suited for studies of the ^{3}He melting curve and of liquid and solid ^{3}He at melting in the Pomeranchuk cell itself. In the latter two cases one would like to be able to control the location of the liquid and solid in the cell, which is possible to some extent. Because the melting curve slope is negative, solid will tend to form first in the hotter regions of the cell. At the expense of some loss in cooling ability, heat can be supplied in the region where the solid is desired (Sites *et al.*, 1969). Also since the melting curve is depressed by a magnetic field, the solid will tend to form in regions where the field is strongest. If the temperature gradients are not too large, the solid can be induced to form in other than the warmest region, if desired, by placing it in the strongest field.

V.4. Pomeranchuk Effect in Strong Magnetic Fields

As we have discussed previously, a strong magnetic field affects the entropy of the solid and the behavior of the melting curve. Goldstein (1970a) was the first to point out that use could be made of this to lower the final temperature attainable in the Pomeranchuk affect. Goldstein's molecular-field calculation implicitly assumed that there is an anisotropic spin interaction of sufficient magnitude to prevent the spin-flop configuration in the fields of interest. However, as has been pointed out by Walstedt *et al.* (1971) and by Wolf, Thorpe, and Alben (1971), there is only a very small anisotropy in bcc ^{3}He, making Goldstein's implicit assumption incorrect although the basic idea has merit. Using a spin-wave calculation, Walstedt *et al.* and Wolf *et al.* evaluate the entropy of anitferromagnetically ordered solid ^{3}He (also see Bonner and Nagle, 1972). If there is an applied field equal to the $(T=0)$ value $H_c = 2zIJ/\mu$ (where z is the coordination number) necessary to produce the spin-flop-to-paramagnetic phase transition, a disordering effect is produced. In the paramagnetic phase, the configuration of the system is identical to that in a ferromagnetic phase, with the spin-wave entropy going as $T^{3/2}$ instead of T^3 for the antiferromagnet. This is shown in Fig. 50. The critical field is a function of T, being 74 kG at $T=0$, and going to zero at T_N. Thus the entropy curve for $H=0$ merges with that for $H=H_c$ at T_N. Since the entropy curve for the solid in a nonzero field lies to the left of the zero-field entropy, lower temperatures may be reached in performing the compression in a field $H \geq H_c$. The theoretical minimum temperature attainable, which is determined by $S_S(T, H_c) = S_L(T)$, is about two orders of magnitude below the minimum for $H=0$. As illustrated by the arrow at point A in Fig. 49, Walstedt *et al.* have suggested that the last few mK of the cooling

process be carried out by adiabatic magnetization, thereby reducing frictional losses due to compression. Although this process would occur at constant pressure, it would be accompanied by distortion of the cell and motion within it due to the change in volume as solid forms. Thus it is not clear that there would be a significant reduction in frictional heating. In addition, the magnetization itself might not be completely reversible. So far these ideas have not been put to the experimental test required to determine their usefulness. Should such tests establish the viability of this approach, the fact that in the final state a field of 74 kG is present will somewhat restrict the range of experiments to which the method is suited.

V.5. ^{3}He Melting Pressure Thermometry

The Pomeranchuk effect, discussed previously, provides a beautiful example of the Simon (1952) statement concerning the ability to reach temperatures in some given region of interest: "when the system has lost practically all its entropy, ···only a desert lies before us and so we are not interested in going further···. If, on the other hand, some new phenomenon is going to occur at lower temperatures then we will be able to make use of it to reach this oasis of interest." As a corollary to this, we offer the following: use can also be made of the phenomenon to provide a means of thermometry at the temperatures of interest. Use of the ^{3}He melting pressure for thermometry in the millikelvin region is an example of this. The idea was first proposed by Adams (1967), and has been elaborated by Scribner *et al.* (1969, 1970, 1972), Only a brief outline will be given here; the reader is referred to these papers, particularly the latter, for details.

Finding suitable temperature-dependent parameters for thermometry in the millikelvin region and below is one of the outstanding problems faced in low-temperature research. The ^{3}He melting pressure $P_m(T)$ offers one possibility, with one of its main advantages being the extremely high resolution available. Over most of the range between 2 mK and the minimum in P_m the magnitude of the slope is $|dP_m/dT| \sim 40$ atm/K. With present strain guages (Straty and Adams, 1969), changes in pressure of 2×10^{-6} atm are detectable. Thus one has a temperature resolution of 5×10^{-8} K. In analogy with vapor pressure thermometry, the melting pressure is measured by the strain-guage technique, and $P_m(T)$ used to determine the temperature. The major problem which remains is establishing with good accuracy the relationship $P_m=P_m(T)$. Several approaches to this are possible: (1) Measurement of $P_m(T)$ by some other means of thermometry to empirically establish the relationship. The work of Scribner *et al.* (1968, 1969) and of Johnson *et al.* (1970a) are major steps in this direction; (2) The Clausius–Clapeyron equation, Eq. (5.1), may be integrated using known or extrapolated values for the quantities occuring in it. Goldstein (1969) has made extensive calculations toward this end; (3) Some other thermometric parameter $\alpha=\alpha(T)$ (such as the susceptibility of CMN) with a known temperature dependence, but with the constants in the equation undetermined, may be used in conjunction with P_m and the *known* values of $(dP/dT)_m$ to self-consistently determine T. This apprach has been used by Johnson *et al.* (1970a); (4) In analogy with

$$T=\frac{dQ/dT^*}{dS/dT^*}$$

used to establish the $T-T^*$ relation for a paramagnetic salt, the relation

$$T=\frac{dQ/dP_m}{dS/dP_m}$$

could be used along the melting curve. This approach has not been used since it would be rather laborious. Some values of P_m versus T determined by CMN thermometry are given in the Appendix.

This method of thermometry is a natural one to use in experiments on the ^{3}He melting curve, since in this case the ^{3}He under study can provide its own means of cooling and thermometry! Use has been made of it in a number of recent experiments (Johnson *et al.*, 1970a, Kirk and Adams, 1971, Osheroff *et al.*, 1972). Because of problems in making thermal contact with another specimen being studied, the method may receive only limited use in experiments not involving melting ^{3}He. In the experiment of Kirk and Adams (1971), the sample cell was first filled with melting ^{3}He which was used to calibrate a carbon resistor. The cell was then filled with solid ^{3}He under study and the carbon resistor used as a thermometer.

VI. PHASE SEPARATION IN SOLID ^{3}He–^{4}He MIXTURES

Although for some time phase separation had been known to occur in liquid helium mixtures, it does not seem to have been considered in the solid before its discovery by Edwards, McWilliams, and Daunt (EDM, 1962a). These authors were doing a specific heat study of ^{3}He to look for evidence of nuclear-spin ordering. As was common at that time, their sample had sizable ^{4}He impurities present. They observed that, at a certain temperature depending on the impurity concentration, there was a large anomaly in the specific heat, as shown in Fig. 51. After their original observation of the phenomenon, the work was extended to a wider range of concentrations (Edwards *et al.*, 1962b).

The large specific heat indicates that some ordering process is occurring. Such an anomaly might occur as a result of an order-disorder transition as occurs in some alloys, or as a result of separation of the solid into two phases similar to that which occurs in liquid ^{3}He–^{4}He

mixtures. That the anomaly is due to phase separation was shown clearly by EMD by study of a sample of 82% ^{4}He at a pressure of ~30 atm. This pressure is below the freezing pressure of pure ^{3}He at $T \lesssim 0.1$ K. Therefore, if phase separation occurs, the enriched ^{3}He portion should begin to melt at lower temperatures, which was observed to occur (see Fig. 51).

The temperature at which phase separation occurs is shown as a function of concentration of ^{3}He in Fig. 52. In addition to indicating the phase-separation temperature T_{ps} for a given x (concentration), this curve gives the concentrations of the two phases for temperatures below T_{ps}. To date there has been no study to show how the two phases are distributed. The separation is probably not on a bulk scale as in the liquid, but may instead consist of small clusters of each phase intermingled.

The work of EMD was interpreted by them in terms of the thermodynamic regular solution theory (see, for example, Slater, 1939). Since then there has been a microscopic theory given by Mullin (1968a) which makes some further predictions concerning the phase separation. Most of these predictions have been verified quantitatively by Panczyk, Scribner, Gonano, and Adams (PSGA, 1968). All these points will be elaborated in this section.

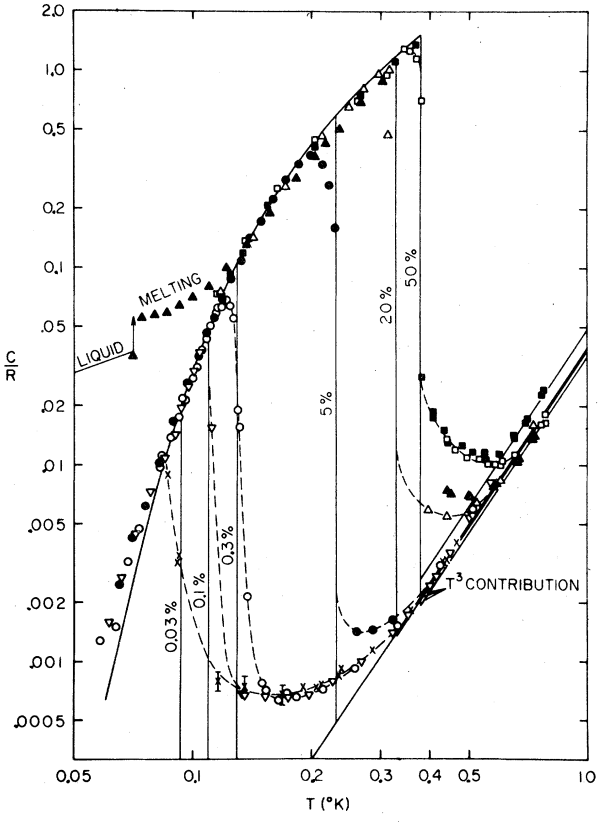

FIG. 51. The specific heat of ^{3}He–^{4}He solid mixtures as a function of temperature. Percentages shown refer to the ^{4}He concentrations. (After Edwards *et al.*, 1962b).

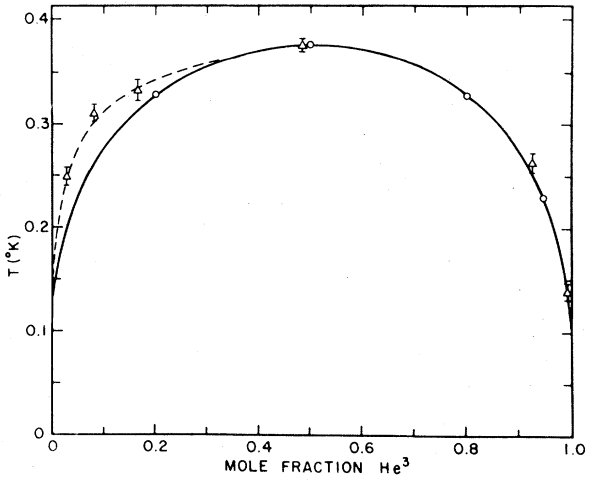

FIG. 52. Phase-separation temperature of solid ^{3}He–^{4}He mixtures versus concentration of ^{3}He. Triangles: Panczyk *et al.* (1968). Circles: Edwards *et al.* (1962b). Solid line: regular solution theory.

In the following, all quantities will be molar (whether indicated by lower case letters or not), and $x = N_3/(N_3+N_4)$ will denote the ^{3}He concentration. In the thermodynamic regular-solution theory, the equilibrium concentration is found as a function of temperature by minimizing the Helmholtz free energy $A = U - TS$. U contains a term in ΔE which is the energy of mixing, and S is the usual entropy of mixing. (Lattice energy and entropy do not need to be included since these remain roughly unaffected by separation.) With $\Delta E > 0$, separation is favored at $T = 0$; at $T \neq 0$ the equilibrium concentration is determined by a balance between ΔE and $-T\Delta S$. Minimizing A gives for the phase-separation curve

$$T_{ps}(x) = \frac{\Delta E}{R}\left(\frac{1-2x}{\ln[(1-x)/x]}\right). \qquad (6.1)$$

This curve is symmetrical about $x = 0.5$ where T_{ps} has a maximum value $T_{max} \equiv T_c = \Delta E/(2R)$. Here $\Delta E/(2R)$ or T_c is taken as an adjustable parameter. When T_c was given the value 0.38 K, the fit of Eq. (6.1) to the points of EMD was amazingly good, in view of the simplicity of the theory. T_c is a function of pressure; the value quoted here is for $P \approx 30$ atm.

The specific heat in the two phase region is given by

$$C_V = 2RT_c(1-2x)\,(\partial x/\partial T)_V, \qquad (6.2)$$

where $(\partial x/\partial T)_V$ is to be obtained from Eq. (6.1). This is the form shown by solid lines (see Fig. 51) in the data of EMD (1962a, b). The equation gives a sharp peak with a discontinuous drop to zero as mixing is completed on raising the temperature. The data show some rounding at the peak and a high-temperature "tail" which is probably due to short-range order not

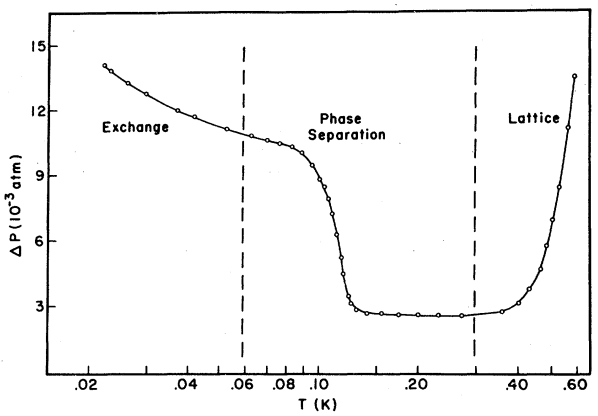

FIG. 53. Isochoric pressure of solid ^{3}He with 1600 ppm ^{4}He versus temperature. ΔP indicates changes in P_V relative to an arbitrarily chosen reference value. The designations lattice, phase separation, and spin ordering indicate the regions where these have the major effect on $P_V(T)$.

considered in this thermodynamic treatment. Otherwise, the fit is again surprisingly good.

Other thermodynamic properties also show anomalous behavior. In particular the "excess" volume and "excess" pressures are obtained from

$$V^E=(\partial G^E/\partial P)_T \quad \text{and} \quad P^E=-(\partial A^E/\partial V)_T,$$

where the excess quantities are related to the increase in that quantity on mixing, and G is the Gibbs free energy. We have

$$G^E=\Delta E x(1-x)=2RT_c x(1-x), \tag{6.3}$$

$$V^E=2Rx(1-x)(dT_c/dP), \tag{6.4}$$

and

$$P^E=-2Rx(1-x)(dT_c/dV), \tag{6.5}$$

where P^E and V^E are not independent but are related by $V^E=VK_TP^E$, where K_T is the compressibility of the mixture. A point to note is that in a measurement of V^E or P^E one obtains dT_c/dP or dT_c/dV from data at a single pressure or volume, rather than requiring measurements at several pressures to give $T_c(P)$. This method of studying the phase separation has been used by PSGA and will be discussed after giving the results of the Mullin (1968a) theory.

The Mullin theory of quantum crystal mixtures is based on the Nosanow theory for pure crystals. Thus the ground state trial wave function is

$$\psi_0=\prod_i \varphi_3(i)\prod_j \varphi_4(j)\prod_{k<l} f_{33}(kl)\prod_{m<n} f_{44}(mn)\prod_{p,q} f_{34}(pq), \tag{6.6}$$

where the φ's are single-particle Gaussians, and the f's are short-range correlation functions. Each of the φ and f contains a parameter which could be adjustable, but only those in φ were varied by Mullin. Those in the f's were given values based on the results for pure crystals. The energy was evaluated by the cluster expansion technique (Nosanow, 1966) and from this was obtained the excess Gibbs free energy

$$G^E=x\Delta e_3+(1-x)\Delta e_4+x(1-x)\Delta E+PV^E. \tag{6.7}$$

Here ΔE has the same meaning as before but turns out to be very small in this case. The Δe are defined by

$$\Delta e_i=e_i[V_{\text{mix}}(P)]-e_i[V_{\text{pure}}(P)],$$

where e is the internal energy.

Classically we have $V_3=V_4$ and $\Delta e_i=0$. But because of the difference in zero-point energy of ^{3}He and ^{4}He, $V_3\neq V_4$ and $\Delta e_i\neq 0$. Thus the difference in zero-point energy plays the crucial role rather than $\Delta E_{(\text{classical})}$. Again V^E is the change in volume on mixing,

$$V^E=V(x,P)-xV_3(P)-(1-x)V_4(P). \tag{6.8}$$

Once Δe_3, Δe_4, and $V(x,P)$ are calculated, the thermodynamic quantities are determined. The major results of the Mullin theory are as follows:

(1) At $P=35.8$ atm, we have $V^E=-0.4x(1-x)$. This is of the regular solution form, i.e., it has an x dependence of $x(1-x)$, with $2R\ dT_c/dP=-0.4$ [see Eq. (6.4)].

(2) Instead of the regular solution form for G^E, we have

$$G^E=x(1-x)[a+bx].$$

The effect of the term in bx is to make the $T_{\text{ps}}(x)$ curve somewhat asymmetrical, with $T_{\text{ps}}(x<0.5)>T_{\text{ps}}(1-x)$. The asymmetry of the curve arises through the difference in compressibility of the two pure phases and is therefore expected to be a real effect.

(3) We find $T_c=0.47$ K, not at $x=0.5$ but at $x=0.45$. The agreement with the experimental $T_c=0.38$ K must be considered rather good.

(4) At $P=55$ atm, we have $T=0.45$ K, or $(dT_c/dP)_{\text{Av}}\approx -1$ mK/atm.

(5) At $x=0.5$, we have $P^E\approx -1$ atm, independent of pressure (note error in Mullin's original value and errata).

We now describe the $P_V(T)$ study of ^{3}He–^{4}He mixtures, which is able to test the predictions of the Mullin theory. In this type of experiment, the strain-gauge technique was used to measure $P_V(T)$ of the mixtures in going through the phase separation region. Typical results of PSGA are shown in Fig. 53. It is fortunate that, for most concentrations of interest, the phase separation occurs in a region where the phonon and spin-ordering contributions to $P_V(T)$ are quite small. At $T\ll T_{\text{ps}}$, phase separation is almost complete. Therefore, the increase in pressure in going from $T\ll T_{\text{ps}}$ to T well above T_{ps} is the excess pressure, P^E. In this type of study one finds $P^E(x)$ and $T_{\text{ps}}(x)$, which is identified as the inflection point of $P_V(T)$ in the phase-separation region. Results, in the phase-separation region only, are shown in Fig. 54 for $x=0.485$, for several values of applied pressure (in the mixed phase

region). Quite large values of P^E (≈ -1 atm) were observed in this case, in agreement with Mullin's calculation. The section of the curve labeled bcc–hcp indicates the onset of a crystallographic change in one of the phases. At the temperature and pressures involved, the crystal structure of pure ^{3}He is bcc while that of ^{4}He is hcp. In the single-phase region, the structure depends on the concentration. Hence we expect a crystallographic change in one of the two almost pure phases after separation. Such changes frequently occurred, accompanied by large pressure changes. This complicated the study of the phase separation since both phase separation and crystallographic changes contributed to observed changes in pressure.

Several samples in the range $0.007<x<0.996$ at $P\approx 30$ atm were studied by PSGA. (Phase separation was seen for all these concentrations, in contrast to the situation in the liquid, which is stable for $x<0.06$.) In view of the asymmetry predicted by Mullin, particular attention was paid to the region $x<0.2$, which was not covered earlier by EMD. The results of PSGA are shown by the triangles of Fig. 52. A slight asymmetry in the direction predicted by Mullin was seen. Verification that T_c occurs at $x<0.5$ was not possible because of the flatness of the curve. (We point out that the calculation of Mullin is for a bcc lattice for all x.

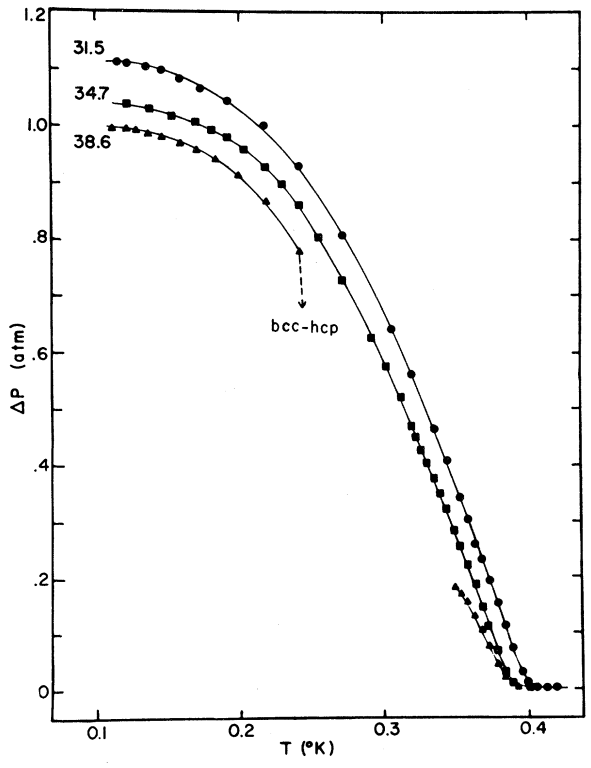

FIG. 54. The pressure change due to phase separation for $x_3=0.485$ at the indicated sample pressures. The line labeled bcc–hcp is explained in the text. (After Panczyk *et al.*, 1968).

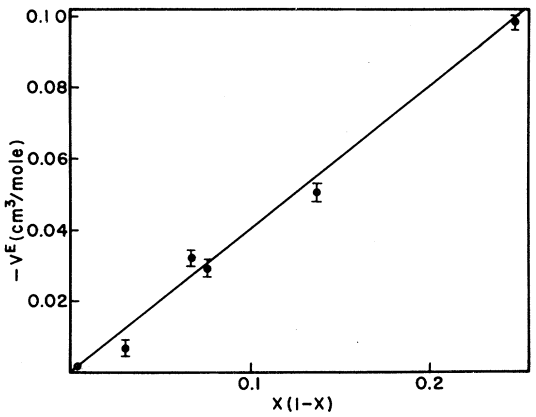

FIG. 55. The excess volume of mixing of ^{3}He and ^{4}He. Solid line: Mullin (1968a); Solid circles: Panczyk *et al.* (1968). (After Adams *et al.*, 1969).

As noted above, for $x\to 1$ the lattice is bcc, while for $x\to 0$ it is hcp. Just how this should affect the phase separation is not known, although Mullin argued that the effect is small.)

Using the observed P^E and a value of K_T appropriate to the mixture, $V^E=VK_TP^E$ was calculated (PSGA, 1968; Adams, Panzcyk, Scribner, and Gonano, 1969). The results are shown by the points in Fig. 55 with the straight line being the Mullin value $V^E=-0.4x(1-x)$. The agreement is quite good. As seen from Eq. (6.8), V^E is a useful quantity for an experimentalist studying mixtures since it allows the volume of the mixture to be determined from that of the pure phases under the same pressure. Using the regular solution relation Eq. (6.4), $V^E=2Rx(1-x)dT_c/dP$, it was found that $dT_c/dP\approx -2$ mK/atm for $P\approx 30$ atm, compared to an average value of -1 mK/atm calculated by Mullin between 35 and 55 atm.

In all of the experimental work described, the solid was at a pressure only slightly above the melting pressure. One would like to study the separation at higher pressures. Zimmerman (1965) has reported a decrease in the phase-separation temperature with increasing pressures. However, long time constants for the phase separation made it impractical to obtain quantitative information. This same difficulty was encountered by PSGA. Although this has not been verified, it may be that the time constant depends on the geometry of the sample. In the work of PSGA, the smallest sample dimension was ~ 1 mm, while in the EMD experiment time constants of ~ 15 sec were found in a geometry in which the helium was in pores of approximately 10 μm diameter of a copper sponge.

An investigation of P^E and time constants for phase separation for various molar volumes or pressures at $x_4=N_4/(N_3+N_4)=2.5\times 10^{-3}$ was made by Henriksen, Panczyk, and Adams (1970). This was done by quickly cooling the sample from above T_{ps} to well below T_{ps} and then watching $P(t)$ as the separation progressed,

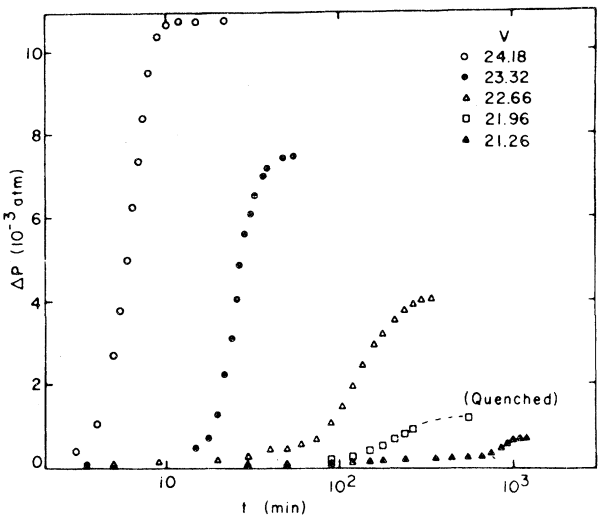

FIG. 56. A study of phase separation as a function of time through observation of the excess pressure. The curves are for various molar volumes with the ^{4}He concentration $x_4=2.5\times10^{-3}$, $T_{ps}\approx0.12$ K. The temperature was held constant well below T_{ps} as the phase separation took place. (After Henriksen *et al.*, 1970).

with the results shown in Fig. 56. For $V=24$ or $P\approx35$ atm, separation was complete in 10 min. At $V=21.3$ cm^3/mole very little separation occurred in the first 10 hr. The value of $P^E=-\Delta P(t\to\infty)$ was strongly dependent on V or P (applied). (This is in contradiction to the Mullin prediction of P^E independent of P.)

Using the regular solution result $P^E=-2Rx(1-x)\times dT_c/dV$, we can take the values of P^E reported by Henriksen *et al.* to determine $dT_c(V)/dV$ in the range $V>21$ cm^3/mole. Then by numerical integration we find $T_c(V)$, which has not been reported previously. Alternatively, we may use P^E to calculate V^E and from this dT_c/dP. The results for dT_c/dP and T_c versus pressure are given in Fig. 57. We see that dT_c/dP, decreases rapidly with increasing pressure. Hence T_c quickly reaches an essentially constant value of 0.34 K for $P\geq50$ atm. If some $T_{ps}(x, P)$ other than $T_c(P)$ is required, it can be found by scaling $T_{ps}(x, P)$ with pressure in the same way as $T_c(P)$.

Although no clear understanding has yet emerged, some recent experiments on mixtures have given information on the dimensions involved in the separation. Greenberg, Thomlinson, and Richardson (1972) have studied the "hopping time" τ_{34} for interchange of a ^{3}He atom with its neighbor in dilute mixtures of ^{3}He in ^{4}He. In one experiment, the pressure was 26.9 atm so that the enriched ^{3}He formed in liquid "bubbles" within the solid ^{4}He lattice. Assuming that the bubbles formed by a diffusion process with the atoms hopping a nearest neighbor distance every τ_{34} sec, and with the total time of 500 sec required for the bubbles to form (observed by a strain gauge as in the experiment of Henriksen *et al.*), a diffusion distance $d\approx5\times10^{-4}$ cm was obtained. If all the ^{3}He atoms within a sphere of radius d form a bubble of radius r, then $r^3=xd^3$, which with $x=0.02$ gives $r\approx2\times10^{-4}$ cm.

Burgess and Crooks (1972) have measured the thermal conductivity of mixtures with $x_3=0.1$ and 0.9 and find a decrease in thermal conductivity below T_{ps}. They interpret this decrease as due to phonon scattering from enriched domains of the less-abundant isotope embedded in a matrix rich in the more-abundant isotope. Again assuming a diffusion process, taking the time constant for separation to be $\tau=140$ sec (Adams *et al.*, 1969), and $\tau_{34}=1.4\times10^{-5}$ sec (Greenberg *et al.*, 1972), the estimated radius of the domain is $r\approx0.75\times10^{-4}$ cm, which compares favorably with the above bubble radius. These numbers should be considered only as a rough indication of dimensions involved in the phase separation.

VII. SUMMARY AND CONCLUDING REMARKS

Results from a wide variety of experiments on solid helium have been presented and discussed with an objective of pointing out relationships among them. A probing of the long-wavelength portion of the phonon dispersion curve of hcp ^{3}He and ^{4}He through the specific heat shows no unusual features. In both cases, the specific heat is quite similar to that of the heavier rare-gas solids and is reasonably well understood. A closer look (at a smaller region) through sound velocities corroborates this conclusion; for elastic Debye θ's are in good agreement with the zero-T calorimetric values. A detailed investigation of the dispersion curves of hcp ^{4}He by neutron scattering reveals that they are in fact rather normal, particularly for the lower frequencies. Some attempt to determine the extent of the high-frequency phonon broadening in this phase, as well as in the fcc phase, would be useful and could

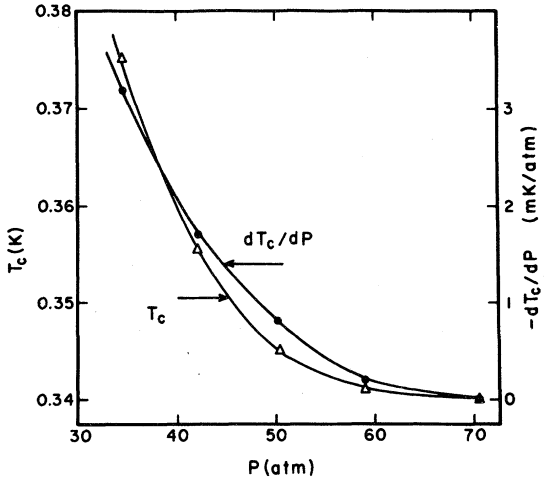

FIG. 57. Critical temperature for phase separation and its pressure derivative versus pressure. Based on the data of Henriksen *et al.* (1970).

provide a rather stringent test of line-broadening theories.

In the bcc phase of ^{3}He the situation is very different, there being anomalous behavior in the specific heat at both low and high temperatures. The high-T anomaly has been discussed in terms of vacancies, although there is no conclusive experimental evidence that this mechanism can account for all the excess specific heat and it has been questioned on theoretical grounds. Thus, results of x-ray investigation of thermally activated vacancy concentrations will be most welcome. That there is a low-T specific heat anomaly has been generally accepted because of strong supporting evidence from $(\partial P/\partial T)_V$, thermal conductivity, and sound velocities. Theoretical calculations attributing the departure from Debye behavior to anomalous dispersion are inconclusive. Because of the large capture cross section for neutrons, the neutron-scattering technique cannot be used to investigate the dispersion curves. Although technically demanding, additional ultrasonics studies would be very useful if they could provide velocities for the soft transverse branch along the [110] direction, attenuation coefficients, and velocities at very high frequencies. Extension of high-precision specific heat measurements to much lower temperatures would provide needed quantitative information on the anomaly. (See *Note added in proof* at end of Sec. II.4.)

Because it exists over such a narrow range in pressure and temperature, investigations of bcc ^{4}He are limited. The question of specific heat anomalies such as those in bcc ^{3}He cannot be answered from calorimetric data. Sound velocities adequate for evaluation of θ_0[e1] are not available. Extensive studies of the dispersion curves by neutron scattering have been made. While the dispersion curves do not appear strikingly unusual, the precision with which they are known is not sufficient to allow the extraction of high-precision information about bulk properties. One aspect of the bcc ^{4}He neutron scattering which is not at all understood is the high intensity second-zone scattering. (See *Note added in proof* at end of Sec. III.3.)

Considerable progress has been made on the question of nuclear-spin ordering in solid ^{3}He, long protected from inquiry by the remoteness of the temperature at which it is expected to occur. A rather satisfactory picture has emerged from several studies, including $P_V(T)$ and magnetic susceptibility, in the high-temperature, low-field limit. Good values of the exchange energy have been obtained and it has been shown that the ordering should be antiferromagnetic. A common element of these experiments, which have been analyzed using the Heisenberg model, is that all are sensitive to only the lowest-order term in J. A recent experiment at high magnetic field has yielded results inconsistent with the Heisenberg model when only nearest-neighbor, two-particle exchange is included. It has been suggested that this inconsistency can be removed by the inclusion of ferromagnetic three-particle exchange. Further experimental work is needed to establish fully that three-particle exchange is responsible for the observed high-field results. Measurements in the hcp phase would be useful toward this end; however, because of the small values of J and possibly long relaxation times which will be encountered, these may be extremely difficult. It seems certain that the long standing tacit assumption that bcc ^{3}He is a good example of a simple Heisenberg antiferromagnet can no longer be made. Whether the investigation of magnetism in solid ^{3}He will lead to a simple conceptual understanding of a real magnetic system (as once was hoped) or to a considerably more subtle and complicated model remains to be seen.

Various properties along the ^{3}He melting curve including the liquid and solid molar volumes, volume changes on melting, and melting pressure have been established well into the millikelvin region. The latter quantity has been pursued into the vicinity of T_N itself, expected to occur at 2.0 mK for the solid at melting. A study of the rate of change of the melting pressure with time in Pomeranchuk cooling has indicated a transition at $\approx$2.6 mK. These results have been interpreted to indicate that the transition is not the expected second-order magnetic transition but is first-order. However, because of the non-equilibrium nature of the work, this interpretation is subject to question.[10] If the observed transition does, under closer investigation, prove to be the second-order magnetic transition, its occurrence at 2.6 rather than 2.0 mK might be connected with the high-field behavior of $P_V(T, H)$ in the solid and its possible interpretation through higher-order exchange processes. Although such a suggestion is highly speculative, it does offer a possibility for restoring some conceptual order and relative simplicity to the situation. Clearly, much more work is needed for an understanding of these intriguing problems and this promises to be an area of rewarding but difficult activity.

Considerable use has been made of Pomeranchuk cooling, although primarily for experiments on melting ^{3}He itself. If problems of thermal contact can be solved, the method may see wider application in the future. The possibility of reducing the final temperature attainable in the process by application of a large magnetic field has been investigated theoretically but no experimental study has been reported. ^{3}He melting pressure thermometry has been used in several experiments, again principally in the study of the melting curve.

Most aspects of the phase separation of ^{3}He–^{4}He solid mixtures are well understood, in terms of the behavior of bulk properties. For the most part, these behave as expected from a thermodynamic regular-solution model. However, there are quantum-mechanical effects which have been successfully predicted. A detailed picture of how the phase separation occurs and

the physical dimensions involved are not available. Some progress has been made in providing this information by the study of dynamic properties such as thermal conductivity and NMR relaxation times.

ACKNOWLEDGMENTS

We have benefited greatly from conversations with our many colleagues in the study of quantum crystals. We are particularly indebted to G. Ahlers, F. W. deWette, A. Greenberg, D. Greywall, R. A. Guyer, J. A. Krumhansl, D. M. Lee, V. Minkiewicz, A. K. McMahan, H. Meyer, L. H. Nosanow, N. E. Phillips, S. K. Sinha, and R. O. Simmons, many of whom have provided us with information prior to publication or with commentary on their published work. One of us (EDA) takes pleasure in acknowledging the hospitality of Professor Olli Lounasmaa and the Technical University of Helsinki during the latter half of 1971, during which period lecture notes were prepared which served as an early version of some portions of this review. Finally, our heartiest thanks go to the Secretarial Staff of the Quantum Theory Project of the University of Florida, Michele Ellis, Josephine Larrauri, and Charlotte Rustin, for doing a superb job of a difficult task.

APPENDIX

A.I Heisenberg Hamiltonian Conventions

A number of conventions are used for the definitions of the exchange energy (or operator) in solid ^{3}He; hence, the probability of erroneously interpreting the values of J from various experiments and theories is great. An illuminating discussion regarding this problem and its possible clarification has been offered by McMahan (1971, 1972a) which, with his kind consent, is reproduced below.

If E_{ij}^+ and E_{ij}^- are appropriately defined singlet and triplet energies for the pair (i,j) then we have

$$J_{ij}=\alpha(E_{ij}^+-E_{ij}^-), \tag{A1}$$

where α has been taken as $\frac{1}{2}$, 1, and 2. These conventions cannot affect the exchange Hamiltonian as a whole since it must generate the singlet–triplet energy splittings for each pair of atoms; nor can they affect the predicted nuclear-spin ordering temperature, T_N, for the same reason. The particular convention used for J_{ij} must then be balanced by an appropriate numerical factor in front of the Heisenberg Hamiltonian.

To illustrate these matters we give a brief intuitive derivation of the Heisenberg Hamiltonian. Note that

$$E_{ij}^{\pm}=\tfrac{1}{2}(E_{ij}^+ + E_{ij}^-)\pm\tfrac{1}{2}(E_{ij}^+ - E_{ij}^-). \tag{A2}$$

Now if $\mathbf{I}_i$ is the nuclear spin operator of atom i, then we have

$$\begin{aligned}\langle\tfrac{1}{2}+2\mathbf{I}_i\cdot\mathbf{I}_j\rangle &= -1 \quad \text{in the singlet state}\\ &= +1 \quad \text{in the triplet state}\end{aligned} \tag{A3}$$

[Note, the above expression is similar to the Dirac vector model expression referred to in Sec. IV.1.] Thus we have

$$E_{ij}^{\pm}=\text{Direct terms}-(E_{ij}^+-E_{ij}^-)\mathbf{I}_i\cdot\mathbf{I}_j. \tag{A4}$$

Now, one sums over all of the pairs (i,j) making sure not to count them twice. The Heisenberg Hamiltonian comes from the spin dependent terms:

$$\mathcal{H}=-\sum_{i<j}(E_{ij}^+-E_{ij}^-)\mathbf{I}_i\cdot\mathbf{I}_j. \tag{A5}$$

In terms of Eq. (A5), the Néel temperature for bcc solid ^{3}He is given by Baker *et al.* (1967)[12]

$$T_N=1.38\,|\,E^+-E^-\,|/k, \tag{A6}$$

where $E^{\pm}$ correspond to a nearest-neighbor pair.

According to the above, the following expressions must be consistent:

$$J_{ij}=\alpha(E_{ij}^+-E_{ij}^-), \tag{A1}$$

$$\mathcal{H}=\alpha^{-1}\sum_{i<j}J_{ij}\mathbf{I}_i\cdot\mathbf{I}_j, \tag{A7}$$

$$T_N=(1.38/\alpha)\,|\,J\,|/k. \tag{A8}$$

In those cases where an exchange operator is defined, one replaces $E_{ij}^{\pm}$ by $(E_{ij}^{\pm})_{mn}$, and J_{ij} by $(\mathcal{J}_{ij})_{mn}$. Various different factors may be seen in front of the Heisenberg Hamiltonian according to whether one writes

$$\sum_{i<j}=\tfrac{1}{2}\sum_{i,j}'$$

or uses the Pauli spin operators $\boldsymbol{\sigma}_i=2\mathbf{I}_i$. The more standard convention is $\alpha=\frac{1}{2}$. We list some of the papers and the conventions they use:

$\alpha=\frac{1}{2}$
- Herring (1968)
- Thouless (1965)
- Bernardes and Primakoff (1960)
- Ebner and Sung (1971)
- McMahan (1971, 1972a)
- Panczyk and Adams (1969)
- Kirk and Adams (1971)
- Kirk, Osgood, and Garber (1969)
- Sites, Osheroff, Richardson, and Lee (1969)
- This review

$\alpha=1$
- Guyer and Zane (1969)
- Reich (1963)

[12] Baker *et al.* have studied (with the Padé approximant) the singularities of $F_1(x)$ [Eq. (4.4)] and its derivatives. With proper interpretation, the locations of certain singularities correspond to physically significant transition temperatures such as T_N.

Richards, Hatton and Giffard (1965)
Richardson, Hunt, Meyer (1965)
Johnson and Wheatley (1970a, c)

$\alpha=2$
Nosanow and Mullin (1965)
Nosanow and Varma (1969)

A.II Properties of Melting ^{3}He

Data for $T\geq 0.3$ K are those of Grilly (1971); for $T<0.3$ K, data of Scribner *et al.* (1969) are used, except that P_m for $T<40$ mK are those of Johnson *et al.* (1970a). All melting pressures have been adjusted to the same minimum value taken to be $P_{\min}=28.94$ atm. The molar-volume data, V_L, V_S, ΔV_m, of Scribner *et al.* have been reanalyzed using the Grilly results for $T>T_{\min}$ rather than the older data of Mills *et al.* (1961).

T (K)	P_m (atm)	V_L (cm^3/mole)	V_S (cm^3/mole)	ΔV_m (cm^3/mole)
1.80	67.69	22.425	21.486	0.940
1.70	63.55	22.681	21.721	0.961
1.60	59.55	22.949	21.967	0.982
1.50	55.73	23.225	22.222	1.004
1.40	52.07	23.513	22.487	1.026
1.30	48.65	23.804	22.756	1.048
1.20	45.45	24.100	23.030	1.070
1.10	42.39	24.408	23.316	1.092
1.00	39.59	24.712	23.599	1.114
0.90	36.96	25.022	23.886	1.136
0.80	34.71	25.308	24.152	1.157
0.70	32.77	25.573	24.397	1.176
0.60	31.13	25.811	24.618	1.194
0.50	29.91	26.003	24.792	1.212
0.40	29.14	26.135	24.907	1.228
0.32	28.94	26.181	24.939	1.241
0.30	28.95	26.183	24.937	1.245
0.28	28.98	26.180	24.931	1.249
0.26	29.03	26.174	24.922	1.252
0.24	29.12	26.166	24.910	1.256
0.22	29.23	26.156	24.895	1.261
0.20	29.37	26.137	24.871	1.266
0.18	29.55	26.121	24.848	1.273
0.16	29.79	26.092	24.812	1.280
0.14	30.07	26.057	24.771	1.286
0.12	30.41	26.014	24.723	1.291
0.10	30.80	25.962	24.668	1.294
0.08	31.26	25.898	24.600	1.298
0.06	31.80	25.830	24.530	1.300
0.04	32.44	25.740	24.443	1.297
0.03	32.78	25.691	24.397	1.295
0.02	33.16	25.639	24.346	1.293
0.015	33.35			
0.01	33.55			

A.III Comparison of the Molar Volumes of Solid ^{3}He at Melting

Below we give a short table for converting solid ^{3}He molar volumes at melting determined by Mills *et al.* (1961) to the newer values of Grilly (1971). The melting pressure, rather than temperature, has been used as the independent variable since it is felt that this was measured with greater precision and reproducibility.

V_{MGS} (cm^3/mole)	V_G (cm^3/mole)
23.00	23.05
23.20	23.27
23.40	23.49
23.60	23.71
23.80	23.93
24.00	24.14
24.20	24.36
24.40	24.56
24.60	24.76
24.80	24.95

REFERENCES

Abel, W. R., A. C. Anderson, and J. C. Wheatley, 1961, Phys. Rev. Letters **7,** 299.
——, A. C. Anderson, W. C. Black, and J. C. Wheatley, 1966, Phys. Rev. **147,** 111.
Adams, E. D., 1967, Quantum Fluids, Gordon Conference, Crystal Mountain, unpublished.
——, 1970, in *Proceedings of the XIIth International Conference on Low Temperature Physics*, edited by Eizo Kanda (Keigaku Publ. Co., Kyoto, Japan), p. 37.
——, H. Meyer, and W. M. Fairbank, 1960, in *Helium Three*, edited by J. G. Daunt, (Ohio State U. P., Columbus, Ohio), p. 57.
——, M. F. Panczyk, R. A. Scribner, and J. R. Gonano, 1969, in *Proceedings of the XIth International Conference on Low Temperature Physics*, edited by J. F. Allen, D. M. Finlayson, and D. M. McCall (University of St. Andrews Printing Dept.), p. 461.
Ahlers, G., 1964, Phys. Rev. **135,** A10.
——, 1970, Phys. Rev. A **2,** 1505.
——, 1972, private communication to SBT. This work is unpublished because of a thermometer failure which prematurely ended the investigation.
Alder, B. J., W. R. Gardner, J. K. Hoffer, N. E. Phillips, and D. A. Young, 1968, Phys. Rev. Letters, **21,** 732.
Ambegaokar, V., J. M. Conway, and G. Baym, 1965, in "Lattice Dynamics" edited by R. F. Wallis (Pergamon, London, 1965).
Anderson, A. C., W. Reese, and J. C. Wheatley, 1963, Phys. Rev. **130,** 1644.
——, W. Reese, and J. C. Wheatley, 1961, Phys. Rev. Letters **7,** 366.
Anderson, P. W., 1963, *Solid State Physics* **14** (Academic, New York).
Anufriyev, Yu. D., 1965, Zh. Eksperim. i Teor. Fiz.-Pis'ma Redakt. **1,** No. 6, 1, [JETP Letters **1,** (1965) 155].
Baker, Jr., G. A., H. E. Gilbert, J. Eve, and G. S. Rushbrooke, 1967, Phys. Rev. **164,** 800.
Balzer, R., and R. O. Simmons, 1972, *Proc. 13th Intern. Conf. Low Temp. Phys.*, in press.
Barron, T. H. K., and J. A. Morrison, 1957, Can. J. Phys. **35,** 799.
Baum, J. L., D. F. Brewer, J. G. Daunt, and D. O. Edwards, 1959, Phys. Rev. Letters **3,** 127.
Bernardes, N., and H. Primakoff, 1960, Phys. Rev. **119,** 968; Phys. Rev. Letters **2,** 290, (1959).
——, and D. F. Brewer, 1962, Rev. Mod. Phys. **34,** 190.
Bertman, B., H. A. Fairbank, W. W. White, and M. J. Crooks, 1966, Phys. Rev. **142,** 74.

Bitter, M., W. Gissler, and T. Springer, 1967, Phys. Stat. Solidi **23,** K155.
Bonner, J. C., and J. F. Nagle, 1972, Phys. Rev. **A5,** 2293.
Brandow, B. H., 1971, Phys. Rev. **A4,** 422; Ann. Phys., to be published.
Burgess, A. E., and M. J. Crooks, 1972, Phys. Lett. **39A,** 183.
Carr, W. J., 1953, Phys. Rev. **92,** 28.
Chell, G. G., 1970, J. Phys. C.: Solid State Physics **3,** 1861.
——, V. V. Goldman, M. L. Klein, and G. K. Horton, 1970, Phys. Rev. **B2,** 560.
Crepeau, R. H., O. Heybey, D. M. Lee, and S. A. Strauss, 1971, Phys. Rev. **A3,** 1162.
——, and D. M. Lee, 1972, Phys. Rev. **A6,** 516.
Cohen, H. D., P. B. Pipes, K. L. Verosub, and W. M. Fairbank, 1968, Phys. Rev. Letters, **21,** 677.
Corruccini, L. R., D. D. Osheroff, D. M. Lee, and R. C. Richardson, 1971, Phys. Rev. Letters **27,** 650.
Cowley, R. A., and A. D. B. Woods, 1971, Can. J. Phys. **49,** 177.
deWette, F. W., 1963, Phys. Rev. **129,** 1160.
——, L. H. Nosanow, and N. R. Werthamer, 1967, Phys. Rev. **162,** 824.
——, and N. R. Werthamer, 1969, Phys. Rev. **184,** 209.
Dirac, P. A. M., 1929, Proc. Roy. Soc. (London) **A123,** 714.
Dugdale, J. S., and J. P. Franck, 1964, Phil. Trans. Roy. Soc. London, **A257,** 1.
Edwards, D. O., A. S. McWilliams, and J. G. Daunt, 1962a, Phys. Letters **1,** 218.
——, 1962b, Phys. Rev. Letters **9,** 195.
——, and R. C. Pandorf, 1965, Phys. Rev. **140,** A816.
——, and R. C. Pandorf, 1966, Phys. Rev. **144,** 143.
Ebner, C., and C. C. Sung, 1971, Phys. Rev. A **4,** 1099.
Fain, Jr., S. C., and D. Lazarus, 1970, Phys. Rev. A **1,** 1460.
Fairbank, W. M., and G. K. Walters, 1957, in *Proceedings of the Symposium on Solid and Liquid Helium Three* (Ohio State Research Foundation, Columbus, Ohio), p. 220.
——, and E. D. Adams, 1958, in *Proceedings of the Kammerlingh-Onnes Conference on Low Temperature Physics*, Leiden, Holland, Suppl. Physica **24,** 134.
Fedorov, F. I., 1968, *Theory of Elastic Waves in Crystals* (Plenum, N.Y.) pp. 339–354.
Finegold, L., and N. E. Phillips, 1969, Phys. Rev. **177,** 1383.
Franck, J. P., and R. Wanner, 1970, Phys. Rev. Letters, **25,** 345.
Gardner, W. R., J. K. Hoffer, N. E. Phillips, 1972, unpublished; see also Hoffer, 1968.
Gillis, N. S., T. R. Koehler, and N. R. Werthamer, 1968, Phys. Rev. **175,** 1110.
Glyde, H. R., 1969, Phys. Rev. **177,** 262; **A1,** 296 (1970).
——, 1970, J. Low. Temp. Phys. **3,** 559.
——, 1971, Can. J. Phys. **49,** 761.
——, and F. C. Khanna, 1971, Can. J. Phys. **49,** 2997.
Goldman, V. V., G. K. Horton, and M. L. Klein, 1970, Phys. Rev. Letters **24,** 1424.
Goldstein, L. 1961, Phys. Rev. **122,** 726.
——, 1967, Phys. Rev. **159,** 120; **164,** 270.
——, 1968a, Phys. Rev. **171,** 194.
——, 1968b, Phys. Rev. **176,** 311.
——, 1969, Phys. Rev. **188,** 349.
——, 1970a, Phys. Rev. Letters **25,** 1094.
——, 1970b, Phys. Rev. **A2,** 1964.
Greenberg, A. S., W. C. Thomlinson, and R. C. Richardson, 1972, J. Low. Temp. Phys. **8,** 3.
Greywall, D. S., 1971a, Phys. Rev. **A3,** 2106.
——, 1971b, Phys. Letters **35A,** 67.
——, and J. A. Munarin, 1970a, Phys. Letters **31A,** 469.
——, and J. A. Munarin, 1970b, Phys. Rev. Letters **24,** 1282; Erratum, 1970, Phys. Rev. Letters, **25,** 261.
Grilly, E. R., 1971, J. Low Temp. Phys. **4,** 615.
——, and R. L. Mills, 1959, Ann. Phys. (N.Y.) **8,** 1.
Guyer, R. A., 1969, *Solid State Phys.* **23,** 413.
——, 1970, Phys. Rev. Letters **24,** 810.
——, 1971, private communication to SBT.
——, 1972, J. Low. Temp. Phys. **6,** 251.
——, and L. I. Zane, 1969, Phys. Rev. **188,** 445; Phys. Rev. Letters, **24,** 660, 1325 (1970).
——, R. C. Richardson, and L. I. Zane, 1971, Rev. Mod. Phys. **43,** 532.
Harris, A. B., 1971, Solid State Comm. **9,** 2255.
Hartmann, S. R., 1964, Phys. Rev. **133,** A17.
Henriksen, P. N., M. F. Panczyk, and E. D. Adams, 1970, Solid State Comm. **8,** 735.
——, M. F. Panczyk, S. B. Trickey, and E. D. Adams, 1969, Phys. Rev. Letters, **23,** 518.
Herring, C., 1962, Rev. Mod. Phys. **34,** 631.
——, 1968, in *Magnetism II*, edited by G. Rado and H. Suhl (Academic Press, Inc., New York).
Hetherington, J. H., 1968, Phys. Rev. **176,** 231.
——, W. J. Mullin, and L. H. Nosanow, 1967, Phys. Rev. **154,** 175.
Hoffer, J. K., 1968, Thesis, Univ. Calif. (Berkeley), unpublished.
Hogan, E. M., R. A. Guyer, and H. A. Fairbank, 1969, Phys. Rev. **185,** 356.
Horner, H., 1970a, Phys. Rev. Letters **25,** 147.
——, 1970b, Phys. Rev. **A1,** 1722.
——, 1971, Solid State Comm. **9,** 79.
——, and L. H. Nosanow, 1972, Phys. Rev. Letters **29,** 88.
Horton, G. K., 1968, Am. J. Phys. **36,** 93.
Jarvis, J. F., D. Ramm, and H. Meyer, 1968, Phys. Rev. **170,** 320.
Johnson, R. T., O. G. Symko, and J. C. Wheatley, 1969a, Phys. Rev. Letters, **22,** 449.
——, O. G. Symko, R. Rosenbaum, and J. C. Wheatley, 1969b, Phys. Rev. Letters **23,** 1017.
——, O. V. Lounasmaa, R. Rosenbaum, O. G. Symko, and J. C. Wheatley, 1970a, J. Low. Temp. Phys. **2,** 403.
——, and J. C. Wheatley, 1970b, J. Low Temp. Phys. **2,** 423.
——, and J. C. Wheatley, 1970c, Phys. Rev. A **1,** 1836.
——, R. E. Rapp, and J. C. Wheatley, 1971, J. Low Temp. Phys. **6,** 445.
——, R. E. Rapp, and J. C. Wheatley, 1972a, preprint.
——, D. N. Paulson, R. P. Giffard, and J. C. Wheatley, 1972b, preprint.
——, O. G. Symko, and J. C. Wheatley, 1972c, Phys. Letters **39A,** 173.
Keller, W. E., 1969, *Helium-3 and Helium-4* (Plenum Press, N.Y.).
Kirk, W. P., 1970, Thesis, State University of New York at Stony Brook, (unpublished).
——, E. B. Osgood, and M. Garber, 1969, Phys. Rev. Letters **23,** 833; See also Kirk (1970) and Osbood, Garber, and Kirk (1970).
——, and E. D. Adams, 1971, Phys. Rev. Letters **27,** 392.
——, and E. D. Adams, 1972, Bull. Am. Phys. Soc. **17,** 452; submitted to LT 13; and to be published.
Klein, M. L., and D. L. Martin, 1972, Phys. Letters **38A,** 430.
Koehler, T. R., and N. R. Werthamer, 1972, Phys. Rev. **A5,** 2230.
Lee, D. M., H. A. Fairbank, and E. J. Walker, 1959, Bull. Am. Phys. Soc. **4,** 239.
Lipschultz, F. P., and D. M. Lee, 1965, Phys. Rev. Letters **14,** 1017.
——, and D. M. Lee, 1967, *Proc. 10th Intern. Conf. Low Temp. Phys.* (VINITI, Moscow) I, 309.
——, V. J. Minkiewicz, T. A. Kitchens, G. Shirane, and R. Nathans, 1967, Phys. Rev. Letters **19,** 1307.
McMahan, A. K., 1971, Thesis, Univ. of Minn., (unpublished).
——, 1972a, J. Low Temp. Phys. **8,** 115; Bull. Am. Phys. Soc. **17,** 355.
——, 1972b, Bull. Am. Phys. Soc. **17,** 452; and to be published.
——, and R. A. Guyer, 1972, *Proc. 13th Intern. Conf. Low Temp. Phys.*, in press.
Meissner, G., 1971, *Proc. Twelfth Intern. Conf. Low Temp. Phys.* edited by Eizo Kanda (Academic, Tokyo, Japan), p. 143.
Meyer, H., 1968, J. Appl. Phys. **39,** 390.
Mezhov-Deglin, L. P., 1965, J. Exptl. Theoret. Phys. (USSR) **49,** 66; [Sov. Phys. JETP **22,** 47 (1966)].
Mills, R. L., E. R. Grilly, and S. G. Sydoriak, 1961, Ann. Phys. (N.Y.) **12,** 41.
Minkiewicz, V. J., T. A. Kitchens, F. P. Lipschultz, R. Nathans, and G. Shirane, 1968, Phys. Rev. **174,** 267.
Morley, G. L., and K. L. Kliewer, 1969, Phys. Rev. **180,** 245.
Mullin, W. J., 1964, Phys. Rev. **136,** A1126.
——, 1968a, Phys. Rev. Letters **20,** 254; Phys. Rev. Letters **20,** 1550.
——, 1968b, Phys. Rev. **166,** 142.
——, L. H. Nosanow and P. M. Steinback, 1969, Phys. Rev. **188,** 410.
Musgrave, M. J. P., 1959, in *Reports on Progress in Physics*, edited by A. C. Stickland (The Physical Society, London), Vol. XXII, 74.
Nosanow, L. H., 1964, Phys. Rev. Letters **13,** 270.
——, and W. J. Mullin, 1965, Phys. Rev. Letters **14,** 133.
——, 1966, Phys. Rev. **146,** 120.

——, and C. M. Varma, 1968, Phys. Rev. Letters **20,** 912.
——, and C. M. Varma, 1969, Phys. Rev. **187,** 660.
Osgood, E. B., 1971, private Communication.
——, M. Garber, and W. P. Kirk, 1970, in *Proceedings of the XIIth International Conference on Low Temperature Physics,* edited by Eizo Kanda (Keigaku Pub. Co., Kyoto, Japan) p. 137.
——, and M. Garber, 1971, Phys. Rev. Letters **26,** 353.
——, V. J. Minkiewicz, T. A. Kitchens, and G. Shirane, 1972, Phys. Rev. **A5,** 1537, errata, 1972, Phys. Rev. **A6,** 526.
Osheroff, D. D., R. C. Richardson, and D. M. Lee, 1972, Phys. Rev. Letters **28,** 885.
Østgaard, E., 1972, J. Low. Temp. Phys. **7,** 471.
Overton, W. C., Jr., 1971, Phys. Letters **37A,** 287.
Panczyk, M. F., R. A. Scribner, G. C. Straty, and E. D. Adams, 1967, Phys. Rev. Letters **19,** 1102.
——, R. A. Scribner, J. R. Gonano, and E. D. Adams, 1968, Phys. Rev. Letters **21,** 594.
——, and E. D. Adams, 1969, Phys. Rev. **187,** 321.
——, and E. D. Adams, 1970, Phys. Rev. **A1,** 1356.
Pandorf, R. C., and D. O. Edwards, 1968, Phys. Rev. **169,** 222.
Pipes, P. B., and W. M. Fairbank, 1969, Phys. Rev. Letters **23,** 520; Phys. Rev. **A4,** 1590 (1971).
Pollack, G. L., 1964, Rev. Mod. Phys. **36,** 748.
Pomeranchuk, I. I., 1950, Zhur. Eksp. i. Theoret. Fiz. **20,** 919.
Reese, R. A., S. K. Sinha, T. O. Brun, and C. R. Tilford, 1971, Phys. Rev. **A3,** 1688.
Reich, H. A., 1963, Phys. Rev. **129,** 630.
Richards, M. G., 1971, in *Advances in Magnetic Resonance,* edited by J. S. Waugh (Academic, N.Y.) **5,** 305.
——, J. Hatton, and R. P. Giffard, 1965, Phys. Rev. **139,** A91.
——, and J. M. Homer, 1969, Phys. Rev. **182,** 318.
Richardson, R. C., 1970, J. du Physique, Colloque **C.3**. (suppl. Vol. 10), C3–79.
——, E. Hunt, and H. Meyer, 1965, Phys. Rev. **138,** A1326.
——, A. Landesman, E. Hunt, and H. Meyer, 1966, Phys. Rev. **146,** 244.
Roberts, T. R., and S. G. Sydoriak, 1954, Phys. Rev. **93,** 1418.
Ruvalds, J., 1971, Phys. Rev. **B3,** 3556.
Sample, H. H., and C. A. Swenson, 1967, Phys. Rev. **158,** 188.
Scribner, R. A., M. F. Panczyk, and E. D. Adams, 1968, Phys. Rev. Letters **21,** 427.
——, M. F. Panczyk, and E. D. Adams, 1969, J. Low Temp. Phys. **1,** 313.
——, and E. D. Adams, 1970, Rev. Sci. Instr. **41,** 287.
——, and E. D. Adams, 1972, in *Temperature, Its Measurement and Control in Science and Industry,* Vol. 4 (in press).
Seward, W. D., D. Lazarus, and S. C. Fain, Jr., 1969, Phys. Rev. **178,** 345.
Sherman, R. H., and F. J. Edeskuty, 1960, Ann. Phys. (N.Y.) **9,** 522.
Silberglitt, R., 1969, Phys. Rev. **188,** 786.
Simon, F. E., N. Kurti, J. F. Allen, and K. Mendelssohn, 1952, *Low Temperature Physics' Four Lectures* (Academic, New York), p. 28.
Sites, J. R., D. D. Osheroff, R. C. Richardson, and D. M. Lee, 1969, Phys. Rev. Letters **23,** 836.
Slater, J. C., 1939, *Introduction to Chemical Physics* (McGraw-Hill, New York), Chaps. 17 and 18.
Smart, J. S., 1966, *Effective Field Theories of Magnetism* (Saunders, Philadelphia).
Smith, B. L., 1970, Contemporary Phys. **11,** 125.
Straty, G. C., and E. D. Adams, 1968, Phys. Rev. **169,** 232.
——, and E. D. Adams, 1969, Rev. Sci. Instr. **40,** 1393.
Swenson, C. A., 1969, private communication to EDA.
Thomlinson, W. C., 1969, Phys. Rev. Letters **23,** 1330.
——, 1972, to be published.
Thompson, J. R., and H. Meyer, 1967, Cryogenics **7,** 296.
Thomson, A. L., H. Meyer, and P. N. Dheer, 1963, Phys. Rev. **132,** 1455.
Thouless, D. J., 1965, Proc. Phys. Soc. (London) **86,** 893.
Traylor, J. G., C. Stassis, R. A. Reese, and S. K. Sinha, 1971, in *Inelastic Scattering of Neutrons* (I.A.E.A., Vienna) Vol. I, in press.
Trickey, S. B., and E. D. Adams, 1970, Phys. Letters **33A,** 483.
Van Kranendonk, J., and J. H. Van Vleck, 1958, Rev. Mod. Phys. **30,** 1.
Varma, C. M., 1970a, Phys. Rev. Letters **24,** 203.
——, 1970b, Phys. Rev. Letters **24,** 970.
——, and L. H. Nosanow, 1970, Phys. Rev. A **1,** 133.
Vignos, J. H., and H. A. Fairbank, 1966, Phys. Rev. **147,** 185.
Walstedt, R. E., L. R. Walker, and C. M. Varma, 1971, Phys. Rev. Letters **26,** 691.
Wanner, R., 1971, Phys. Rev. A **3,** 448.
——, and J. P. Franck, 1970, Phys. Rev. Letters, **24,** 365.
Werthamer, N. R., 1969, Am. J. Phys. **37,** 763.
——, 1972, Phys. Rev. Letters, **28,** 1102.
Wilks, J., 1967, *Liquid and Solid Helium* (Oxford U. P., London).
Wolf, W. P., M. F. Thorpe, and R. Alben, 1971, Phys. Rev. Letters **26,** 756.
Zane, L. I., 1972a, Phys. Rev. Letters **28,** 420.
——, 1972, J. Low Temp. Phys., to be published.
Zeisse, C. R., 1968, Phys. Rev. **173,** 301.
Zimmerman, G. O., 1965, in *Proceedings of the IXth International Conference on Low Temperature Physics,* edited by J. G. Daunt, D. O. Edwards, F. J. Milford, and M. Yaqub (Plenum, New York) p. 244.